



**UCGE Reports  
Number 20129**

Department of Geomatics Engineering

**DGPS Carrier Phase Networks and Partial Derivative  
Algorithms**

(URL: <http://www.geomatics.ucalgary.ca/GradTheses.html>)

by

**Christopher C. Varner**

**February 2000**



Calgary, Alberta, Canada

THE UNIVERSITY OF CALGARY

**DGPS Carrier Phase Networks and Partial Derivative Algorithms**

by

Christopher Champion Varner

A DISSERTATION

SUBMITTED TO THE FACULTY OF GRADUATE STUDIES IN PARTIAL  
FULFILMENT OF THE REQUIREMENTS FOR THE DEGREE OF DOCTOR OF  
PHILOSOPHY

DEPARTMENT OF GEOMATICS ENGINEERING

CALGARY, ALBERTA

FEBRUARY, 2000

© Christopher Champion Varner 2000

THE UNIVERSITY OF CALGARY  
FACULTY OF GRADUATE STUDIES

The undersigned certify that they have read, and recommend to the Faculty of Graduate Studies for acceptance, a dissertation entitled “Carrier Phase Differential GPS Networks” submitted by Christopher Champion Varner in partial fulfillment of the requirements for the degree of Doctor of Philosophy.

---

Supervisor, Dr. M. E. Cannon, Geomatics Engineering

---

Dr. G. Lachapelle, Geomatics Engineering

---

Dr. E. Krakiwsky, Geomatics Engineering

---

Dr. D. Irvine-Halliday, Electrical and Computer Engineering

---

Dr. D. B. Cox, DBC Communications, Inc.

---

Date

## Abstract

There are a variety of large-scale applications that desire centimetre to decimetre level positioning and navigation accuracy. Some of these applications include surveying, agriculture fertilisation and yield monitoring, aircraft precision landings, intelligent transportation systems, and harbour/river navigation and docking. The Global Positioning System is one of the few, and perhaps the only, service that can meet the requirements of these projects.

Centimetre to decimetre level positioning accuracy requires the use of carrier-phase GPS measurements. The system must be operated in a double differential mode in which a nearby reference station is used to calibrate for errors in the satellite differential measurements. For large-scale applications, a network of multiple differential reference stations is necessary.

While Carrier-Phase Network Differential GPS (CP-NDGPS) is theoretically possible, its implementation is complex and has not been fully developed. This dissertation describes one method of implementing CP-NDGPS using Partial Derivative Algorithms. Partial derivative algorithms are implemented by the network service provider, and are used to estimate signal errors that cannot be measured by a single GPS reference station.

The information sent to the user by the network service provider is communicated through a data link. The amount of information communicated defines the data link bandwidth. A PDA is an efficient method of filtering the information and reducing the data link bandwidth, which is often limited to transfer speeds of 9600 bits per second (bps).

## Acknowledgements

I gratefully acknowledge the support and guidance of Dr. M. Elizabeth Cannon, Dr. Gerard Lachapelle, Dr. Edward Krakiwski, and Dr. J. Rod Blais, Dr. Duncan Cox, and Dr. Dave Irvine-Halliday. I also would like to express my appreciation to John Raquet, Richard Klukas, and Huangqi Sun for the many hours that we debated various aspect of network GPS, ambiguity resolution, and Kalman filtering. I thank my parents for their emotional and financial support.

Thanks also to Michael Heflin for help with understanding the data obtained from the Southern California Integrated GPS Networks. The Holloman data presented in this document is provided through the courtesy of 746th Air Force Test Squadron stationed at Holloman AFB, Alamogordo, New Mexico.

## Dedication

I dedicate this book to my brother, LCDR Andrew B. Varner – who taught me that my flying is good, but my engineering is better.

## TABLE OF CONTENTS

Approval Page	ii
Abstract	iii
Acknowledgements	iv
Dedication	v
Table of Contents	vi
List of Tables	ix
List of Figures	x
Nomenclature	xii
Acronyms	xiii

<b>Section</b>	<b>Page</b>
----------------	-------------

---

### Chapter 1: INTRODUCTION

1.1	Background and History	1
1.2	Research Into High Accuracy Positioning Using GPS	2
1.3	Problem Statement, Objective, and Solution Approach	10
1.4	Document Organisation	12

### Chapter 2: GPS FUNDAMENTALS

2.1	Overview	14
2.2	The Global Positioning System	14
2.3	Determination of Position and Time	16
2.4	Measurements	18
2.4.1	Code-Phase Measurements	19
2.4.2	Carrier-Phase Measurements	20
2.4.2.1	Widelane	23
2.4.2.2	Ionospheric Free Measurement	23
2.4.2.3	Narrowlane	24
2.5	System Errors and Biases	25
2.5.1	Selective Availability (SA)	25
2.5.2	Ephemeris and Clock Errors	26
2.5.3	Atmospheric Errors	28
2.5.3.1	Ionosphere	28
2.5.3.2	Troposphere	31
2.5.4	Receiver Technologies, Noise, and Multipath	32
2.5.4.1	Dual Frequency Technologies	32
2.5.4.2	Noise	35

2.5.4.3	Multipath	36
2.6	GPS Range Error Budgets	37
Chapter 3: CARRIER-PHASE DIFFERENTIAL GPS		
3.1	Overview	39
3.2	Differential GPS	39
3.3	Receiver Single-Difference Measurements	43
3.4	Differential Shift and Distortion Errors	45
3.5	Double-Difference Measurements	47
3.6	DGPS Error Budgets	49
Chapter 4: PARTIAL DERIVATIVE ALGORITHMS THEORY AND IMPLEMENTATION		
4.1	Overview	52
4.2	PDA Theory	52
4.3	Network Measurements	54
4.4	Budgeting for the Network Measurement Noise ( $\zeta_j^i$ )	56
4.5	Measurement Error Modelling (Partial Derivative Algorithms)	60
4.6	Modelling Solutions	67
4.7	Correcting User Measurements with the PDA Model	70
4.8	Short History on the Use of PDAs	72
4.9	Origins of NDGPS	73
4.9.1	Wide, Regional, and Local Area Coverage	75
4.9.2	Common View and Non-Common View Networks	76
4.9.3	Centralised Vs. Decentralised Processing	78
4.9.4	Communications Architecture	78
4.10	Nearest-Station Concept	79
4.11	Combined-Station Concept	81
4.12	Spatial and Non-spatial Error Categories	84
4.13	Network Initialisation and Recovery from Geometry Changes	85
4.13.1	Network Initialisation	86
4.13.2	Network Recovery from Geometry Changes	86
4.13.3	Short Baseline Network Linking	87
4.13.4	Batch Process Filtering	89
4.13.5	Combined Ambiguity and Parameter Estimation	90
4.13.6	Dual Frequency Thinning	91
4.14	Parameter Filtering	92

## Chapter 5: PROCESSING METHODS

5.1	Overview	93
5.2	Processing Software and Concerns	93
5.3	State and Noise Filtering	97
5.4	Ambiguity Resolution	98
5.5	PDA Implementation	100
5.6	Testing Procedure	103
5.7	Real-Time Issues	103
5.7.1	Data Link	103
5.7.2	Latency	105
5.7.3	Software	106

## Chapter 6: TEST CASE RESULTS

6.0	Overview	107
6.1	Calgary and New Mexico Sample Networks	107
6.1.1	PDA Development	111
6.1.2	Performance Analysis	112
6.2	Southern California Integrated GPS Networks (SCIGN)	118
6.2.1	Network Ambiguity Determination	121
6.2.2	Network Measurements	123
6.2.3	Modelling the Errors with Partial Derivatives	125
6.2.4	Positioning with PDA Network Phase Corrections	133
6.2.4.1	Results at the "oat2" Test Site	134
6.2.4.2	Other Test Site Results	139

## Chapter 7: CONCLUSIONS AND RECOMMENDATIONS

7.1	Summary	143
7.2	Specific Results	145
7.3	Network Design Issues	147
7.4	Future Perspectives	148

	References	150
--	------------	-----

	Appendix A: Site Co-ordinates for SCIGN Working Network	160
--	---	-----

## List of Tables

<b>Table</b>	<b>Title</b>	<b>Page</b>
2-1	GPS Range Error Budget (Errors Common to All Measurements)	38
2-2	GPS Code-Phase Measurement Error Budget	38
2-3	GPS Carrier-Phase Measurement Error Budget	38
3-1	Double-Difference (DD) Carrier-Phase DGPS Error Budget (L1)	50
3-2	DD Carrier-Phase DGPS Error Budget (L2)	50
3-3	DD Carrier-Phase DGPS Error Budget (Widelane)	50
3-4	DD Carrier-Phase DGPS Error Budget (Ionospheric Free)	51
3-5	DD Carrier-Phase DGPS Error Budget (Narrowlane)	51
4-1	Horizontal Survey Classifications	59
4-2	Network Measurement Noise Error Budget (L1)	60
4-3	PDA Naming Convention	67
4-4	Data Link Throughput Requirement for Different Algorithms	83
6-1	PDA's Tested with the Holloman Network Data	112
6-2	PDA Models for Satellite DD28-17 at 416052 seconds GPS Time	115
6-3	California Working Net Kilometerage Chart	121
6-4	PDA Parameter Estimates for PRN 29-1 at Epoch 96419	126
6-5	PDA Parameter Estimated Standard Deviations	128
6-6	Non-Spatial Error at the Secondary Reference Stations	130
6-7	Modelling Analysis for Satellite PRN 29-14	131
6-8	Accuracy Comparisons Between NDGPS & DGPS	139
6-9	Ambiguity Resolution Results	141

## List of Figures

<b>Figure</b>	<b>Title</b>	<b>Page</b>
2-1	The Global Positioning System	15
2-2	(a) Sphere of Position, (b) Circle of Position , (c) Points of ...	18
2-3	GPS Error Sources	26
3-1	Differential GPS	43
3-2	Formation of the Double-Difference Measurement	48
4-1	North/South Network	65
4-2	East/West Network	66
4-3	Common View and Non-Common View Networks	77
4-4	Centralised and Decentralised Processing Models	79
4-5	MVA Modelling Modes	82
5-1	Carrier-Phase Solution Architecture	95
5-2	Network Processing Implementation	102
5-3	Generating Range Corrections from Network Measurements	102
5-4	Testing DGPS and PDA Solutions	104
6-1	Test Networks	108
6-2	Survey Accuracy Versus Observation Period	110
6-3	Double Difference Carrier-Range Measurement Residuals ...	114
6-4	PDA Model Comparisons	115
6-5	$\alpha\beta$ PDA Coefficient Time Histories	117
6-6	Positioning Error – Time Histories	118
6-7	Southern California Integrated GPS Network Site Map	119
6-8	IGS Southern California Working Network	120
6-9	Network Linking (Ambiguity Determination for PRN 29-1)	123
6-10	Network Measurements of PRN 29-14 at 111510 seconds	124
6-11	Time History of the Master Station Non-Spatial Error Estimate...	132
6-12	Time History of the PRN 29-14 Spatial Decorrelation Parameters	132
6-13	Time History of the AKAIKE Value	133
6-14	Estimated and Measured Errors for PRN 16-14 at “oat2”	135
6-15	Estimated and Measured Error for PRN 18-14 at “oat2”	135
6-16	Estimated and Measured Error for PRN 22-14 at “oat2”	136
6-17	Estimated and Measured Error for PRN 29-14 at “oat2”	136
6-18	Vertical Positioning Results for “oat2”	137
6-19	Easting Positioning Results for “oat2”	138

6-20	Northing Positioning Results for "oat2"	138
6-21	Resolution Time Vs. Distance	142



## Acronyms

<u>Acronym</u>	<u>Description</u>	<u>Page</u>
AIC	- Akaike Information Criterion	130
C/A	- Course/Acquisition	4
CAA	- Conditional Adjustment Algorithm	73
CP	- Carrier Phase	5
DD	- Double Difference	48
DGPS	- Differential Global Positioning System	4
DOD	- United States Department of Defence	14
DOF	- Degrees of Freedom	63
DOP	- Dilution of Precision	98
FAA	- United States Federal Aviation Administration	75
FLL	- Frequency Lock Loop	21
FOC	- Full Operational Capability	15
GPS	- Global Positioning System	2
IGS	- International GPS Service for Geodynamics	27
ITRF	- International Terrestrial Reference Frame	27
IP	- Innovations Process	129
ITS	- Intelligent Transportation Systems	2
JPL	- Jet Propulsion Laboratory	27
LAAS	- Local Area Augmentation System	75
MCS	- Master Control Station	14
MVA	- Minimum Variance Algorithm	73
NDGPS	- Network DGPS	12
OTF	- On-The-Fly (i.e. resolves CP ambiguities in real-time)	100
PDA	- Partial Derivative Algorithm	8
PDD	- United States Presidential Decision Directive	25
PDOP	- Position DOP	98
PLL	- Phase Lock Loop	21
ppm	- Parts Per Million	44
PPS	- Precision Positioning Service	15
PRDS	- Priddis (IGS reference site)	110
PRN	- Pseudo-Random Noise codes assigned to each GPS satellite	113
RFI	- Radio Frequency Interference	16
RMS	- Root Mean Square	113
RSS	- Root Sum Square	6
RTCM	- Radio Technical Commission for Maritime studies	41
RTK	- Real-Time Kinematic	16
SA	- Selective Availability	3

SCIGN	- Southern California Integrated GPS Networks	118
SEP	- Spherical Error Probable	3
SPS	- Standard Positioning Service	14
TEC	- Total Electron Content	29
USCG	- United States Coast Guard	8
UTC	- Universal Time Coordinated	17
WADGPS	- Wide Area DGPS	8
WGS	- World Geodetic System	27

## Chapter 1

### INTRODUCTION

#### 1.1 Background and History

Knowing our location has been a universal desire since the beginning of human civilisation. It is a powerful tool that has been used for religion, politics, war, and commerce. In 585 BC, the Greek philosopher Thales moved the boundaries of religion and science by predicting a solar eclipse and defined a new scientific theory for determining the positions of celestial bodies [Collier Encyclopædia, 1997]. The boundary markers of land near the Nile were often moved after the spring floods. In order to resolve the ensuing land disputes, the Egyptians turned to surveying as a method of recovering the boundaries. Surveying techniques were also used by Eratosthenes (275-294 BC) to compute the first accurate measure of the size of the Earth. This event was used as evidence to dispel the, then popular, belief that the Earth was flat. A new continent was discovered when Christopher Columbus attempted to sail the unknown waters west of Europe and establish a new trade route to India. In 1759, an English clock maker by the name of John Harrison developed a marine chronometer that allowed a navigator to determine a ship's longitude to within 30 miles [Encarta 97 Encyclopædia, 1997]. Coincidentally, England became the undisputed world naval power at the end of the Seven Years War (1756-1763).

The Persian Gulf War (1990-1991) is likely to become a classic example of the power derived from knowing the precise location of objects. During the war, Coalition forces lead by the United States introduced a new form of determining position by using satellites. This satellite positioning system was called the Global Positioning System

(GPS). GPS proved to be a tremendous advantage during the war, and quickly became a popular method of positioning for commercial applications. In December of 1994, GPS was declared fully operational [GPS World, 1995], and today, commercial applications are the driving force in the system's development. These applications include fishing, farming, surveying, hiking, flying, and driving. GPS is also used for time transfer, geodesy, orbit determination, atmospheric studies, earthquake prediction [Van Dierendonck et al., 1994; Dong and Bock, 1989], and a multitude of other scientific projects.

GPS has given people the ability to determine their location instantly, anywhere on the globe with an accuracy of 10 to 100 metres, but entrepreneurs are designing GPS applications that require even better accuracy. Aeroplanes and boats operating in poor weather need to know their position to within a few metres. Farmers guide combines through their fields with only a metre between the rows of produce, while surveyors and seismologists need to define the location of their reference markers with centimetre level accuracy. Research into the capabilities of GPS has indicated that the system can meet these needs.

## **1.2 Research Into High Accuracy Positioning Using GPS**

Sub-metre positioning accuracy is quickly becoming the reality of modern vehicle navigation. The Intelligent Transportation System (ITS) is an emerging concept in which individual vehicle movement is externally controlled along certain sections of roadway. Each vehicle is monitored and controlled in concert with other vehicle groups by an external traffic management system. In order to control the movement of numerous vehicles in close proximity to one another, the ITS monitoring functions demand high accuracy positioning and navigation [Galijan et al., 1994]. Airport Category III

instrument landings require vertical positioning accuracy of 0.5 m vertical [Beser et al., 1984]. In order to obtain global navigation capabilities many system designers are turning to GPS. Unfortunately, there are a variety of errors in the GPS measurements that prevent the basic system from meeting the high accuracy requirements demanded by modern applications.

In GPS, measurement errors can be grouped into three categories:

- Transmission or source errors include “Selective Availability” (SA), poor satellite ephemeris (orbit), and satellite clock bias.
- Path errors exist in the form of ionospheric effects, troposphere delay, and multipath reflections.
- Reception errors result from measurement tracking noise, and antenna phase centre instability.

The combined effect of these errors causes most civilian GPS to have the range measurement accuracy of 22 metres spherical error probable (SEP) [Parkinson, 1996a]. In order to obtain metre level accuracy, methods of reducing the measurement errors are necessary. A common method of reducing the errors in GPS measurements is to generate relative positions with respect to a surveyed local reference point (site or station). A stationary GPS receiver is placed at the reference point and is called the reference receiver. The measurements collected by the reference receiver are subtracted from the measurements collected by the user’s receiver to form differential measurements. The differential measurements are then used to calculate a differential position. Transmission errors are introduced at the satellite and are the same for both the reference and user receivers. Some path errors can also be common to both receivers. Common errors are eliminated through the differencing process.

This concept is called Differential GPS (DGPS). DGPS eliminates errors introduced by SA and the satellite clock bias. It also reduces the effects of path errors for a user that is in the vicinity of the reference point.

The vector that represents the differential position of the user with respect to the reference station is called the “baseline”. Baselines can be of any length, but DGPS applications typically vary from a few metres to a few hundred kilometres. Errors that are not common to both the user and reference station can be characterised as either “spatial” or “non-spatial”. Spatial errors are errors whose magnitude depends upon the length of the baseline. Non-spatial errors are errors that are independent of the baseline length. Source errors are common to both receivers and are effectively eliminated by the DGPS concept. Path errors (such as ionospheric effects, some tropospheric delay, and satellite orbital errors) are spatial, while errors that occur at the receiver are primarily non-spatial.

GPS measurements come in two forms: Code-Phase and Carrier-Phase. Code-Phase measurements are derived from codes that are embedded in the GPS radio signals. The two fundamental codes are designated as the course/acquisition (C/A) code, and the Precise (P) code. When the P-code is encrypted for the military use, it is called the Y-Code.

In DGPS, the largest errors for code-phase measurements tend to be multipath and receiver noise. The original GPS receivers could experience multipath errors of up to 150 metres. Today, the use of multipath mitigation technology such as Narrow Correlator<sup>TM</sup> can reduce these errors considerably [Van Dierendonck et al., 1992]. For baselines up to 500 kilometres, a positioning accuracy of 5 to 10 metres can be expected [Wells et al., 1987]. NovAtel has developed C/A-code receivers with improved tracking capabilities as exemplified by their Multipath Estimating Delay Lock Loop (MEDLL<sup>TM</sup>) architecture

[Townsend et al., 1995]. These receivers have a code-phase positioning accuracy of 1 to 3 metres [Sams, 1995].

The accuracy of differential code-phase positioning is limited to the 1 to 3-metre level because there are non-spatial errors associated with code-phase multipath and measurement tracking noise [Mueller, 1994a]. More accurate positioning and navigation can be obtained by using the carrier-phase measurements because the measurement tracking noise errors are several orders of magnitude smaller. As a result, centimetre level accuracy has been achieved with carrier-phase DGPS (CP-DGPS), but spatial errors play a more important role in defining the carrier-phase positioning accuracy [Ford and Neumann, 1994].

Carrier-phase measurements are an integration of the Doppler shift affecting the GPS radio signals. The Doppler shift is related to the rate of change of range to the satellite. It is measured in Hz and can sometimes reach a magnitude of 6 kHz. Integration of the Doppler Shift is one method of determining the range to the satellite. Unfortunately, there is a lack of knowledge of the cycle within which the phase is being measured. This means that each carrier-phase measurement has an ambiguity that can take on any value. This ambiguity must be estimated or resolved before the carrier phase measurements are useful.

GPS operates on two frequencies that are allocated within radio navigation bands that are protected world-wide. These frequencies are called L1 (1575.42 MHz) and L2 (1227.6 MHz). Carrier-phase measurements can be obtained for both of these frequencies, but measurements can also be derived from linear combinations of L1 and L2. The most important derived frequencies are the Widelane (347.82 MHz), and the Narrowlane (2803.02 MHz). The Ionospheric Free carrier-phase is also a derived measurement, but it can have a variety of frequencies depending upon how it is formed.

Each carrier-phase measurement has an unknown ambiguity called the integer cycle ambiguity [Parkinson, 1996a]. This ambiguity may be estimated with a floating ambiguity filter, and resolved to an integer by testing the root sum squared (RSS) residuals of the various potential integer solutions. These potential integer solutions are selected from the filter estimate of the ambiguity based upon the estimate's predicted uncertainty. This uncertainty decreases as more measurements are collected. The lower the uncertainty, the greater the potential for successfully resolving the ambiguities by RSS residual testing. The level of uncertainty depends not only on the number of measurements collected (satellites), but also on the strength of the measurement geometry, and the baseline distance between the user and reference receiver. Numerous satellites with strong geometry over a short baseline could provide instantaneous resolution, while poor geometry with few satellites may take tens of minutes [Chen and Lachapelle, 1994; Sauer et al., 1994]. As the baseline length increases, spatial errors grow making it more difficult, and ultimately impossible, to resolve integer ambiguities. Beyond 15 or 20 kilometres, the spatial errors are so large that integer ambiguity resolution on the L1 or L2 frequencies is not typically possible [Weisenberger, 1997]. Lower frequency measurements such as the derived widelane can sometimes resolve to integers on baselines of 45 to 60 km.

For baselines that are more than 10 or 15 km, single frequency (L1 or L2) ambiguity resolution is normally limited by the spatial errors. These errors, which include atmospheric and orbital effects, are not fully correlated between the user and reference station. Spatial errors can result in a positioning error of 1 to 10 parts per million (ppm) of the baseline length [Cannon et al., 1993; Wells et al., 1987]. The use of dual frequency ionospheric free measurements can eliminate the ionospheric portion of the spatial error and reduce the rate of growth with baseline length. Unfortunately, dual frequency measurements have large non-spatial multipath and noise errors. Since spatial errors have

random characteristics over time, the accumulated effect of the spatial errors will decrease if filtering is implemented by adding measurements over time. As a result, the magnitude of the spatial positioning error depends upon the period of time over which the positioning solution can be derived. Sluiter et al. [1994] has shown that static positioning using a geodetic dual frequency receiver can have spatial positioning errors as low as 0.1 ppm when positions are averaged over an hour. Kinematic applications often have little to no ability to apply the time averaging concept. Ford and Neumann [1994], and Cannon and Varner [1995] have shown that kinematic positioning errors may grow at a rate of 10 ppm for baselines of less than 50 km.

Since some positioning applications have a specific accuracy requirement, there exists a baseline length limit beyond which the user's positioning accuracy will not meet the stated requirements. The baseline length limit will primarily depend upon the rate at which the spatial errors grow. By reducing the growth rate of the spatial error, the baselines can be extended for the same level of accuracy, and the DGPS technique can be used over larger areas.

DGPS networks, which combine observations from multiple reference stations, have been shown to reduce the rate of growth of spatial errors [Mueller, 1994a]. One result of combining measurements from multiple reference stations is that the multipath errors of one station are diluted by the random nature of the multipath errors at the other stations in the network. Mueller predicted the positioning accuracy of a code-phase network that covers the United States is between 1 and 4 metres. Lapucha and Huff [1994] have obtained similar results in which the horizontal errors had a standard deviation of 2.5 metres.

DGPS networks can be separated into two logical groups: those employing measurement domain algorithms, and those using state-space domain algorithms [Mueller, 1994b].

Measurement domain algorithms make no attempt to identify the individual error sources. State-space domain algorithms estimate the magnitude and direction of each error as categorized by its source.

Measurement domain networks observe the measurement errors at the reference receivers (also called sites or stations), and then combine these errors using the measurement domain algorithm to form measurement corrections for the user. The corrections are sent to the user, and the adjustments are made [Mueller, 1994b]. These algorithms are simple to implement, but they do not attempt to identify the source of the errors being corrected. As a result, the area over which their application can be justified is usually less than a few hundred kilometres depending upon the type of measurements being observed.

In state-space domain algorithms, each error source is associated with a state-space parameter, and the state vector is a collection of all parameters to be estimated. The components of the state vector are supplied to the user, and the measurement corrections are computed using a function called the state-space algorithm [Mueller, 1994a]. The estimation process in state-space networks is usually complicated, but these networks can be used to provide measurement corrections for areas of continental size.

The U.S. Coast Guard (USCG) operates a code-phase measurement domain DGPS network that covers the coastal United States using more than 50 reference stations [Alsip and Radice, 1993]. The user is expected to determine a position with DGPS using the nearest network reference station. As a result, this network is called a “nearest-station” network, and there is no attempt to combine the measurements of multiple stations.

Wide Area Differential GPS (WADGPS) is one application of a state-space domain algorithm. In WADGPS, the error sources are divided into categories such as SA, ionospheric error, and orbit error [Kee and Parkinson, 1992]. Another state-space

concept is called the Partial Derivative Algorithm (PDA). PDAs have been applied to code-phase networks [Loomis et al., 1991], and divide the errors into spatial, and non-spatial categories. State-space domain algorithms are implemented by the network service provider who can control the amount of information that the user receives by simply changing the mathematical order of the state-space algorithm.

State-space domain algorithms that attempt to estimate the errors according to their source can accurately estimate the non-linear characteristics of the errors over large areas. Unfortunately, the error sources can only be accurately estimated using networks that span large areas. Networks that cover only a few hundred kilometres are unable to distinguish the signatures of the various error sources. This problem is referred to as “lack of observability”.

Carrier-phase networks tend to be small. This means that they are not well suited for identifying the components of state-space domain algorithms that are based upon non-linear source error models. On the other hand, carrier-phase networks have excellent measurement accuracy and can easily detect spatial variations of the measurement errors over baselines of only a few tens of kilometres in length. For this reason, it is possible to design state-space algorithms that attempt to model the measurement errors at the network location.

Varner and Cannon [1997], Raquet [1996], and Wübbena et al. [1996] have developed methods of combining the carrier-phase measurements from multiple stations to reduce the errors in carrier-phase DGPS applications. Corrections can be estimated by the user after receiving error information from all network reference stations, but in order to reduce the data link communications load (bandwidth), the network provider may choose to model the corrections as a low order function and send the correction function

parameters to the user. PDAs are one class of low order functions that may be implemented by the network service provider.

A critical factor affecting the design of carrier phase networks is the relative survey accuracy of the network reference stations. Cannon and Varner [1995] indicate that errors in the relative positions of the network reference stations degrade the performance of the carrier-phase network. If the relative positions of the reference stations are not accurate, the differential integer ambiguities between the reference stations are difficult to resolve. These differential ambiguities (also called “inter-station ambiguities”) must be correctly resolved in order for the network to be useful as a tool for determining position. The amount of time required to resolve these ambiguities can vary from seconds to hours, and can adversely affect the ability of the network to support real-time operations.

### **1.3 Problem Statement, Objective, and Solution Approach**

In this dissertation, GPS data has been collected from three different carrier-phase networks:

- A linear 15-km network of 3 reference stations,
- An 80 by 100-km network having 5 reference stations, and
- A 100 by 100-km network with 13 reference stations.

In the first two networks, the relative positions of the network reference stations are unknown and must be determined from the observed data. The relative positions of the stations in the last network are obtained from prior surveys and are independent of the observed data set. The carrier-phase PDA concept is applied to each of these networks. Methods of resolving the network ambiguities are developed and presented. The

performance of the PDA is compared to that of the “nearest-station” network to show how the PDA concept improves positioning accuracy. A variety of PDA models having different mathematical orders are tested so as to determine which model provides the best set of information without overloading the data link. No attempt is made to apply the PDA concept to kinematic operations and all tests are evaluated against static reference points.

The objectives of this dissertation are:

1. Model the spatial and non-spatial DGPS errors for several carrier-phase networks using PDAs. The results from this model will show that spatial and non-spatial errors can be estimated and removed, thereby improving the accuracy of the DGPS solutions.
2. Identify the prediction error for several PDA models and form some conclusions regarding how the prediction error is affected by the design of the reference network. The design and geometry of the network will be shown to have a strong impact upon the selection of the PDA model.
3. Minimise the prediction error by selecting an appropriate PDA. Through this process, a PDA is found that provides that best match for the observed spatial and non-spatial errors and consequently provides that greatest improvement in positioning accuracy.
4. Minimise the dimension and order of the PDA to conserve data link bandwidth. The results will show that a 2 or 3 dimensional, 1<sup>st</sup> order PDA is usually adequate for small networks.
5. Show that networks surveyed with poor accuracy degrade the performance of NDGPS applications. This objective is met by exploring the performance of several networks having different levels of survey quality.

## 1.4 Document Organisation

A detailed description of GPS is given in Chapter 2. The code and carrier-phase measurements are introduced. The errors affecting the various GPS measurements are also discussed. Chapter 2 concludes with the development of GPS measurement error budgets.

The basic theory of DGPS is given in Chapter 3. The fundamental measurements and errors that are unique to differential measurements are developed. This chapter will show that double-difference measurements are required to solve the carrier-phase ambiguity problem. Finally differential error budgets are described in terms of spatial and non-spatial effects.

The use of DGPS networks (NDGPS) for determining the user's position is outlined in Chapter 4. In this chapter, the implementation of an NDGPS network is also described. Combined-station networks are shown to have the ability to remove some of the spatial and non-spatial errors observed by the network. It is also shown that real-time CP-DGPS networks depend upon the quick resolution of the inter-station ambiguities. Several methods of resolving these ambiguities are provided. The PDA is given as a class of solutions, each of which models the spatial and non-spatial errors. The advantages and disadvantages of different PDA solution models are also discussed.

In Chapter 5, the methods used to process CP-NDGPS data are described. SEMIKIN™ software is introduced as the primary mechanism for processing the raw information required in the PDA analysis. New PDA estimation software is developed and pre- and post-processing requirements are discussed.

Three sets of data are analysed in an effort to define the performance enhancements provided by a PDA carrier-phase network. These data sets are described in Chapter 6. They come from networks established in Alberta, New Mexico, and Southern California. The modelling techniques given in Chapter 4 are applied to the various networks. The PDA models are compared in order to determine the “best” model for each network. Finally, the measurement and positioning accuracy using CP-NDGPS is compared with the measurement and positioning accuracy obtained from standard single reference station techniques.

Chapter 7 is a summary that reiterates the issues and solutions discussed in this document. It highlights the requirements that are imposed when using carrier-phase networks and the advantages offered in terms of accuracy, coverage, and data link development. Logical steps for future research in the area of CP-NDGPS are part of the conclusions in Chapter 7.

## Chapter 2

### GPS FUNDAMENTALS

#### 2.1 Overview

In this chapter, the Global Positioning System is described in terms of the ground, space, and user segments. Receivers in the ground and user segments measure signals emitted by the satellites in the space segment. The measurements collected by GPS receivers are explained, and the errors that affect these measurements are discussed.

#### 2.2 Global Positioning System Overview

The concept for the GPS originated with the United States Department of Defense (DOD) in the early 1970s. Testing and development of the system took place during the 1980s and early 1990s [Parkinson, 1996a]. GPS is divided into ground, space, and user segments, see Figure 2-1. The space segment consists of 24 GPS satellites that broadcast a ranging signal, along with satellite orbit and satellite clock information to the user and ground segments. The transmission of the signal from the satellites to the user and ground segments is called the downlink signal. In the ground segment, monitoring stations send their observations of the GPS satellite constellation to a master control station (MCS) which determines the GPS orbit and clock errors. Orbit and clock information is then uplinked to the satellites through the ground antenna stations. Land, air, and marine users with GPS receivers can determine their position from the information broadcast by the satellites.

When GPS became operational in 1994, the DOD committed itself to sustaining a Standard Positioning Service (SPS) according the specifications outlined in the GPS Interface Control Document [Air Force, 1992]. In July of 1995, GPS reached Full

Operational Capability (FOC) and had 24 fully tested Block II satellites providing a Precise Positioning Service (PPS) to the military community [GPS World , 1995].

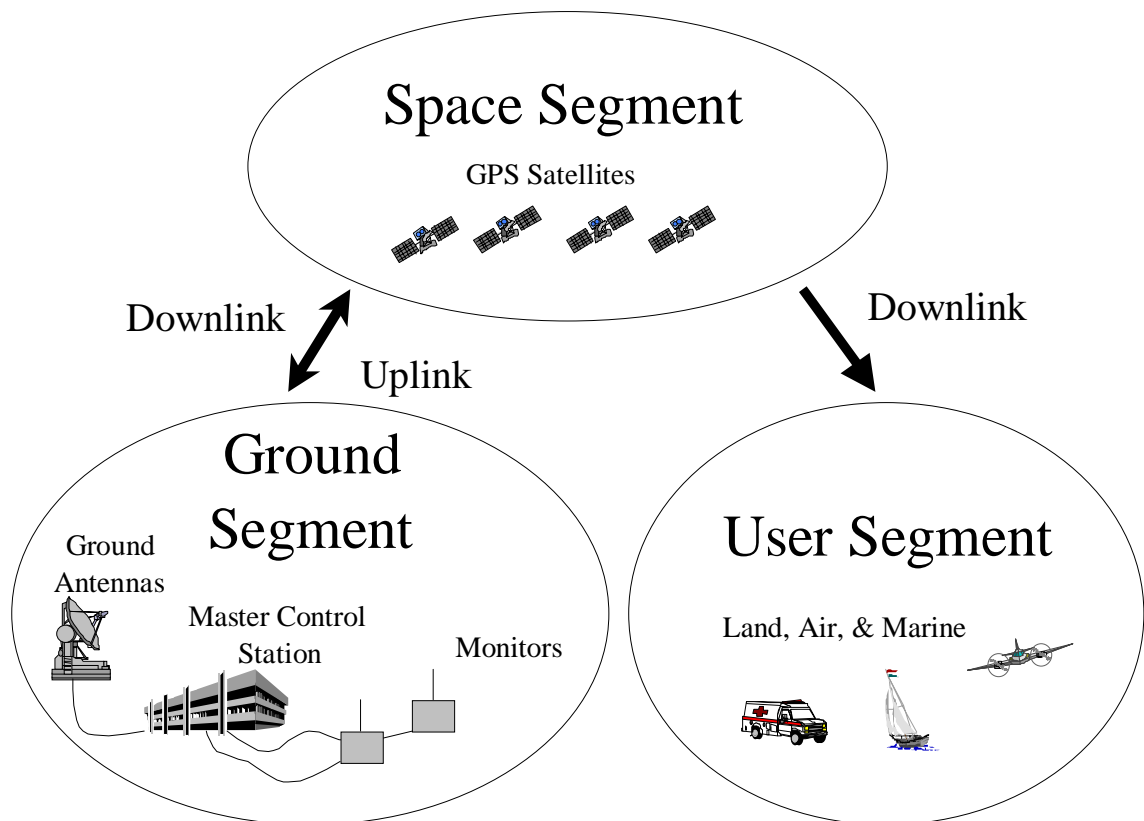


**Figure 2-1: The Global Positioning System**

GPS satellites and receivers operate on two frequencies called L1 (1575.42 MHz) and L2 (1227.6 MHz). Users who have access to the signals on both the L1 and L2 frequencies can remove signal distortions caused by the ionosphere. On the L1 frequency, the C/A-code is a signal that is transmitted “in the clear” and can be used by anyone owning a GPS receiver [Air Force, 1992]. The military “anti-spoofing” code (Y-code) is transmitted on both the L1 and L2 frequencies [Spilker, 1980]. It is a combination of two codes: An encryption (W) code and the P-code, which is known to all users of GPS. Only the users who are authorised by the United States DOD to have anti-spoofing protection

are given information about the W-code. Spoofing is a deliberate attempt to send false signals to users of the GPS. This protection is generally afforded to military groups that are allies with the United States. Since spoofing is generally considered to be an act of war, civilians who use GPS are not given anti-spoofing protection.

Military forces allied with the United States may obtain receivers that are capable of decrypting the Y-code signal and using it without performance loss. Some civilian receivers can strip the encryption sequence and use the underlying carrier and P-code signals. Civilian receivers having this capability are more expensive than single frequency receivers, and they have no protection against signal spoofing. Since they use the L1 signal to aid the tracking of L2, they do not provide independent positions on both frequencies. However, they are capable of measuring and eliminating ionospheric errors that corrupt the GPS signals.

The Vice President of the United States has announced that three frequencies will be made available for transmission of unencrypted GPS signals by the year 2006 [White House Press Release, 1998]. The additional frequencies protect against radio frequency interference (RFI) that can interrupt GPS navigation services on one or more frequencies. They improve the performance of civilian dual frequency receivers in their role of measuring ionospheric errors. They also allow the implementation of widelane networks, which provide some advantages for carrier-phase real-time kinematic (RTK) applications [MITRE, 1998].

### **2.3 Determination of Position and Time**

GPS works according to the theory of multilateration, whereby a user whose three-dimensional location is unknown, determines position by measuring the distance from multiple locations whose positions are known. In the present case, the positions of the

GPS satellites are known from the information provided in the downlink signals. A GPS receiver measures the time difference between the transmission of the signal at the satellite and the reception of the signal at the receiver. This time difference, when multiplied by the speed of light, is a measurement of the range to the satellite. Since the location of the GPS satellite is known, the receiver must be located on the surface of a sphere whose radius is equal to the measured range and whose centre is located at the satellite's position (Figure 2-2a). If the range to a second satellite is available, then the receiver's location is somewhere on a "circle of position" defined by the intersection of the two spheres (Figure 2-2b). By measuring the range to a third satellite, the receiver's position is one of two points defined by the intersection of the three "circles of position" (Figure 2-2c). One of these points is located above the plane containing the three satellites, while the other is on the Earth side of the plane (Figure 2-2d). The position that is on the Earth side is the correct position of the receiver. The other solution is a false mirror point.

Since range is derived from a time difference measurement, timing is a critical factor in the solution. Therefore, it is extremely important that all elements of the system maintain time synchronisation. The master control station in the ground segment synchronises the satellites using a time standard called GPS time. GPS Time is a derivative of Universal Time Coordinated (UTC), which is measured by the United States Naval Observatory using atomic time standards [Spilker, 1996a]. All satellites maintain synchronisation by using atomic clocks that are integrated into their payload. The GPS ground segment constantly monitors any deviations of the satellite clocks with respect to GPS time. These deviations are then relayed to the user segment through the uplink and downlink signals.

Synchronising the user's receiver to GPS time is accomplished as part of the solution for the user's position. When the receiver is turned on, it is not initially synchronised to GPS time. The difference between the receiver's time and GPS time is called the receiver clock offset ( $dT$ ). This offset causes the range measurements to be in error, but the error

is exactly the same for all satellite range measurements collected by the receiver. If the receiver records the range to four satellites simultaneously, the receiver's clock offset can be estimated along with the three unknown coordinates of position. Therefore, the basic GPS positioning problem implicitly involves the synchronisation of the receiver clock to GPS time, and is solved only if the receiver simultaneously observes four or more satellites.

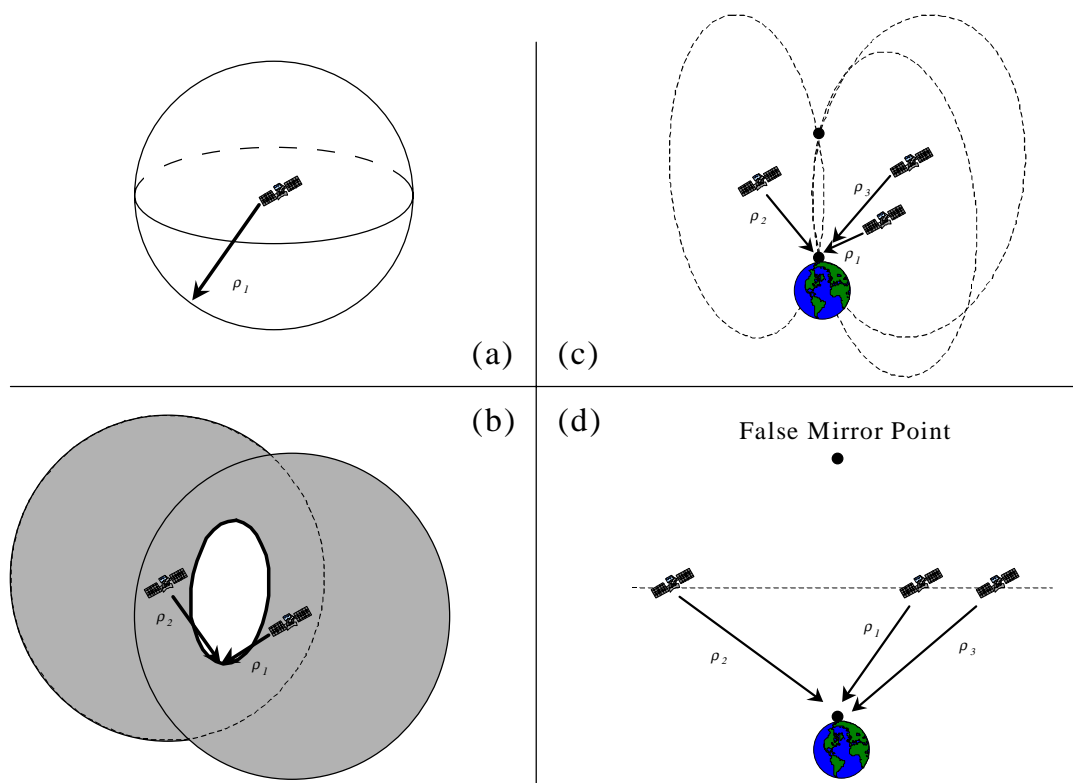


**Figure 2-2: (a) Sphere of Position; (b) Circle of Position; (c, d) Points of Position**

## 2.4 Measurements

The GPS signal is a composite signal that contains a high frequency carrier radio wave (L1 or L2), and a low frequency code (C/A, P, or Y) that is modulated onto the carrier.

There are several types of measurements that can be obtained from the code and carrier-phase components of the signals. The next few sections discuss the fundamental measurement types and the mathematical equations that model them.

### 2.4.1 Code-Phase Measurements

The most common GPS positioning solution available to the user is called the code-phase solution. As mentioned in Section 2.2, a predictable code is embedded in the GPS signal when it is transmitted from the satellite. The C/A-code, and the P(Y)-code are the two basic ranging codes that are modulated onto the carrier signal. The C/A-code has a frequency of 1.023 MHz, and the P(Y)-code frequency is 10.23 MHz. The W-code is a military encryption code that, when modulated with the P-code, forms the Y-code. The frequency of the W-code is not precisely known, but is estimated to be about 500 kHz [Leick 1995].

The user's receiver tracks the C/A and/or the P(Y) codes as part of its normal operation. In the tracking process, the receiver generates a replica of the code and synchronises it with the embedded code in the received signal. The time difference (delay) that synchronises the replica with the incoming signal is a measure of the signal travel time between the receiver and the satellite. This delay includes the receiver's clock offset as well as any timing offset that may exist in the satellite clock. When multiplied by the speed of light, the measured delay is converted to units of distance. This measurement is said to be in the range domain, and is called the code-phase measurement ( $p$ ).

Equation 2.1 is a mathematical model of the code-phase measurement. In this equation, the true range to the satellite ( $\rho$ ) is given in metres. The clock offset of the receiver ( $dT$ ) and satellite ( $dt$ ) have units of seconds. The code-phase measurement also includes the effects of satellite orbit error ( $do$ ), tropospheric delay ( $da$ ), ionospheric delay ( $di$ ), code-

phase multipath ( $dM$ ), and code-phase receiver noise ( $\varepsilon$ ). All of these latter effects are described in units of metres. The accepted value of the speed of light ( $c$ ) for use in GPS applications is  $2.99792458 \times 10^8$  m/s.

$$p = \rho + c(dt - dT) + do + da + di + dM + \varepsilon \quad (\text{m}). \quad (2.1)$$

### 2.4.2 Carrier-Phase Measurements

The frequency ( $f$ ) of the received carrier signal is measured in Hertz, and is slightly shifted from that of the primary carrier frequency (L1 or L2) because of the Doppler effect. The Doppler effect ( $\Delta f$ ) results from the existence of relative motion between the receiver and satellite. It is measured in Hertz and is directly related to the rate of change of the carrier signal delay ( $\dot{\tau}$ ) as expressed in Equation 2.2. The carrier signal delay ( $\tau$ ) is the number of seconds required for the signal to travel from the satellite to the receiver. The rate of change of signal delay is unitless.

$$\Delta f = f \cdot \dot{\tau} \quad (\text{Hz}). \quad (2.2)$$

The GPS receiver is capable of measuring the Doppler effect, and hence the rate of change of carrier delay. The rate of change of carrier delay is affected by many of the same items that affect the code-phase delay and is modelled by Equation 2.3. Note, that the effect of the ionosphere causes the carrier-phase to advance ( $-di$ ) [Klobuchar, 1996]. This is contrary to the effect on the code-phase in which ionospheric effect caused a signal delay ( $+di$ ). The interested reader is referred to Klobuchar [1996], Leick [1995], and Hoffman-Wellenhof et al. [1994] for more information about the physical effects of the ionosphere on code and carrier-phase signals.

$$\dot{\tau} = \frac{1}{c} \cdot \frac{d}{dt} \{ \rho + c \cdot (dt - dT) + do + da - di \} \quad (\text{s/s or unitless}). \quad (2.3)$$

Multipath effects and frequency tracking noise are included in the model only if the receiver is tracking the signal frequency. This is the case for receivers that use a frequency lock loop (FLL) to track the incoming carrier signal, but many receivers perform normal signal tracking using a phase lock loop (PLL). A PLL tracks the phase or the integral of the Doppler. The units for phase are in cycles of wavelength. Using Equations 2.2 and 2.3, the mathematical model for this integral is given by Equation 2.4. In Equation 2.4, “ $N$ ” is measured in cycles and represents a constant of integration called the “ambiguity”.

$$\int \Delta f \, dt = \int f \cdot \dot{\tau} \, dt = \frac{f}{c} \cdot \{ \rho + c \cdot (dt - dT) + do + da - di \} + N \quad (\text{cycles}). \quad (2.4)$$

If the tracking function is performed using a PLL, the receiver noise ( $\eta$ ) is in the phase domain (i.e. measured in cycles) rather than in the frequency domain (hertz). Most authors describe the effects of multipath ( $dm$ ) as being limited to one quarter of a cycle [Braasch, 1996; Leick, 1995]. For this reason, the multipath affecting a PLL is assumed to be a distortion of the signal in the phase domain, rather than the integration of a frequency distortion. A mathematical model of the PLL’s output (Equation 2.5) combines the effects of Equation 2.4 with phase noise and multipath tracking errors. Equation 2.5 is called the “carrier-phase measurement” ( $\phi$ ).

$$\phi = \frac{1}{\lambda} \cdot \{ \rho + c \cdot (dt - dT) + do + da - di \} + N + dm + \eta \quad (\text{cycles}). \quad (2.5)$$

Where:  $\lambda = c/f = \text{Carrier-Phase Wavelength} \quad (\text{m/cycle}).$

The units for the carrier-phase measurement are cycles of wavelength. In order to get the equivalent measurement in range domain units, the carrier-phase measurement must be multiplied by the carrier-phase wavelength ( $\lambda$ ). For L1, the carrier-phase wavelength is about 19 centimetres per cycle. For L2, it is approximately 24 centimetres per cycle.

In the carrier-phase measurement, the ambiguity is unknown because the receiver does not have complete knowledge of the signal's initial conditions at the time that the PLL begins tracking the incoming signal. Even though the ambiguity is unknown, it is not completely arbitrary; the ambiguity is an integer. To prove this, the above condition is stated mathematically according to Equation 2.6. The right-hand side of Equation 2.6 represents the fractional phase of the actual signal being tracked by the receiver's PLL. Note that the actual signal does not have an ambiguity because the ambiguity is a function of the PLL integration process, not the physical radio signal. The left-hand side of the Equation 2.6 is the fractional phase of the carrier-phase measurement, and is the output the PLL<sup>1</sup>.

$$MOD(\phi) = MOD\left(\frac{1}{\lambda}(\rho + c \cdot \{dt - dT\} + do + da - di) + m + \eta\right). \quad (2.6)$$

Equation 2.5 is then substituted into Equation 2.6 to show that the ambiguity must be an integer:

$$\begin{aligned} MOD\left(\frac{1}{\lambda}(\rho + c \cdot \{dt - dT\} + do + da - di) + N + m + \eta\right) &= \\ MOD\left(\frac{1}{\lambda}(\rho + c \cdot \{dt - dT\} + do + da - di) + m + \eta\right) & \\ MOD(N) = MOD(0) = 0. & \\ \therefore N = \text{Integer} \quad (\text{cycles}). & \end{aligned} \quad (2.7)$$

---

<sup>1</sup> Whole cycle values of the phase are stored in an accumulation register and removed from the PLL during the tracking process.

### 2.4.2.1 Widelane

A dual frequency GPS receiver can track the carrier-phase on both the L1 and the L2 frequencies. By subtracting the carrier-phase measurement of L2 from that of L1, a new carrier-phase measurement called the “widelane” is created (Equation 2.8). The frequency of the widelane measurement is 347.82 MHz, and its wavelength is 86 cm.

$$\phi_{WL} = \phi_{L1} - \phi_{L2} \quad (\text{cycles}). \quad (2.8)$$

The mathematical model for the widelane is identical to that of Equation 2.5, and the widelane ambiguity is formed from an integer combination of the L1 and L2 carrier-phase ambiguities. Since the L1 and L2 ambiguities are both integers, the widelane ambiguity is also an integer. The widelane ambiguity is often easier to estimate and/or resolve because its wavelength is 3.5 and 4.5 times larger than the L2 and L1 wavelengths.

### 2.4.2.2 Ionospheric Free Measurement

Another linear combination of the L1 and L2 carrier-phase measurements is important as a method of removing the ionospheric error. The ionosphere is a dispersive electromagnetic medium in which the magnitude of the ionospheric effect depends upon the frequency of the radio signal that is passing through the medium [Klobuchar, 1996]. When two carrier-phase signals are transmitted using different frequencies, there exists a linear combination of those signals that is free of ionospheric effects. For the GPS L1 and L2 carrier-phase measurements, one possible method of generating an ionospheric free measurement is given by Equation 2.9 [Leick, 1995]. This measurement can be

modelled according to Equation 2.10. Notice the absence of the ionospheric error term in this equation.

$$\phi_{IF} = \frac{1}{f_{L1}^2 - f_{L2}^2} \{ f_{L1}^2 \cdot \phi_{L1} - f_{L1} f_{L2} \cdot \phi_{L2} \} = 2.546 \cdot \phi_{L1} - 1.984 \cdot \phi_{L2}. \quad (2.9)$$

$$= \frac{1}{\lambda_{IF}} \{ \rho + c \cdot (dt - dT) + do + da \} + N_{IF} + dm_{IF} + \eta_{IF}. \quad (2.10)$$

The wavelength ( $\lambda_{IF}$ ) of this measurement is the same as that of  $\phi_{L1}$ . Unfortunately, since  $\phi_{IF}$  is not an integer combination of  $\phi_{L1}$  and  $\phi_{L2}$ , the ionospheric free ambiguity ( $N_{IF}$ ) is not an integer. Since  $N_{IF}$  is not an integer,  $\phi_{IF}$  can be scaled to have any frequency or wavelength desired.

### 2.4.2.3 Narrowlane

The “narrowlane” is another dual frequency measurement that is created by adding the L1 and L2 carrier-phase measurements (Equation 2.11). This measurement has a wavelength of 11 cm. The widelane and the narrowlane measurements have the same level of phase noise when measured in cycles. But when the phase noise is converted into the range domain using the measurement wavelength, the narrowlane range error is nearly 8 times smaller than its widelane counterpart. While the narrowlane measurement is capable of reducing noise in the range domain, the wavelength is short and ambiguities are difficult to resolve. Wübbena [1987] has discussed some uses for the narrowlane measurement.

The narrowlane can be modelled according to Equation 2.5 by substituting the 11-cm wavelength. Even though the ambiguity for the narrowlane is an integer, it is difficult to resolve because of the short wavelength.

$$\phi_{NL} = \phi_{L1} + \phi_{L2} \quad (\text{cycles}). \quad (2.11)$$

## 2.5 System Errors and Biases

The accuracy of the position obtained from GPS depends upon the accuracy of the range measurements and the location of the satellites with respect to the user (satellite geometry). The range measurements differ from the true range in that they incorporate a variety of errors (Figure 2-3). These errors were briefly mentioned when the measurement types were introduced. In this section, the causes and magnitudes of these errors are investigated.

### 2.5.1 Selective Availability (SA)

Since March of 1990, the DOD has implemented SA [Van Grass and Braasch, 1996]. Under this policy, the satellite clock and ephemeris information is deliberately corrupted in order to limit the accuracy of the position derived by non-military users. When SA is in effect, civilian users of GPS can expect their position errors to have a SEP of 72 metres [Parkinson, 1996a]. This translates into a 1 sigma ranging error of 23 metres, and allows users to determine their horizontal position with an accuracy of 100 metres 95% of the time [DOD/DOT, 1997].

In a recent Presidential Decision Directive (PDD), the President of the United States has declared that SA will be turned off by 2006 [PDD, 1998]. Until this occurs, SA will be the dominant error affecting GPS range measurements.

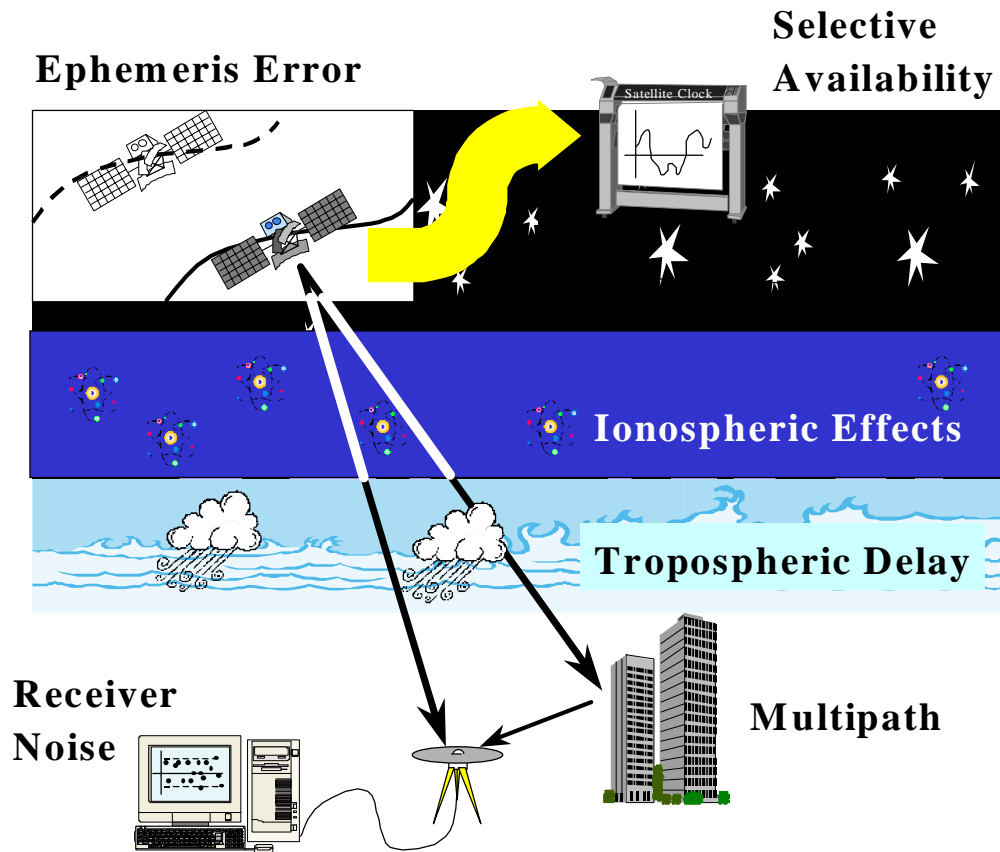


**Figure 2-3: GPS Error Sources**

### 2.5.2 Ephemeris and Clock Errors

Even without SA, errors in the satellite's orbit ( $do$ ) and clock ( $dt$ ) exist. The predicted orbital ephemeris is broadcast by the satellites and has an specified accuracy of 8 metres 95% of the time for authorised PPS users [GPS JPO, 1991]. Experience has shown that the broadcast ephemerides have a 1 sigma accuracy of about 2 metres [Zumberge and Bertiger, 1996], but SPS users must remember that 20 or 30 metre errors could be applied to the satellite ephemerides as part of the SA policy.

The U.S. National Geodetic Survey, the U.S. Naval Surface Weapons Center, Natural Resources Canada, Jet Propulsion Laboratory (JPL), the University of Berne, and the University of Texas all provide precise ephemerides. Natural Resources Canada, and JPL have estimated the accuracy of their precise ephemerides to between 10 and 20 cm [Skone et al., 1996; Zumberge and Bertiger, 1996]. Precise ephemerides require as much as 30 hours to generate, and are primarily used for post mission analysis. Some organizations are suggesting that predicted precise ephemerides can be used for real time operations [Yunck et al., 1996; Skone et al., 1996]. Predicted precise ephemerides are not commonly available, but an orbital accuracy of 20 to 80 cm (1 sigma) is considered achievable.

The International Terrestrial Reference Frame 1994 (ITRF94) has been used by the International GPS Service for Geodynamics (IGS) since 1996 [Boucher and Altamimi, 1996]. The ITRF is the primary reference frame for precise ephemerides. The broadcast ephemerides are given with respect to the World Geodetic System 1984 Version G873 (WGS-84) coordinate frame [Malys et al., 1997]. Without coordinate conversion, the ITRF and WGS-84 agree to within 10 cm.

Even though the satellite clock is an atomic standard and is stable, it is a free running clock and is not perfectly synchronised with GPS time as measured on the ground. If left uncorrected, the satellite clock may differ from GPS time by a millisecond or more [Spilker, 1996]. Clock errors of this magnitude can cause ranging errors of at least 300,000 m. Corrections for the satellite clock errors are computed by the GPS ground segment, uplinked to the satellites, and broadcast to the user segment as part of the downlink. If the corrections are applied by the user, the standard deviation of the satellite clock error is reduced to 11 ns [Zumberge and Bertiger, 1996]. A timing error of this magnitude has an equivalent ranging error of about 3 metres.

### 2.5.3 Atmospheric Errors

Atmospheric errors are separated into two classes: ionospheric effects ( $di$ ), and tropospheric delay ( $da$ ). The ionosphere is a region of the atmosphere between 70 and 1000 km above the surface of the Earth. Tropospheric delay is not frequency dependent, and occurs as the signal passes through the lower atmosphere between the surface and 50 km.

#### 2.5.3.1 Ionosphere

Interaction of the GPS signal with atomic ions in the ionosphere causes a delay in the code-phase range measurements collected by the receiver. It also advances the phase of the received carrier signal [Klobuchar, 1996]. The magnitude of the ionospheric effect depends upon the time of day and the level of solar activity. During periods of high solar activity, the daytime vertical ionospheric range error (1 sigma) may vary between 5 and 10 metres with maximums being recorded at about the 20 metre level [Klobuchar et al., 1995]. For satellites that are not directly above the user, the signal path does not travel vertically through the ionosphere. Klobuchar [1996] has shown that the resulting slant delays may be as great as a 100 m. During periods of low solar activity, the vertical ranging error is lower by a factor of about 3 (i.e. 1 to 3 metres typical).

Rapid variations of the ionospheric error – called “scintillation” – can occur at auroral and equatorial latitudes [Klobuchar, 1996]. These variations may cause the GPS receiver to stop tracking the signal. At equatorial latitudes, scintillation is most prevalent after sunset during periods of high solar activity. In the auroral regions however, it can occur at almost any time.

The sun's solar activity level follows an 11-year cycle and is characterised by an increase in the number of sunspots, solar flares, and ion discharge events called solar storms. Maximum solar activity has been recorded in the years of 1980 and 1990. Future solar maximums are expected to occur in the year 2001 and 2012. During years of maximum solar activity, 20 to 30 solar storms may be recorded [Klobuchar 1996].

Ionospheric models are available for predicting ionospheric errors. Simple algorithmic models have been developed and are recommended by the GPS interface control document [Air Force, 1992]. These models remove about 50% of the ionospheric error, but provide little or no protection against scintillation. More sophisticated network/grid models have been recommended by the Federal Aviation Administration for use with GPS-based aircraft navigation systems [El-Arini et al., 1995]. These models have been shown to reduce the ionospheric error by a factor of 6. Network/grid models provide an excellent method of reducing the effects of ionosphere; but at auroral latitudes, even these models have been shown to have degraded performance [Skone and Cannon, 1998].

Equation 2.12 is a mathematical representation of the ionospheric error affecting the measurements. The frequency ( $f$ ) is measured in Hertz. The error is an advance for the carrier-phase and a delay for the code-phase measurements. The ionospheric error depends upon the Total Electron Content (TEC) that exists along the path between the satellite and the receiver. The TEC is a function of the satellite elevation, the solar activity level, the time of day, and the magnetic latitude from which the user is operating. For satellites that are directly above the receiver (elevation =  $90^\circ$ ), the value of TEC is typically between  $10^{16}$  and  $10^{18}$  electrons per metre<sup>2</sup>.

$$di = \frac{40.3}{c \cdot f^2} \cdot TEC \quad (\text{m}). \quad (2.12)$$

Equation 2.12 shows that the range error is dependent upon the square of the GPS signal frequency. The lower the frequency, the greater is the error. For example, this equation can be used to show that the error on the L2 signal is 1.65 times larger than it is on the L1 signal.

$$\frac{di_{L2}}{di_{L1}} = \frac{f_{L1}^2}{f_{L2}^2} = \left( \frac{1575.42 \text{ MHz}}{1227.6 \text{ MHz}} \right)^2 = 1.647. \quad (2.13)$$

The ionospheric effect on a derived measurement can be determined by breaking the measurement into its L1 and L2 range components. For example, the widelane range is related to the L1 and L2 ranges as follows:

$$\begin{aligned} \text{Widelane Phase Range } (r_{WL}) &= \lambda_{WL} \phi_{WL} = \lambda_{WL} (\phi_{L1} - \phi_{L2}) \\ &= \frac{c}{f_{WL}} \left( \frac{1}{\lambda_{L1}} \lambda_{L1} \phi_{L1} - \frac{1}{\lambda_{L2}} \lambda_{L2} \phi_{L2} \right) = \frac{c}{f_{WL}} \left( \frac{f_{L1}}{c} r_{L1} - \frac{f_{L2}}{c} r_{L2} \right). \end{aligned}$$

Therefore, the ionosphere error has a similar relationship:

$$\begin{aligned} \therefore di_{WL} &= \frac{c}{f_{WL}} \left( \frac{f_{L1}}{c} di_{L1} - \frac{f_{L2}}{c} di_{L2} \right), \\ &= \frac{f_{L1} di_{L1} - f_{L2} di_{L2}}{f_{WL}} = \frac{f_{L1} di_{L1} - 1.647 \cdot f_{L2} di_{L1}}{f_{WL}}, \\ \frac{di_{WL}}{di_{L1}} &= \frac{f_{L1} - 1.647 \cdot f_{L2}}{f_{WL}} = \frac{1575.42 - 1.647 \cdot 1227.6}{347.82} = -1.284. \end{aligned} \quad (2.14)$$

Using the same analysis, it is possible to show that:

$$\frac{di_{NL}}{di_{L1}} = -10.34. \quad (2.15)$$

$$\frac{di_{IF}}{di_{L1}} = 0.000. \quad (2.16)$$

### 2.5.3.2 Troposphere

Tropospheric delay occurs as a result of the GPS signal's passage through the Earth's lower atmosphere. By formal definition, the troposphere is that portion of the Earth's atmosphere that lies below the tropopause (usually within 10 km of the Earth's surface). The stratosphere is also considered part of the lower atmosphere. It extends upward from the tropopause to an altitude of approximately 50 kilometres. In these two sections of the atmosphere, electromagnetic refraction slows the GPS radio signal causing a delay in its arrival at the receiver. The refractive index of the wet atmosphere is different from that of the dry atmosphere. The combined delay caused by both the wet and the dry atmosphere is called tropospheric delay. In the range domain, the tropospheric delay is the same regardless of the measurement frequency, and cannot be removed by forming linear combinations of the L1 and L2 measurements.

The dry atmospheric delay can cause a range error of as much as 2 to 3 metres. However, the effects of the dry atmospheric delay can be accurately predicted using surface pressure and temperature measurements. Since the dry component is 90 percent of the total tropospheric error, a large portion of the tropospheric error is removed from the range measurements by using a tropospheric model. According to Mendez and Langley [1994], a user who employs a tropospheric model for predicting the delay can expect the residual tropospheric error to be less than 30 centimetres. The residual delay is caused mostly by the signal passing through the "wet atmosphere" (i.e. clouds and areas of high humidity).

As a result, the rate of change of this delay depends largely upon the form and motion of the cloud layers in the lower atmosphere.

## **2.5.4 Receiver Technologies, Noise, and Multipath**

Receivers today are designed to tackle many problems. For example, dual frequency receivers are useful for removing the effects of the ionosphere. Some receivers use correlation processing techniques to reduce the chances of receiving reflected GPS signals (multipath). In this section, several of these technologies are discussed.

### **2.5.4.1 Dual Frequency Technologies**

Civilian dual frequency receivers are classified according to the processing technology that they use to remove the W-code encryption sequence. There are four classifications [Leick, 1995]: Squaring, Code-Aided Squaring, Cross-Correlation, and Z-Tracking.

#### **Squaring:**

The squaring process squares the received L2 signal and strips all code modulation from the signal. This severely degrades the signal's strength. After the signal is free of code modulation, the receiver is able to track the L2 carrier. Ionospheric changes can be measured, and L2 ranges along with the absolute ionospheric error can be derived once the carrier-phase ambiguities have been estimated. Squaring reduces the carrier wavelength by half, which doubles the noise level in the signals. The result of stripping the code and doubling the noise causes the signal to noise ratio to be 30 to 40-dB less than that which is expected when using full Y-code correlation [Leick, 1995; Van Dierendonck, 1995].

#### Cross-Correlation:

The Y-code signal is the same on both the L1 and L2 frequencies. The cross correlation process takes the received Y-code signal on L1 and correlates it with the arriving signal on L2. This means that the receiver can track the time of arrival difference between the L1 and L2 signals without solving for carrier-phase ambiguities. To track the L2 signal, the Y-code is stripped using Y-code that was received on L1. Stripping the Y-code degrades the signal strength. The noise level is not increased because the signal is not squared. Therefore, the carrier-phase measurement is of full wavelength and the signal-to-noise ratio is 3 dB greater than that which is possible from “squaring” (i.e. 27 dB below the signal-to-noise ratio for full correlation of the L2 Y-code). If the C/A code measurement is tracked on L1, then adding the time of arrival difference to the L1 code measurement derives the L2 code measurement. For this case, the L2 measurement is not an independent measure of the distance to the satellite, where as the fully correlated L2 Y-code is an independent measurement for positioning purposes.

#### Code-Aided Squaring:

In code-aided squaring the receiver correlates the received Y-code signal with a replica of the P-code. This allows the receiver to track the P-code portion of the Y-code and provide code measurements. By correlating with the P-code, the bandwidth of the received signal can be reduced from 10 MHz to about 500 kHz (the bandwidth of the W-code). This increases the signal strength by 13 dB. The reduced signal is then squared to strip the W-code and the receiver tracks the half-wavelength carrier. The result is that code-aided squaring provides a signal to noise ratio that is 13 dB greater than that of “squaring”. It also provides a code measurement for

L2. The performance is, however, still 17 dB below that which is achievable with full Y-code correlation.

#### Z-Tracking:

Z-Tracking combines the concepts of code-aiding and cross-correlation, whereby the received signals on L1 and L2 are correlated with the P-code to provide code-phase measurements on both frequencies. Removing the P-code reduces the bandwidths of the two signals – increasing signal strength by 13 dB. After which, the reduced L1 signal is cross-correlated with the L2 signal in order to track the full wavelength L2 carrier. Since squaring is avoided, the noise level is reduced by an additional 3 dB. Therefore, the signal to noise ratio of the Z-Tracking process is 16 dB better than the “squaring” technique (14 dB weaker than the full correlation of the Y-code). L2 code measurements can be derived from L1 C/A code measurements according to the method described for cross-correlation. These measurements are not independent measures of distance.

The above discussion highlights the fact that there is a significant advantage to be gained from having the ability to fully correlate signals on multiple frequencies. Civilian receivers cannot operate in a dynamic environment on the L2 frequency alone. While L1 code-aiding of the L2 signal allows a civilian dual frequency receiver to estimate the ionospheric effects, redundant navigation using the separate L1 and L2 frequencies is not possible in most dynamic environments. If unencrypted signals are provided on additional frequencies, civilian dual frequency receivers would be able to navigate in a dynamic environment using each frequency independently. This can be of great benefit in situations where RFI causes one of the signals to become unusable.

#### 2.5.4.2 Noise

The measurements taken by a GPS receiver have thermal noise errors resulting from the fact that the receiver cannot track the incoming signal with exact precision. The tracking error is random, and is assumed to have a Gaussian distribution. The magnitude of the noise is a function of the measurement type and the signal strength. The C/A-code measurement can be tracked with a typical accuracy of 1.5 metres [Leva et al., 1996], but it may vary between 0.2 and 3 metres depending upon the strength of the received signal [Parkinson and Enge, 1996; Van Dierendonck, 1992; Van Dierendonck, 1996]. The typical receiver noise for Y-code measurements is 10 to 30 cm. The P-code noise is the same as the Y-code because the two codes have the same fundamental frequency.

At normal signal levels, the receiver noise of the carrier-phase measurement is about 1% of a carrier-phase wavelength [Martin, 1980]. This error may vary between 10% and 0.1% depending upon the type of receiver and the power of the signal being tracked [Van Dierendonck, 1996]. Geodetic receivers tracking strong signals can have L1 frequency noise that is equivalent to 0.2 mm [Langley, 1997].

Since both the L1 and L2 carrier-phase measurements are required to derive the widelane, the tracking noise error for the widelane is larger than for the L1 or L2 carrier measurements individually. The widelane noise (measured in cycles) is the RSS of L1 and L2 noise (measured in cycles).

The widelane noise error in cycles is scaled by the widelane wavelength to determine the noise error in range units. Since the wavelength of the widelane cycle is 4.5 times greater than the L1 wavelength, the range error caused by tracking noise is significantly larger for the widelane than it is for L1. The statistical relationship between the tracking noise on the widelane and the L1 frequencies is given by Equation 2.17. This equation shows that, if the tracking noise on L2 is 25% greater than that of L1, the widelane tracking error is

7.2 times greater than the L1 tracking error. By example, if the L1 and L2 noise are assumed to be 2 mm and 2.5 mm respectively, Equation 2.17 indicates that the widelane noise level is about 14 mm (1.4 cm).

$$\varepsilon_{WL} = \lambda_{WL} \sigma_{WL} = \lambda_{WL} \sqrt{\sigma_{\eta_{L1}}^2 + \sigma_{\eta_{L2}}^2} \approx \sqrt{2.56} \lambda_{WL} \sigma_{\eta_{L1}} = 7.2 * \lambda_{L1} \sigma_{\eta_{L1}} \quad (2.17)$$

### 2.5.4.3 Multipath

The normal GPS position solution assumes that the signal travels directly from the satellite to the receiver. Unfortunately, the signal can be reflected by a variety of materials, including metal and water. When a reflected signal arrives at the receiver's antenna, it combines with, or distorts, the direct signal. The range error that results from this distortion is called multipath. The frequency and magnitude of multipath depends greatly upon the environment surrounding the GPS receiver antenna. In static applications, multipath errors can persist for extended periods of time because the satellite geometry changes slowly with respect to the antenna. The magnitude and number of occurrences of multipath can be reduced if care is taken to properly site the receiver's antenna. Using an antenna that is insensitive to low-elevation signals can also provide some multipath protection. In kinematic applications, the environment surrounding the antenna is continuously changing. Even though the environment is more difficult to control, the time constant over which the multipath errors are correlated is much shorter than for static applications. In fact, the error often changes so rapidly that it is said to be "randomized", and modelled as uncorrelated noise.

Braasch [1996] has shown that multipath can cause a delay in the C/A code-phase measurement of as much as 120 metres. Employing multipath mitigation technologies in the receiver's code correlator can significantly reduce the multipath affecting C/A code-

phase measurements. Examples of these multipath mitigation technologies include Narrow Correlator™ [Van Dierendonck et al., 1992], Strobe Correlator [Garin et al., 1996], and the Multipath Estimation Technology™ correlator [Townsend et al., 1995]. If care has been taken to reduce the potential for multipath and appropriate receiver technologies are used, a typical level for the code-phase multipath error is 1 to 2 metres [Parkinson and Enge, 1996]. This same level of performance is expected from receivers using P/Y-code correlation [Braasch, 1996].

Carrier-phase multipath is much more difficult to mitigate than code-phase multipath. Ray, Cannon, and Fenton [1998] are currently studying methods of using multiple closely spaced antennas to reduce the effects. Carrier-phase multipath is limited to one quarter of the carrier-phase wavelength [Leick, 1995]. For L1, this means that the maximum carrier-phase multipath is about 5 centimetres.

## **2.6 GPS Range Error Budgets**

Based upon the discussions in this Chapter, a summary of the errors that affect the GPS signals is provided in Tables 2-1, 2-2, and 2-3. Errors that are common to all measurement types are listed in Table 2-1. Errors whose magnitude depends upon the measurement type are given in Tables 2-2, and 2-3. Table 2-2 shows the magnitudes of code-phase errors, while Table 2-3 gives the magnitudes of carrier-phase errors.

From the above descriptions of receiver noise and multipath, it is obvious that the carrier-phase measurement has significantly lower errors than the code-phase measurement. If the other sources of error can be controlled, there is a natural desire by the users to take advantage of the carrier-phase measurement accuracy.

**Table 2-1: GPS Range Error Budget  
(Errors Common to All Measurements)**

Parameter	1 Sigma Error (metres)
Selective Availability	23.0
Ephemeris	2.0 to 23 <sup>†</sup>
Satellite Clock	3.0
Troposphere (Modelled / Unmodelled)	0.3 / 2.0 – 3.0

**Table 2-2: GPS Code-Phase Measurement Error Budget**

Parameter	1 Sigma Range Error (metres)		
	L1 C/A	L1-P/Y	L2-P/Y
Ionosphere	1.0 to 30	1.0 to 30	1.7 to 50
Multipath <sup>††</sup>	1.0 to 2.0	1.0 to 2.0	1.0 to 2.0
Receiver Noise	0.2 to 1.0	0.3 to 0.7	0.3 to 0.7

**Table 2-3: GPS Carrier-Phase Measurement Error Budget**

Parameter	1 Sigma Range Error (metres)				
	L1	L2	L1-L2	$\phi_{IF}$	L1+L2
Ionosphere	1.0 to 30	1.7 to 50	1.3 to 40	0.0	10 to 300
Multipath <sup>†††</sup>	0.020	0.030	0.10	0.020	0.010
Receiver Noise	0.002	0.0025	0.013	0.007	0.013

<sup>†</sup> Ephemeris SA is rare – 2 metre errors are considered typical.

<sup>††</sup> Assumes the use of Narrow Correlator™ or equivalent technology.

<sup>†††</sup> Assumes the normal level of multipath is equal to 0.4 times one-quarter wavelength.

## Chapter 3

### CARRIER-PHASE DIFFERENTIAL GPS

#### 3.1 Overview

In this chapter, the concept of DGPS is introduced. While the stand-alone code-phase GPS position solution can be smoothed using the carrier-phase measurements, the carrier-phase measurements on their own are not suitable for the purposes of determining stand-alone positions. In DGPS, however, the carrier-phase measurements can be used without code-phase measurements to derive extremely accurate position solutions. This chapter focuses exclusively on the sole use of carrier-phase measurements in the DGPS positioning process. The theory behind DGPS involves the derivation of two new classes of measurements called single-difference and double-difference measurements. These measurements can be derived for any of the undifferenced measurement types described in Table 2-3. The ranging accuracy obtained when using single and double-difference measurements is considerably better than that of undifferenced measurements because errors that are spatially correlated are removed. This chapter will show how and why the improved ranging accuracy allows DGPS to provide better positioning performance.

#### 3.2 Differential GPS

DGPS has been developed in order to reduce or eliminate the effects of SA, orbital error, ionosphere, and troposphere. In DGPS, the position of the user is calculated with respect to a reference point rather than with respect to the absolute GPS coordinate frame. The reference point is surveyed and its location is specified in GPS coordinates ( $\mathbf{X}_{R_{True}}$ ). A static GPS receiver is set up at the reference point and is called the “reference receiver”.

DGPS operates on the theory that the range measurement errors are nearly the same (correlated) at both the reference and the user locations. The amount of correlation will be investigated later in this Chapter. First it is important to describe the concept by which DGPS is implemented.

Solving the GPS problem using differential measurements results in the user's position being defined as a relative vector with respect to the reference point. If the user's absolute position is desired, the estimated relative position ( $\Delta\mathbf{X}$ ) is added to the GPS coordinates of the reference receiver as shown in Equation 3.1.

$$\mathbf{X}_{\Delta} = \mathbf{X}_{R_{True}} + \Delta\mathbf{X}. \quad (3.1)$$

Where:  $\mathbf{X}_{\Delta}$  = Absolute Position Using Relative Positioning.

DGPS can also be implemented using corrected positioning instead of relative positioning. In corrected positioning, the estimated position of the reference station ( $\mathbf{X}_R$ ) is subtracted from the station's true position to derive a position correction (Equation 3.2).

$$\text{Position Correction } (\delta\mathbf{X}) = \mathbf{X}_{R_{True}} - \mathbf{X}_R. \quad (3.2)$$

The user's corrected position ( $\mathbf{X}_C$ ) is then computed by adding the position correction to the user's estimated position ( $\mathbf{X}$ ) as given by Equation 3.3.

$$\mathbf{X}_C = \mathbf{X} + \delta\mathbf{X}. \quad (3.3)$$

The user's estimated position is output by the user's receiver, but it can also be computed by adding the user's relative position to the reference station's estimated position (Equation 3.4).

$$\mathbf{X} = \mathbf{X}_R + \Delta\mathbf{X}. \quad (3.4)$$

Substituting Equation 3.4 and 3.2 into Equation 3.3 shows that “corrected positioning” and “relative positioning” are mathematically equivalent concepts (Equation 3.5).

$$\begin{aligned} \mathbf{X}_C &= \mathbf{X}_R + \Delta\mathbf{X} + \mathbf{X}_{R_{True}} - \mathbf{X}_R. \\ &= \mathbf{X}_{R_{True}} + \Delta\mathbf{X}. \\ \therefore \mathbf{X}_C &= \mathbf{X}_\Delta. \end{aligned} \quad (3.5)$$

Corrected and relative DGPS concepts are not usually implemented in the position domain, as indicated above. These concepts are actually implemented in the measurement domain. As a result, the observed satellite code (or carrier-phase) measurements recorded the reference station are sent to the user to form differential measurements. These differential measurements are used to generate the relative position ( $\Delta\mathbf{X}$ ). Alternatively, measurement corrections are generated at the reference station by subtracting the observed measurements from measurement predictions that are based upon the reference station’s true position. The measurement corrections are then transmitted and applied to the user’s observed measurements before a corrected position ( $\mathbf{X}_C$ ) is generated.

The Radio Technical Commission for Maritime Services (RTCM) has developed a method of transmitting differential and corrected measurements from the reference station [RTCM 104, 1994]. Taveira-Blomenhofer and Hein [1993] have described how to use carrier-phase corrections in to generate carrier-phase DGPS solutions for the user’s position.

In terms of its digital representation, measurement corrections are physically smaller than the reference station’s observed measurements. This means that it is more efficient to transmit corrections (as opposed to the observed measurements) through a digital data

link. Even though data link applications can realise a greater information throughput when using measurement corrections, it is more natural to use the differential measurements when the data is being post-processed and the data link is not a factor. Data links were not used for any of the analysis within this dissertation. Therefore, all of the results presented herein are based upon the use of differential carrier-phase measurements (relative positioning).

DGPS introduces two significant complications to the GPS concept:

- 1) The reference receiver measurements must be provided to the user. Since the user is normally in transit, a physical line data link is generally not desirable. For post-processing analysis, the best method for bringing the two sets of data together is to collect and store the data at each location. The stored data is then transferred to a common location where the analysis is to be performed. In real-time operations, a radio data link is normally used.
- 2) Inaccuracies in the reference receiver's absolute location cause a one-for-one error in the computed location of user. These inaccuracies can also distort the relative solution.

The set-up for a generic DGPS application is shown in Figure 3-1. For relative positioning, the user's receiver subtracts the reference station measurement ( $\phi_R$ ) from its own measurement ( $\phi_U$ ), and forms a new measurement called the single-difference measurement ( $\Delta\phi_{UR}$ ). In this figure, the reference station measurement is sent to the user through a radio data link.

In DGPS, the satellite clock offset – which includes SA – is almost fully correlated (identical) between the user and reference receivers. As a result, the satellite clock offset and SA are eliminated in the single-difference measurement.

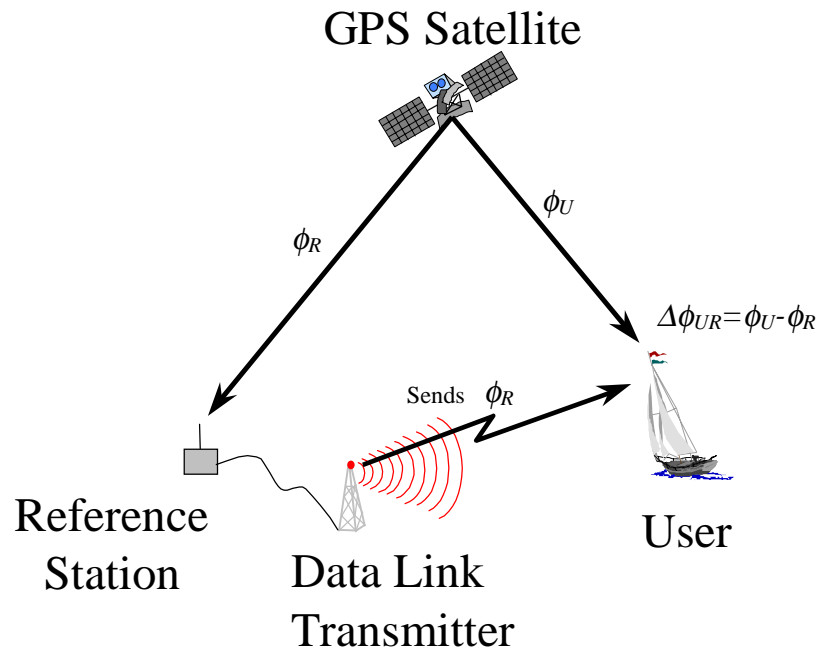


**Figure 3-1: Differential GPS**

The distance between the user and the reference station is called the baseline. The magnitude of other errors such as orbital error, ionospheric effects, and tropospheric delay depend upon the baseline length because they are spatially correlated throughout a geographic region. If the baseline is short in comparison to the size of the region for which the errors are correlated, single differencing will reduce the effects of these spatially correlated errors.

### 3.3 Receiver Single-Difference Measurements

For DGPS, the receiver single-difference carrier-phase measurement is modelled by Equation 3.6. It is the difference in the carrier-phase between two GPS receivers and is derived from Equation 2.5.

$$\Delta\phi_{UR}^s = \frac{1}{\lambda} \left\{ \Delta\rho_{UR}^s - c \cdot (dT_U^s - dT_R^s) + \Delta do_{UR}^s + \Delta da_{UR}^s - \Delta di_{UR}^s \right\} \quad (3.6)$$

$$+ \Delta N_{UR}^s + \Delta dm_{UR}^s + \Delta \eta_{UR}^s.$$

$$\text{Where:} \quad \Delta \otimes_{UR}^s = \otimes_U^s - \otimes_R^s.$$

The subscript U refers to the user's measurement, and the subscript R refers to the reference receiver's measurement. The superscript "s" refers to the satellite for which the measurement applies. The ionospheric term is zero if ionospheric free measurements are used.

The satellite clock offset and SA are completely eliminated in Equation 3.6. The magnitude of  $\Delta N_{UR}^s$  is unknown and depends upon the time at which the two receivers established a tracking lock on the satellite, as well as the method by which the receivers initialise their carrier-phase measurements.

The noise and multipath ( $\eta$ , and  $dm$ ) are assumed to be uncorrelated between the user and reference receivers. From a statistical point of view,  $\Delta \eta_{UR}^s$ , and  $\Delta dm_{UR}^s$  are expected to be larger than their undifferenced counterparts.

The magnitude of the ionospheric error, the tropospheric error, and the orbital error are dependent upon the length of the baseline between the user and the reference receivers. Parkinson and Enge [1996] have shown that ephemeris errors have linear growth rates for short baselines. If ephemeris SA is not applied, the rate of growth is about 0.1 mm per km or parts per million (ppm) of the baseline length. If ephemeris SA were to be applied, the rate of growth could potentially reach 5 ppm. At 0.1 ppm, the differential orbital error on a 100-km baseline is expected to be 1 cm. Parkinson and Enge [1996] also estimated the spatial decorrelation for the ionospheric and the tropospheric effects to be 2 ppm and

1 ppm respectively. Accordingly, it is expected that the ionosphere is the most troublesome source of spatial error followed by troposphere, and then the satellite orbit error.

### 3.4 Differential Shift and Distortion Errors

The user's relative position can be derived very accurately using DGPS, but if the reference station's absolute position is in error, the user's absolute position will be shifted by an amount equal to that error. This error is called differential shift. Differential shift is not a problem for user's that position themselves with respect to objects whose location has been determined using the same DGPS reference station. However, if the user is determining position with respect to objects whose locations are not derived from the user's DGPS reference station, the effects of differential shift must be considered.

Tang [1996] has shown that relative positioning solutions using DGPS can be distorted if the reference station position is error. This error is called differential distortion and is usually small. Under some circumstances however, this error can become significant. The differential distortion is a second order effect that is modelled by Equation 3.7 [Tang, 1996].

$$\text{Differential Distortion} = \{ \mathbf{A}_U^T \mathbf{C}_l^{-1} \mathbf{A}_U \}^{-1} \mathbf{A}_U^T \mathbf{C}_l^{-1} \{ \mathbf{A}_R - \mathbf{A}_U \} \delta \mathbf{x}. \quad (3.7)$$

Where:

- $\mathbf{A}_U$  = Network Design Matrix at the User's Location.
- $\mathbf{A}_R$  = Design Matrix at the Reference Location.
- $\mathbf{C}_l$  = Measurement Variance/Covariance Matrix.
- $\delta \mathbf{x}$  = Differential Shift.

Tang also derived Equation 3.8, which describes the  $\{ \mathbf{A}_R - \mathbf{A}_U \}$  term in Equation 3.7. Equation 3.8 clearly shows that the term is proportional to the baseline length (  $|\Delta \mathbf{X}_{UR}|$  ),

but is also related to the difference in inverse distances  $\left(\frac{1}{\rho^n}\right)$  to the various satellites used in the DGPS solution.

$$\{\mathbf{A}_R - \mathbf{A}_U\} = \begin{bmatrix} \left(\frac{1}{\rho^1} - \frac{1}{\rho^k}\right) [\Delta \mathbf{X}_{UR}]^T \\ \left(\frac{1}{\rho^2} - \frac{1}{\rho^k}\right) [\Delta \mathbf{X}_{UR}]^T \\ \vdots \\ \left(\frac{1}{\rho^n} - \frac{1}{\rho^k}\right) [\Delta \mathbf{X}_{UR}]^T \end{bmatrix}. \quad (3.8)$$

Where:  $\rho^k = \text{Range to Satellite "k"}$ .

The maximum range to a GPS satellite is about 26,000,000 metres. The minimum range is about 20,000,000 metres. Therefore, it is possible to quantify the maximum value of the  $\{\mathbf{A}_R - \mathbf{A}_U\}$  term.

$$\text{MAX} \left[ \left( \frac{1}{\rho^n} - \frac{1}{\rho^k} \right) \right] = \left( \frac{1}{20,000,000} - \frac{1}{26,000,000} \right) = \frac{1}{90,000,000}.$$

The worst case conditions for range distortion occur for an orthogonal network in which the design matrix at the user's location is the identity matrix. In this situation, all terms to the left of the  $\{\mathbf{A}_R - \mathbf{A}_U\}$  term evaluate to an identity matrix and the worst case range distortion would be given by Equation 3.9. In this equation, the distortion is converted from units of distance to ppm units by dividing by the baseline length.

Since the differential distortion is directly related to differential shift, distortion can be minimised by using WGS-84 surveyed coordinates for the reference point location. As long as the reference stations absolute position error (differential shift) is less than 10

metres, differential distortion can be ignored because ionospheric, tropospheric, and orbital errors will dominate the error budget.

$$\begin{aligned}
 \text{Range Distortion (Worst Case)} &= \frac{\{\mathbf{A}_R - \mathbf{A}_U\}_{Max}}{|\Delta\mathbf{X}_{UR}|} \delta\mathbf{x}, & (3.9) \\
 &= MAX \left[ \left( \frac{1}{\rho^n} - \frac{1}{\rho^k} \right) \right] \delta\mathbf{x}, \\
 &\approx 0.01 \cdot \delta\mathbf{x} \text{ (ppm)}.
 \end{aligned}$$

In order to determine the significance of the differential distortion error, an estimate of the differential shift must be available. This estimate must take into account the accuracy of any coordinate transformations and the quality of the data used to derive the reference point's position. A reference point that is not tied to a known control network can have its location derived by long term averaging of GPS measurements. If the reference location is derived using a few hours of GPS measurements, it may have a differential shift error a few tens of metres. On the other hand, reference points that are part of the IGS network have differential shift errors of between 0.3 and 3 cm [Zumberge et al., 1994].

### 3.5 Double-Difference Measurements

Single-difference carrier-phase measurements, on their own, are of limited use because it is not possible to separate the differential receiver clock offset ( $dT_U - dT_R$ ) from the differential ambiguity ( $\Delta N_{UR}$ ). This is quite troublesome because the clock offset is not generally constant. Carrier-phase solutions are made possible by assuming that the ambiguity is constant. If the clock offset varies and cannot be separated from the ambiguity, a solution for the position using carrier-phase measurements becomes

extremely difficult. One method of overcoming this problem is to use double-difference measurements [Hoffman and Wellenhof, 1994].

Figure 3.2 depicts the situation that exists when double-difference measurements are formed. When the single-difference carrier-phase measurement of a satellite “b” is subtracted from that of another satellite “s”, a double-difference (DD) measurement is created for Satellite “s” (Equation 3.10). When this measurement is formed, Satellite *b* is called the “base satellite”. The DD measurement does not have a clock parameter to be estimated because the user’s differential clock offset is the same for both single-difference measurements. Since a base satellite must be selected to form DD measurements, there are “n-1” DD measurements available when single-difference measurements are derived from “n” satellites.

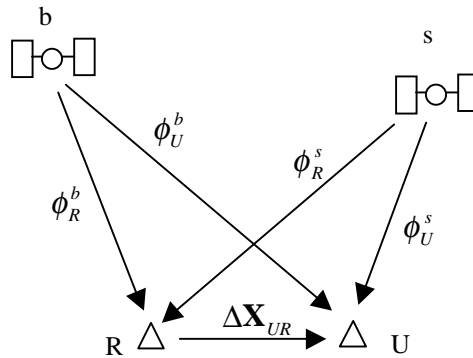


**Figure 3.2: Formation of the Double-Difference Measurement**

$$\begin{aligned} \nabla \Delta \phi^s &= \Delta \phi^s - \Delta \phi^b & (3.10) \\ &= \frac{1}{\lambda} (\nabla \Delta \rho + \nabla \Delta do + \nabla \Delta da - \nabla \Delta di) + \nabla \Delta N + \nabla \Delta dm + \nabla \Delta \eta. \end{aligned}$$

The drawback to using DD measurements is that the measurement errors are magnified. Under the assumption that the errors affecting the single-difference measurements are uncorrelated, the standard deviation of the DD errors is a factor of  $\sqrt{2}$  greater than for the single-difference errors.

### 3.6 DGPS Error Budgets

The accuracy of DGPS is driven by the errors that exist in the observations. As explained in Chapter 2, these errors can be classified according to their source. For the error budgets given by Table 3-1 through 3-5, these errors are classified according to five separate categories: orbital error, the ionospheric error, the tropospheric delay, multipath, and receiver noise. Since only relative position performance is being analysed, differential shift is ignored. Differential distortion is also ignored based upon the assumption that reference station absolute positioning accuracy is 10 metres or better. The error budget for the DD L1 carrier-phase measurement is summarised in Table 3-1. All error budget tables have two columns: The column titled “Range Error” is the error associated with using a GPS receiver on a DGPS baseline of zero length. The second column is the error associated with DGPS spatial decorrelation. The spatial decorrelation value (in ppm) is multiplied by the baseline length (in kilometres) to determine the actual error budget for a particular error source (in millimetres).

Based upon the frequency relationships derived in Chapter 2, the error budgets for the L2 carrier-phase, widelane, ionospheric free, and narrowlane can also be estimated. These budgets are given as Tables 3-2, 3-3, 3-4, and 3-5 respectively.

**Table 3-1: Double-Difference (DD) Carrier-Phase DGPS Error Budget (L1)**

Parameter	Carrier-phase DGPS Errors (1 Sigma)	
	L1 Frequency	
	Range Error (cm)	Decorrelation (ppm)
Ephemeris	0.0	0.14
Ionosphere	0.0	2.0
Troposphere (Max = 30 cm when Modelled)	0.0	1.0
Multipath (Max = 4.8 cm)	1.9	0.0
Receiver Noise (See p. 37; $\times \sqrt{2}$ for DD)	0.27	0.0
Reference Station Noise	0.27	0.0
<b>Total Measurement Error (RMS)</b>	<b>1.9</b>	<b>2.2</b>

**Table 3-2: DD Carrier-Phase DGPS Error Budget (L2)**

Parameter	Carrier-phase DGPS Errors (1 Sigma)	
	L2 Frequency	
	Range Error (cm)	Decorrelation (ppm)
Ephemeris	0.0	0.14
Ionosphere	0.0	3.4
Troposphere (Max = 30 cm when Modelled)	0.0	1.0
Multipath (Max = 6 cm)	2.4	0.0
Receiver Noise (See p. 37; $\times \sqrt{2}$ for DD)	0.34	0.0
Reference Station Noise	0.34	0.0
<b>Total Measurement Error (RMS)</b>	<b>2.4</b>	<b>3.5</b>

**Table 3-3: DD Carrier-Phase DGPS Error Budget (Widelane)**

Parameter	Carrier-phase DGPS Errors (1 Sigma)	
	Widelane	
	Range Error (cm)	Decorrelation (ppm)
Ephemeris	0.0	0.2
Ionosphere	0.0	2.6
Troposphere (Max = 30 cm when Modelled)	0.0	1.0
Multipath (Max = 21.5 cm)	8.6	0.0
Receiver Noise (See p. 37; $\times \sqrt{2}$ for DD)	1.72	0.0
Reference Station Noise	1.72	0.0
<b>Total Measurement Error (RMS)</b>	<b>8.9</b>	<b>2.8</b>

**Table 3-4: DD Carrier-Phase DGPS Error Budget (Ionospheric Free)**

Parameter	Carrier-phase DGPS Errors (1 Sigma)	
	Ionospheric Free	
	Range Error (cm)	Decorrelation (ppm)
Ephemeris	0.0	0.2
Ionosphere	0.0	0.0
Troposphere (Max = 30 cm when Modelled)	0.0	1.0
Multipath (Max = 4.8 cm)	1.9	0.0
Receiver Noise (See p. 37; $\times \sqrt{2}$ for DD)	0.38	0.0
Reference Station Noise	0.38	0.0
<b>Total Measurement Error (RMS)</b>	<b>2.0</b>	<b>1.0</b>

**Table 3-5: DD Carrier-Phase DGPS Error Budget (Narrowlane)**

Parameter	Carrier-phase DGPS Errors (1 Sigma)	
	Narrowlane	
	Range Error (cm)	Decorrelation (ppm)
Ephemeris	0.0	0.2
Ionosphere	0.0	20
Troposphere (Max = 30 cm when Modelled)	0.0	1.0
Multipath (Max = 2.8 cm)	1.1	0.0
Receiver Noise (See p. 37; $\times \sqrt{2}$ for DD)	0.22	0.0
Reference Station Noise	0.22	0.0
<b>Total Measurement Error (RMS)</b>	<b>1.1</b>	<b>20</b>

## Chapter 4

### PARTIAL DERIVATIVE ALGORITHMS THEORY AND IMPLEMENTATION

#### 4.1 Overview

The previous chapters have been a review of the techniques and methods that determine positions using GPS and DGPS. This chapter seeks to define a method for modelling the errors that affect the DGPS measurements. The application of this model is designed to reduce the measurement errors and improve the positioning accuracy. The models developed in this chapter are called PDAs. A network of DGPS reference stations is required to implement a PDA. The performance when using a PDA is compared against the performance of some alternative models. The trade-offs between network design, model complexity, and communications requirements are discussed.

#### 4.2 PDA Theory

The mathematical origin of a PDA is based upon a Taylor series spatial expansion of the GPS measurement error function ( $g$ ) about a specified reference point ( $\mathbf{P}_0$ ) [Swokowski, 1979]. The Taylor series can be expanded to any order desired, but a second order series is the most complicated form that will be considered for analysis in this dissertation. Equation 4.1 gives an example of a second order Taylor series PDA expanded in three-dimensional coordinates. The constant  $g(\mathbf{P}_0)$ , represents a fixed/non-spatial characteristic of the error being estimated. The first order partial derivative term,  $\frac{\partial g}{\partial \mathbf{P}_0}$ , accounts for spatial decorrelation. The second order term,  $\frac{\partial^2 g}{\partial \mathbf{P}_0^2}$ , may be used to

characterise non-linear aspects of the DGPS error. The reference point can be located anywhere near the user. However, when a network of reference stations is available, the reference point is normally selected to be the location of a reference station near the middle of the network area. The network station whose location corresponds to the PDA reference point is called the master reference station. All other reference stations are called secondary reference stations.

$$g(\mathbf{P}) = g(\mathbf{P}_0) + \frac{\partial g}{\partial \mathbf{P}_0} \cdot \{\mathbf{P} - \mathbf{P}_0\} + \frac{1}{2} \{\mathbf{P} - \mathbf{P}_0\} \frac{\partial^2 g}{\partial \mathbf{P}_0^2} \cdot \{\mathbf{P} - \mathbf{P}_0\}^T + O(h_3). \quad (4.1)$$

Where:  $g(\mathbf{P}_0) = 0^{\text{th}}$  Order Partial Derivative (mm).

$$\frac{\partial g}{\partial \mathbf{P}_0} = \begin{bmatrix} \frac{\partial g}{\partial x} & \frac{\partial g}{\partial y} & \frac{\partial g}{\partial z} \end{bmatrix} = 1^{\text{st}} \text{ Order Partial Derivative Vector (ppm)}.$$

$$\frac{\partial^2 g}{\partial \mathbf{P}_0^2} = \begin{bmatrix} \frac{\partial^2 g}{\partial x^2} & \frac{\partial^2 g}{\partial x \partial y} & \frac{\partial^2 g}{\partial x \partial z} \\ \frac{\partial^2 g}{\partial y \partial x} & \frac{\partial^2 g}{\partial y^2} & \frac{\partial^2 g}{\partial y \partial z} \\ \frac{\partial^2 g}{\partial z \partial x} & \frac{\partial^2 g}{\partial z \partial y} & \frac{\partial^2 g}{\partial z^2} \end{bmatrix} = 2^{\text{nd}} \text{ Order Partial Derivative Matrix} \left( \frac{\text{ppm}}{\text{km}} \right).$$

$$\mathbf{P} = \begin{bmatrix} P_x & P_y & P_z \end{bmatrix}^T = \text{Position (km)}.$$

In Equation 4.1, the partial derivatives  $g(P_0)$ ,  $\frac{\partial g}{\partial \mathbf{P}_0}$ , and  $\frac{\partial^2 g}{\partial \mathbf{P}_0^2}$  are unknowns that must be estimated using the reference station CP-DD measurements and the known locations of the reference station receivers.

A CP DD measurement ( $\Delta \nabla \phi_{PR}^{sb}$ ) is formed for each secondary reference station,  $P$ , using the CP measurements of two satellites ( $s$  and  $b$ ) collected at the secondary and master reference stations. The predicted CP DD measurement ( $\Delta \nabla \tilde{\phi}_{PR}^{sb}$ ) is computed from the

known positions of the satellites and the reference stations. The DD ambiguity on the baseline between the secondary and master reference stations must have been estimated or resolved before the predicted CP DD measurement can be computed. As shown in Equation 4.2, the difference between the predicted and actual CP DD measurements is the measurement error ( $\kappa_{PR}^{sb}$ ) observed at the secondary station. This measurement error is called the “network measurement” for Secondary Reference Station  $P$  and satellite combination ( $sb$ ). The PDA given by Equation 4.1 is used to model the actual these measurement errors. The difference between the value of the model ( $g^{sb}$ ) and the network measurement is the modelling error ( $\xi^{sb}$ ). The relationship between the model, the model error, and the network measurement is also given by Equation 4.2. If the model is a perfect reflection of the errors affecting the network, then  $\xi^{sb}$  will equal zero.

$$\kappa_{PR}^{sb} = \Delta\nabla\phi_{PR}^{sb} - \Delta\nabla\tilde{\phi}_{PR}^{sb} = g^{sb}(P) + \xi^{sb}(P). \quad (4.2)$$

A set of network measurements for satellite combination  $sb$  is formed when the network measurements from all secondary reference stations are collected together. This set of network measurements can be used to estimate the parameters of the PDA for the  $sb$  satellite combination. Before developing the estimation process, it is important to understand what physical errors are present in the network measurement, and how they are reflected in the parameters of the PDA model.

### 4.3 Network Measurements

The network measurement only occurs at secondary stations and is recorded for each non-base satellite. It is defined according to Equation 4.2, but a simplified nomenclature is introduced in Equation 4.3. In this nomenclature, the base satellite superscript and the

master reference station subscript are dropped. As a result, the symbol  $(\nabla\Delta\tilde{\phi}_j^i)$  is the predicted DD carrier-phase for “non-base satellite” ( $i$ ) observed at “secondary station” ( $j$ ) under the implicit assumption that a “base satellite” ( $b$ ) and a “master reference station” ( $R$ ) are required to form the DD measurement.

$$\kappa_j^i = \nabla\Delta\phi_j^i - \nabla\Delta\tilde{\phi}_j^i. \quad (4.3)$$

The predicted CP DD measurement includes the true range  $(\nabla\Delta\rho_j^i)$ , the survey range error for Station  $j$   $(\nabla dr_j^i)$ , and the estimated ambiguity  $(\nabla\Delta\hat{N}_j^i)$ , and is modelled according to Equation 4.4.

$$\nabla\Delta\tilde{\phi}_j^i = \frac{1}{\lambda}(\nabla\Delta\rho_j^i + \nabla dr_j^i) + \nabla\Delta\hat{N}_j^i. \quad (4.4)$$

By substituting Equation 3.10 and 4.4 into Equation 4.3, the network measurement is shown to be an accumulation of the errors in the CP-DD signal (Equation 4.5).

$$\kappa_j^i = \frac{1}{\lambda}(\nabla\Delta do_j^i + \nabla\Delta di_j^i + \Delta\nabla da_j^i + \nabla dr_j^i) + \Delta\nabla dm_j^i + \Delta\nabla\eta_j^i + \{\Delta\nabla N_j^i - \Delta\nabla\hat{N}_j^i\}. \quad (4.5)$$

If the ambiguities have been correctly resolved, the last term of Equation 4.5 is zero and the equation can be rewritten as Equation 4.6.

$$\kappa_j^i = \frac{1}{\lambda}(\nabla\Delta do_j^i + \nabla\Delta di_j^i + \nabla\Delta da_j^i) + \nabla dm_R^i + \nabla\eta_R^i + \zeta_j^i. \quad (4.6)$$

Where:  $\zeta_j^i = \left\{ \nabla dm_j^i + \nabla\eta_j^i + \frac{1}{\lambda}\nabla dr_j^i \right\} \equiv \text{Network Measurement Niose}.$

In Equation 4.6, the spatial errors are ionospheric ( $\nabla\Delta di_j^i$ ), orbital error ( $\nabla\Delta do_j^i$ ) and tropospheric ( $\nabla\Delta da_j^i$ ). The non-spatial errors result from multipath occurring at the master reference station ( $\nabla dm_R^i$ ), and master reference station phase noise ( $\nabla d\eta_R^i$ ). All other errors are noise that is not modelled by the PDA. The accumulation of these errors is called network measurement noise ( $\zeta_j^i$ ). This noise determines the ultimate accuracy to which the PDA model parameters can be estimated. It includes secondary reference station multipath ( $\nabla dm_j^i$ ), secondary reference station phase noise ( $\nabla d\eta_j^i$ ), and range errors caused by inaccuracies in the surveyed positions of the secondary reference stations ( $\nabla dr_j^i$ ).

#### 4.4 Error Budget for the Network Measurement Noise ( $\zeta_j^i$ )

Most of the network measurement noise can be estimated from the tables at the end of Chapter 3. These tables provide estimates for the magnitude of the multipath and phase noise affecting the network measurements.

The measurement range errors that result from errors in the network survey are obtained from the network adjustment process. The adjusted network survey yields an estimate of the relative position of the secondary reference stations. The position of each secondary reference station is represented as a three-element state vector  $\Delta\hat{\mathbf{X}}_j$  (Equation 4.7).

$$\Delta\hat{\mathbf{X}}_j = [\Delta\hat{x}_j \quad \Delta\hat{y}_j \quad \Delta\hat{z}_j]^T. \quad (4.7)$$

The vector given by Equation 4.7 is used to generate the predicted CP DD measurement. This is accomplished by projecting the state vector onto the line of sight unit vector ( $\mathbf{e}^i$ )

for both satellites in the DD measurement. For a particular satellite, the line of site unit vector is defined by the satellite's direction cosines. In the local horizontal / local vertical coordinate system, the line of site unit vector is computed according to Equation 4.8.

$$\mathbf{e}^i = [e_x^i \quad e_y^i \quad e_z^i]. \quad (4.8)$$

Where the direction cosines are:

$$\begin{aligned} e_x^i &= \cos(Az^i)\cos(El^i), \\ e_y^i &= \sin(Az^i)\cos(El^i), \\ e_z^i &= \sin(El^i), \end{aligned}$$

And:

$Az^i$  = Azimuth of Satellite  $i$  at the master reference station.

$El^i$  = Elevation of Satellite  $i$  at the master reference station.

The single difference range ( $\Delta\hat{r}_j^i$ ) for Secondary Reference Station  $j$  and Satellite  $i$  is then given by Equation 4.9.

$$\Delta\hat{r}_j^i = \mathbf{e}^i \bullet \Delta\hat{\mathbf{X}}_j. \quad (4.9)$$

To form a DD range, the single difference range of the base satellite is subtracted from that of the non-base satellite. To obtain a CP DD prediction, the DD range is converted into units of phase by dividing by the carrier-phase wavelength. Afterwards the estimated DD ambiguity is added as described in Equation 4.10. Equation 4.10 is the method by which a predicted CP DD measurement is computed. The physical model of a predicted measurement is given by Equation 4.4.

$$\nabla\Delta\tilde{\phi}_j^i = \frac{1}{\lambda}(\Delta\hat{r}_j^i - \Delta\hat{r}_j^b) + \nabla\Delta\hat{N}_j^i. \quad (4.10)$$

In Equation 4.10 the single difference ranges are obtained from the surveyed positions of the network reference stations. The survey accuracy is normally provided by the network adjustment in the form of a variance/covariance matrix ( $\sigma_{\Delta X_j}^2$ ). The variance/covariance matrix has the form shown in Equation 4.11. The diagonal elements represent the survey error variances along the primary axes (usually east, north, and up). The off-diagonal elements are the result of error correlation between these axes.

$$\sigma_{\Delta X}^2 = \begin{bmatrix} \sigma_{\Delta x}^2 & \tau_{xy} & \tau_{xz} \\ \tau_{xy} & \sigma_{\Delta y}^2 & \tau_{yz} \\ \tau_{xz} & \tau_{yz} & \sigma_{\Delta z}^2 \end{bmatrix}. \quad (4.12)$$

It is always possible to rotate the primary axes to eliminate the horizontal covariance components of the variance/covariance matrix. After applying this transformation (Equation 4.12), the matrix values represent the error variances in a new set of horizontal coordinates called the primary axes ( $x', y', z$ ).

$$\sigma'^2 = \mathbf{T}[\sigma^2]\mathbf{T}^T = \begin{bmatrix} \sigma_{\Delta x'}^2 & 0 & \tau_{x'z} \\ 0 & \sigma_{\Delta y'}^2 & \tau_{y'z} \\ \tau_{zx'} & \tau_{zy'} & \sigma_{\Delta z}^2 \end{bmatrix}. \quad (4.12)$$

Where:  $\mathbf{T}$  is an Orthogonal Transformation Matrix.

The accuracy of a horizontal network is categorised according to Equation 4.13.

$$\text{Horizontal Station Accuracy } (\sigma_H) = \sqrt{\sigma_{\Delta x'}^2 + \sigma_{\Delta y'}^2} \quad (\text{mm}). \quad (4.13)$$

When the horizontal station accuracy in millimetres is divided by the baseline length in kilometres, an accuracy statistic having units of ppm is created. This statistic is derived

for each station in the network, and the largest value of this statistic among all stations defines the accuracy of the network. Networks are classified by their accuracy according to Table 4-1 [Thomson, et al., 1987].

The survey accuracy of a secondary reference station located 100 km from the network master station has a magnitude that is given in the last column of the Table 4-1. The accuracy of the single difference range measurements is derived from the covariance propagation law (Equation 4.14). This equation converts the position errors into errors of satellite range using the direction cosines and is equivalent to dividing the horizontal position accuracy by the dilution of precision. The horizontal dilution of precision is typically about 2. Therefore, the accuracy of the single difference range for a secondary station 100 kilometres from the master reference station can be as low as 0.6 cm (0.06 ppm) for a high precision GPS network.

**Table 4-1: Horizontal Survey Classifications**

<u>Type</u>	<u>Description</u>	<u>Accuracy</u>	<u>Accuracy @ 100 km</u>
–	Carrier-Phase GPS Network (SCIGN)	0.03 – 0.3 ppm	0.3 – 3.0 cm
1 <sup>st</sup> Order	National Control Networks	10 ppm	1.0 m
2 <sup>nd</sup> Order	State/Provincial Control Networks	25 ppm	2.5 m
3 <sup>rd</sup> Order	Municipal Control Networks	60 ppm	6.0 m
4 <sup>th</sup> Order	Local Surveys	150 ppm	15.0 m

$$\sigma_{\Delta\hat{r}_j}^2 = [\mathbf{e}^i]^T [\sigma_{\Delta X}^2] [\mathbf{e}^i]. \quad (4.14)$$

Where:  $\sigma_{\Delta\hat{r}_j}$  = Accuracy of the Range Measurement for Satellite  $i$  at Station  $j$ .

The accuracy of the predicted DD carrier-phase measurement ( $\sigma'_{\Delta\tilde{\phi}_j}$ ) is obtained from Equation 4.15. In this equation,  $\tau_{\Delta\hat{r}_j^i\Delta\hat{r}_j^b}$  is the covariance between two Satellites  $i$  and  $b$ .

The worst case errors occur when the covariance is zero.

$$\sigma'^2_{\nabla\Delta\tilde{\phi}_j} = \frac{1}{\lambda^2} \left( \sigma'^2_{\Delta\hat{r}_j^i} - 2\tau_{\Delta\hat{r}_j^i\Delta\hat{r}_j^b} + \sigma'^2_{\Delta\hat{r}_j^b} \right) \quad (4.15)$$

Therefore, under worst case conditions where the accuracy of the single difference range is 0.06 ppm, the accuracy of the predicted DD carrier-phase is  $\sqrt{2} \cdot 0.06$  ppm (0.085 ppm).

A summary of the range domain errors affecting the network measurement is provided in Table 4-2. Note that the spatial error associated with the network measurement noise is very small for networks that have been surveyed to reasonably accurate standards.

**Table 4-2: Network Measurement Noise Error Budget (L1)**

Parameter	Non-Spatial Error	Spatial Error
	(cm)	(ppm)
Secondary Multipath	1.9	-
Secondary Receiver Noise	0.4	-
Network Survey Accuracy (Rel. Diff. Shift)	-	0.085
Measurement Error RMS	1.9	0.085

#### 4.5 Measurement Error Modelling (Partial Derivative Algorithms)

The network measurements from the various secondary stations are used to estimate the parameters of the PDA. Since the spatial errors are assumed to be linear in the horizontal axes, only 1<sup>st</sup> order partial derivatives are estimated for the x and y coordinates. This

assumption means that the spatial errors do not exhibit second order (non-linear) behaviour in the horizontal axes, and the following relations are applied to Equation 4.1.

$$\frac{\partial^2 g}{\partial x^2} = \frac{\partial^2 g}{\partial y^2} = \frac{\partial^2 g}{\partial x \partial y} = \frac{\partial^2 g}{\partial x \partial z} = \frac{\partial^2 g}{\partial y \partial z} = \frac{\partial^2 g}{\partial y \partial x} = \frac{\partial^2 g}{\partial z \partial x} = \frac{\partial^2 g}{\partial z \partial y} = 0. \quad (4.16)$$

If non-linear behaviour is suspected in the vertical axis because of ionospheric or tropospheric sensitivity, the 2<sup>nd</sup> order partial derivative  $\left( \frac{\partial^2 g}{\partial z^2} \right)$  needs to be estimated.

One possible cause of non-linear behaviour is scintillation, but this behaviour is temporal and generated from discrete cellular structures of high ion content [Klobuchar (1996)]. The effects on signals passing through these cellular structures become unpredictable over short distances. As a result it is assumed that scintillation cannot be accurately modelled as a with a 2<sup>nd</sup> order PDA. If scintillation exists, it increases the network measurement noise and degrades the accuracy of the PDA parameter estimates.

Given the conditions expressed by Equation 4.16, Equation 4.1 can be simplified to the following:

$$g(P) = \alpha + \chi(x_P - x_{P_0}) + \beta(y_P - y_{P_0}) + \delta(z_P - z_{P_0}) + \gamma(z_P - z_{P_0})^2 + O(h_3). \quad (4.17)$$

Where:

$\alpha = g(\mathbf{P}_0) = 0^{\text{th}}$  Order Partial Derivative – Non-Spatial Error at the Master Station (mm).

$\beta = \frac{\partial g}{\partial y} = 1^{\text{st}}$  Order Partial Derivative Along the Horizontal Y Axis (ppm).

$\chi = \frac{\partial g}{\partial x} = 1^{\text{st}}$  Order Partial Derivative Along the Horizontal X Axis (ppm).

$\delta = \frac{\partial g}{\partial z} = 1^{\text{st}} \text{ Order Partial Derivative Along the Vertical Z Axis (ppm)}$ .

$\gamma = \frac{1}{2} \frac{\partial^2 g}{\partial z^2} = 2^{\text{st}} \text{ Order Partial Derivative Along the Vertical Z Axis (ppm/km)}$ .

Any PDA selected for a carrier-phase network should, at a minimum, contain a non-spatial parameter ( $\alpha$ ). This parameter is the best estimate for the receiver noise, and the multipath at the master reference station. Such an algorithm is called a 0<sup>th</sup> Order (or Non-Spatial) PDA. This model is given by Equation 4.18.

Non-Spatial:

$$g_j = g(P_j) = \alpha + \varepsilon_g(P_j). \quad (4.18)$$

Where :

$P_j \equiv \text{Position of the Secondary Station } j$ .

$\varepsilon_g(P_j) \equiv \text{Model Prediction Error at the Secondary Station } j$ .

The non-spatial model has one unknown parameter, which can be estimated from a single network measurement. One network measurement can be obtained from a network comprised of two reference stations, a master station and a secondary station. If three or more reference stations are available to provide network measurements, then second moment information, such as the accuracy of the estimate for  $\alpha$  can be generated. This is useful for comparing the performance of the model against that of other models.

A PDA that is based only on non-spatial errors is useful if the network is small, or if the number of reference stations is too limited to support a more complex PDA model. The definition of “small” as it refers to network resolution depends upon the network

frequency. If the network is single frequency on L1 or L2, spatial errors manifest themselves on baselines as short as 15 km [Weisenberger, 1997]. Therefore, if the network has more than three stations and has a scale in excess of 15 km, a more complicated PDA is recommended. If the network frequency is widelane, then the network can be 4 to 5 times larger before spatial error become noticeable. Therefore, the network scale may expand to 60 or 75 km before the network designer begins to consider a more complicated PDA.

Following the theory suggested by Loomis et al. [1991], spatial decorrelation can be estimated using a 1<sup>st</sup> order PDA. The basic PDA would be of the form shown in Equation 4.19.

$$g_j = \alpha + \chi * \Delta x_j + \beta * \Delta y_j + \delta * \Delta z_j + \varepsilon_g(P_j). \quad (4.19)$$

In solving this equation for the PDA parameters, the degrees of freedom (DOF) is equal the number of equations minus the number of unknowns. Each PDA parameter represents one unknown. In Equation 4.19, there are 4 unknowns. Each measurement of  $g$  (network measurement) is an equation. If there are  $l$  reference stations in the network, and network measurements are collected at each secondary reference station, then there are  $l-1$  equations available to solve for the unknowns. From this information, the DOF for the model given by Equation 4.19 is  $l-5$ :

$$DOF = (l - 1) - 4 = l - 5. \quad (4.21)$$

Where:  $l$  = Number of reference stations in the network.

The importance of analysing the DOF is that it helps determine the number of reference stations required in the network. In order to use a PDA model, the number of reference

stations must be sufficient for the DOF to be equal to or greater than zero. Therefore, the model given by Equation 4.19 requires a network with 5 or more reference stations.

The PDA model of Equation 4.19 assumes that the rate of growth of the network measurement is constant along orthogonal lines of reference. These directions may be selected arbitrarily, but East, North, and Up are convenient for situational awareness. There are certain network geometries that will naturally dictate directions that are non-cardinal. The selection non-cardinal directions for the primary axes of a PDA are dictated by layout of the network reference stations. Networks in which the reference stations are not aligned with the East and North directions can justify the use of non-cardinal axes in the PDA model. This concept will become clearer in the next few paragraphs. In this dissertation, all networks have reference stations that are aligned roughly with the East and North directional axes. Therefore, axes based upon cardinal directions are used for all PDAs analysed herein.

Estimation of all three spatial decorrelation parameters ( $\chi$ ,  $\beta$ , and  $\delta$ ) may not be possible or desirable for certain types of networks. The accuracy of the estimate for the spatial decorrelation parameter(s) is directly related to the projected expanse of the network along the selected line of reference. In order to achieve maximum accuracy, the line of reference should be chosen to be parallel to the line of greatest expanse in the network.

For example, a network that spans a great distance North and South (Figure 4-1) should use a North/South line of reference. If the network does not cover a large distance East and West, the parameter for the East/West axis will be poorly determined. Since the estimate of the East/West parameter will have high uncertainty, the network designer may be justified in removing the parameter from the PDA model. If an East/West parameter is not estimated, the users of the network should be warned that the East or West limits of the network are very narrow. The model for such a North/South PDA is given Equation 4.20.

$$g_j = \alpha + \beta * \Delta y_j + \varepsilon_g(P_j). \quad (4.20)$$

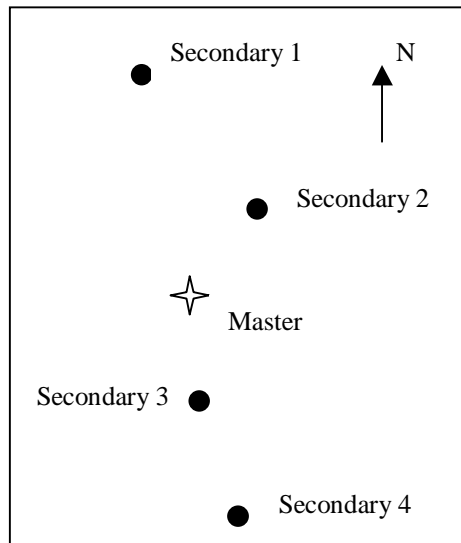


**Figure 4-1: North / South Network**

The best PDA model for a network having an East / West layout (Figure 4-2) would have a mathematical formulation as shown in Equation 4.21.

#### Non-Spatial and Spatial Decorrelation in Easting

$$g_j = \alpha + \chi * \Delta x_j + \varepsilon_g(P_j). \quad (4.21)$$

If the network is not aligned to a particular azimuth and it has three or more secondary reference stations, the spatial decorrelation in two orthogonal directions can be estimated. This is accomplished by using a PDA of the form shown in Equation 4.22.

$$g_j = \alpha + \chi * \Delta x_j + \beta * \Delta y_j + \varepsilon_g(P_j). \quad (4.22)$$

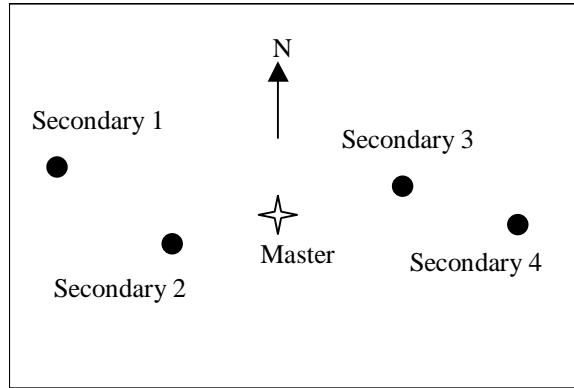


**Figure 4-2: East / West Network**

With four or more secondary stations having significant distribution in altitude, a vertical dimension can also be included as shown by Equation 4.23.

$$g_j = \alpha + \chi * \Delta x_j + \beta * \Delta y_j + \delta * \Delta z_j + \xi_g(P_j). \quad (4.23)$$

The tropospheric error and, to a lesser extent, the ionospheric error are extremely sensitive to changes in vertical position [Cosentino and Diggle, 1996]. As a result, the spatial decorrelation in the zenith direction is at least an order of magnitude greater than the spatial decorrelation in the horizontal direction. For this reason, it is a good practice to keep the horizontal and vertical decorrelation parameters separate by not choosing a reference axis that is inclined to the horizon plane.

Since the spatial decorrelation along the zenith line of reference is suspected to be large, there is the possibility that 2<sup>nd</sup> order (non-linear) effects may be present. Therefore, in addition to the PDAs already mentioned, a PDA of 2<sup>nd</sup> order in the vertical direction will also be investigated in this dissertation. This PDA is given by Equation 4.24.

$$g_j = \alpha + \chi * \Delta x_j + \beta * \Delta y_j + \delta * \Delta z_j + \gamma * \Delta z_j^2 + \xi_g(P_j). \quad (4.24)$$

Where :  $\gamma \equiv$  Curvature of Zenith decorrelation  $\left( \frac{\text{ppm}}{\text{km}} \right)$ .

In this text, the naming convention adopted for PDAs is given by Table 4-3. Since the directions of North and East are the reference axes for all networks studied in this document,  $\beta$  and  $\chi$  refer to the Northing and Easting spatial decorrelation parameters respectively.

**Table 4-3: PDA Naming Convention**

PDA Name	<u>Equation #</u>
$\alpha$	4.18
$\alpha\beta$	4.20
$\alpha\chi$	4.21
$\alpha\beta\chi$	4.22
$\alpha\beta\chi\delta$	4.23
$\alpha\beta\chi\delta\gamma$	4.24

#### 4.6 Modelling Solutions

Once the network designer has selected the PDA model that is most appropriate for the network, a method of estimating the PDA parameters must be developed. The solution is to employ the weighted least squares technique. When the weighting matrix is derived from the *a priori* accuracy estimates of the measurements (as given by Table 4-2), the least squares solution is called a *minimum variance* solution. Even though the PDA model may be the same for all satellites, the model parameters must be estimated for each non-base / base satellite pair separately.

Since the PDA parameters for each satellite pair are time varying, “lumping” the observations of multiple non-base satellites is possible only when the satellites have the same azimuth and elevation at the same time epoch. Such conditions are infrequent, therefore “lumping” several satellites together to estimate a single set of PDA parameters is not attempted. Additional research in this area is worth pursuing because the multipath is the major component of non-spatial error and the multipath characteristics are largely driven by the azimuth and elevation of the satellite. Two satellites that occupy the same azimuth and elevation point in the sky at different times will have similar multipath characteristics. These common points are called cross-over points. The non-spatial error for the two satellites should be nearly the same at the cross-over points, regardless of any temporal separation that may exist between the satellites. If future research proves that this is true, then the non-spatial parameters for the two satellites could be lumped together to improve the accuracy of the parameter estimate.

The minimum variance solution for the PDA parameters (field parameters) for a particular non-base / base satellite pair is expressed as  $(\mathbf{x})$  in Equation 4.25. The size of the matrix/vector is given in parentheses as rows and columns. This solution assumes that the statistical properties of the network measurements are known *a priori*. The information is contained in the Network Measurement Covariance ( $\mathbf{C}_l$ ), which is initially obtained from the estimated network measurement error. The minimum variance solution uses measurement covariance information to weight the measurements and account for correlation between measurements. In many cases the covariance of the network is unknown, but the accuracy of the relative survey is provided from the survey classification of the network as given in Table 4-1. In these situations, it is a common practice to assume that the standard deviation of the network measurement noise is the same and uncorrelated for all secondary stations. The value of the standard deviation is square root of the unit variance ( $\sigma_0$ ). According to Table 4-2,  $\sigma_0$  should be approximately 2 cm – assuming that the network has been surveyed with GPS or first

order accuracy as given by Table 4-1. Since the network measurements are assumed to be uncorrelated, the covariance is obtained from the product of the unit variance scalar and an identity matrix. The identity matrix is sized according to the number of secondary reference stations as shown in Equation 4.25(g). The actual survey covariance for the networks analysed in this document was unknown. The assumed covariance was generated according to the process described by Equation 4.25(g) with a unit variance of  $4 \text{ cm}^2$ .

$$\mathbf{x} = \mathbf{P}\mathbf{H}^T\mathbf{C}_l^{-1}\mathbf{y} \quad (\tau \times 1). \quad (4.25)$$

Where:

$$\mathbf{P} = [\mathbf{H}^T\mathbf{C}_l^{-1}\mathbf{H}]^{-1} \equiv \text{PDA Covariance Matrix } (\tau \times \tau). \quad 4.25(a)$$

$$\tau \equiv \text{Number of PDA Parameters}. \quad 4.25(b)$$

$$\mathbf{H} = \begin{Bmatrix} \mathbf{H}_1 \\ \mathbf{H}_2 \\ \vdots \\ \mathbf{H}_{l-1} \end{Bmatrix} \equiv \text{Network Design Matrix } (l-1 \times \tau). \quad 4.25(c)$$

$$l \equiv \text{Number of Network Reference Stations}. \quad 4.25(d)$$

$$\mathbf{H}_j = [1 \quad X_j \quad Y_j \quad Z_j \quad Z_j^2] \equiv \text{Observation Mapping Vector} \quad 4.25(e)$$

(1 × τ) -- Example shows an  $\alpha\beta\chi\delta\gamma$  PDA model

$$X_j, Y_j, Z_j \equiv \text{Coordinates of Secondary Station "j"} \quad 4.25(f)$$

w.r.t. the Master Station

$$\mathbf{C}_l \approx \sigma_0^2 \mathbf{I} \equiv \text{Network Measurement Covariance Matrix (Diagonal)} \quad 4.25(g)$$

(l-1 × l-1)

$$\sigma_0^2 \equiv \text{Unit Variance of Network Measurements (mm}^2\text{)}. \quad 4.25(h)$$

$$\mathbf{y} = \begin{Bmatrix} \kappa_1 \\ \kappa_2 \\ \vdots \\ \kappa_{l-1} \end{Bmatrix} \equiv \begin{array}{l} \text{Network Measurement Vector for Satellite "i"} \\ \text{Using Base Satellite "B"} \\ (l-1 \times 1) \end{array} \quad 4.25(i)$$

$$\mathbf{x} = \begin{Bmatrix} \alpha \\ \beta \\ \chi \\ \delta \\ \gamma \end{Bmatrix} \equiv \begin{array}{l} \text{PDA Parameters Vector for Satellite "i"} \\ \text{Using Base Satellite "B"} \\ \text{(Assumes an } \alpha\beta\chi\delta\gamma \text{ PDA model)} \\ (\tau \times 1) \end{array} . \quad 4.25(j)$$

Five network measurements are required to solve for the five unknown field parameters in Equation 4.25. This means that the network must have six reference stations, i.e. five secondary stations and a master station. The Network Design Matrix ( $\mathbf{H}$ ) is only a function of the relative geometry of the network reference stations. A residual analysis [Leick, 1995] following the *minimum variance* solution for the PDA parameters provides an *apostori* estimate of the unit variance. If the *apriori* and *apostori* estimates are not consistent, the *minimum variance* solution should be repeated using the *apostori* estimate for the unit variance. The covariance output from the maximum likelihood solution is a statistical measure of the “error” term given in Equations 4.18 through 4.24.

#### 4.7 Correcting User Measurements with the PDA Model

After the parameters for  $g^{sb}$  ( $\mathbf{x}$  in Equation 4.25) have been derived, the code-phase estimate of the user’s position ( $\hat{X}$ ) can be used with the PDA model to determine the correction that needs to be applied to each CP DD measurement taken by the user. If  $\hat{X}$  is the estimated location of the user and  $R$  is the location of the master reference station, the baseline ( $\Delta\hat{X}$ ) between the user and the master reference station can be computed. This baseline is then substituted into the selected PDA model (Equations 4-18 to 4-24) to generate an estimate of the CP DD error for each non-base satellite. The error is then subtracted from the CP DD measurement taken by the user at the user’s true position ( $X$ ). This process is described mathematically in Equation 4.26.

$$\nabla \Delta \tilde{\phi}_{XR}^{sb} = \nabla \Delta \phi_{XR}^{sb} - g^{sb}(\Delta \hat{X}). \quad (4.26)$$

A physical model of the corrected CP DD measurement can be derived from Equations 3-10, 4-2, and 4-6. This model is given by Equation 4.27.

$$\begin{aligned} \nabla \Delta \tilde{\phi}_{XR}^{sb} &= \nabla \Delta \phi_{XR}^{sb} - k_{\hat{X}R}^{sb} + \xi^{sb}. \\ \nabla \Delta \tilde{\phi}_{XR}^{sb} &= \frac{1}{\lambda} \left\{ \nabla \Delta \rho_{XR}^{sb} + \nabla \Delta do_{XX}^{sb} - \nabla \Delta di_{XX}^{sb} + \nabla \Delta da_{XX}^{sb} \right\} \\ &\quad + \nabla \Delta N_{XR}^{sb} + \nabla dm_X^{sb} + \nabla \eta_X^{sb} + \xi^{sb}. \end{aligned} \quad (4.27)$$

Since  $g^{sb}(\hat{X})$  provides an estimate of the spatial errors between  $\hat{X}$  and R,  $\nabla \Delta do_{XX}^{sb}$ ,  $\nabla \Delta di_{XX}^{sb}$ ,  $\nabla \Delta da_{XX}^{sb}$  are removed in the corrected measurement. The remaining spatial errors result only from the difference between the user's true and estimated positions ( $X$  and  $\hat{X}$ ).  $g^{sb}(\hat{X})$  also removes the non-spatial errors that occur at the master reference station (R). Non-spatial errors at the user's location are not predicted by  $g^{sb}(\hat{X})$ . The modelling error  $\xi^{sb}$  is a function of both the quality of the model and the network measurement noise at each secondary reference station. It must be minimised by selecting an appropriate function for  $g^{sb}(\hat{X})$ .

The modelling error depends upon the type of function used to model the spatial and non-spatial DGPS receiver errors as well as the geometry of the network. One of the objectives of this dissertation is to identify the expected modelling error for several types of models and form some conclusions regarding how the modelling error is affected by the design of the reference network. This dissertation focuses on the evaluation of a specific class of models called PDAs. The PDA that are evaluated are described by Equations 4-18 through 4-24.

To summarise the process:

The network observations are formed according to Equation 4.3 and 4.10. At each epoch, a base satellite is selected, and separate PDA parameters are estimated for each non-base satellite using Equation 4.25. The PDA parameters for all satellites are then sent to user, who computes carrier-phase corrections using the PDAs, and corrects the DD carrier-phase measurements according to Equation 4.26.

#### **4.8 Short History on the Use of PDAs**

Loomis et al. [1991] proposed the use of a PDA as a method of modelling the errors across a code-phase network. The method has never been widely used because noise tends to dominate code-phase measurements and a PDA cannot estimate the non-spatial error at the user's location. In order for the PDA to be effective, the errors being estimated need to be significantly greater than the non-spatial errors affecting the user. The non-spatial errors at the well-controlled location of the reference station should be small. Therefore, the benefit of using the PDA is derived mostly from the correction of spatial errors. Since spatial errors grow at a rate of 2 to 3 mm/km, a code-phase network must be hundreds of kilometres in diameter if the spatial errors are to exceed the user's measurement noise. For a network of this magnitude, the spatial errors are not linear and do not lend themselves to being easily modelled as partial derivatives. Kee et al. [1991] developed a non-linear technique that estimates state-space parameters and models the effects of SA, orbital, and ionospheric errors separately. This technique has become known as WADGPS, and is now a standard for large-scale code-phase navigation networks.

Even though PDAs are not the most elegant method of estimating spatial errors in code-phase networks, the application of PDAs to carrier-phase networks has strong merits.

First of all, carrier-phase noise at the user's location is an order of magnitude smaller than code-phase noise. As a result, the spatial effects are observable on networks of only a few tens of kilometres in size. On small networks, spatial errors tend to be linear, and can be accurately modelled as a first order PDA [Loomis et al., 1991].

Carrier-phase navigation networks have been established and analysed by Raquet [1998], Varner and Cannon [1997], Han and Rizos [1997], as well as Wübbena et al. [1996]. Raquet's work has concentrated on the implementation of the Conditional Adjustment Algorithm (CAA). Wübbena et al. described a multi-station one-dimensional PDA approach to estimating distance dependent errors. According to the concept described by Mueller [1994a], Han and Rizos developed a Minimum Variance Algorithm (MVA) solution using a Gauss-Markov spatial decorrelation function. This dissertation is an outgrowth of previous work by Varner and Cannon [1997]. In that work, the focus was on using multi-dimensional PDAs. This dissertation describes some of the results previously reported for networks in Calgary and New Mexico, as well as presents new results conducted on a network in Southern California.

#### **4.9 Origins of NDGPS**

GPS networks are used to establish survey control points, study land deformation and identify changing atmospheric conditions [Van Dierendonck et al., 1994; Dong and Bock, 1989]. They can also provide positioning services for aviation, land, and marine vehicles [Lapucha, and Barker, 1994].

Code and carrier-phase solutions have been applied to both DGPS and NDGPS concepts. Traditionally, code-phases solutions were used for dynamic applications, while carrier-phase solutions were used for high precision static applications. Today however, the relationship between the applications and their solution methodology is not as clearly

defined. With the introduction of semi-kinematic techniques and on-the-fly ambiguity resolution, CP-DGPS is becoming a more common technique for satisfying the requirements of many dynamic applications. Unfortunately, the difficulty in resolving ambiguities still limits the range for dynamic CP-DGPS to a few tens of kilometres [Weisenberger, 1997], and real-time applications are still having problems achieving satisfactory levels of integrity. Integrity of the CP-DGPS problem has been discussed by [Sennott et al., 1996] and [Braff et al., 1996], but further research is needed to validate the use of these systems as dependable methods of navigation.

NDGPS has been successfully used in code-phase applications to expand the areas of coverage [Alsip and Radice, 1993], and to reduce the levels of ground-based multipath [Braff, 1997]. It has not been well developed for use with dynamic carrier-phase operations.

NDGPS applications can be categorised as being Wide Area, Regional Area, or Local Area. They can also be subdivided into common view or non-common view networks. In addition, processing and communications architectures can have a significant impact the design and development of NDGPS networks.

#### **4.9.1 Wide, Regional, and Local Area Coverage**

Algorithms for use in NDGPS can be logically divided into two domain categories:

- Measurement domain algorithms combine the measurements from multiple reference stations in such a way as to minimise the user's differential measurement error.

- State space domain algorithms use multiple reference station measurements to estimate the state parameters of an error model. This model is then used to correct the user's differential measurement or positioning information.

Though it is a misnomer, the processing of state space domain algorithms is generally referred to as “Wide Area” processing [Kee, 1996; Kee and Parkinson, 1992]. A network that uses this concept is called a Wide Area network. The connection between this concept and the term “Wide Area” resulted from the fact that code-phase networks generally cover large (wide) areas, and they have gravitated toward the use of state-space algorithms.

Measurement domain algorithms are often called “Local Area” algorithms. Networks that use these algorithms are called “Local Area” networks. One high profile example is the Local Area Augmentation System (LAAS), which is being promoted by the United States Federal Aviation Administration (FAA) [Braff, 1997]. LAAS uses a single reference station to provide standard DGPS navigation capabilities to aircraft as they attempt to land at airports during periods of poor weather. In 1996, Wübbena et al. [1996] used the measurement domain technique to improve the carrier phase DGPS positioning performance on a network near Hamburg, Germany. Unfortunately, the “Local Area” terminology has caused some confusion because standard DGPS positioning (DGPS using only a single reference station) is sometimes called “Local Area” DGPS. The result is that it is not always obvious whether “local area” refers to a network or a single reference station configuration. Today, the term “local area” is becoming synonymous with “standard (single reference station) DGPS”, particularly when the overall system is composed of multiple reference stations operating independently.

Because of the confusion introduced by the “Local Area” terminology, some authors refer to the concept of NDGPS as “Wide Area” DGPS regardless of whether the system uses

state-space algorithms or measurement domain algorithms. John E. Chance and Associates offer a “wide area” systems called StarFix II and OmniStar that combine the code-phase measurements from a network of reference stations spread across the North American continent [Lapucha and Barker, 1994]. Many authors are beginning to use the term “Regional Area” DGPS to refer to networks that employ measurement domain algorithms [Basker, 1995]. Regional area is a term that is also being used to describe small networks that use state-space domain algorithms.

#### **4.9.2 Common View and Non-Common View Networks**

The carrier-phase networks can be “common view” or “non-common view” networks. A common view network requires a satellite to be visible at all network reference stations in order for it to be available to the user for the purposes of determining position [Loomis et al., 1991]. As the size of the network increases, low elevation satellites tend to be rejected by common view networks. The curvature of the Earth these satellites from being observed at all stations simultaneously. A non-common view network will process the satellite observations even if the satellite is not visible to all stations in the network (Figure 4-3).

In a common view network, the network mask angle is the minimum elevation angle for which a satellite is visible to all stations. It increases at a rate of about  $0.9^\circ$  for every 100-kilometre increase in the network’s size. Therefore, a common view network that is 500 km across will be unable to use satellites below an elevation of about  $5^\circ$ . The growth of the mask angle limits the size of a single common view network because the loss of satellite visibility eventually becomes unacceptable.

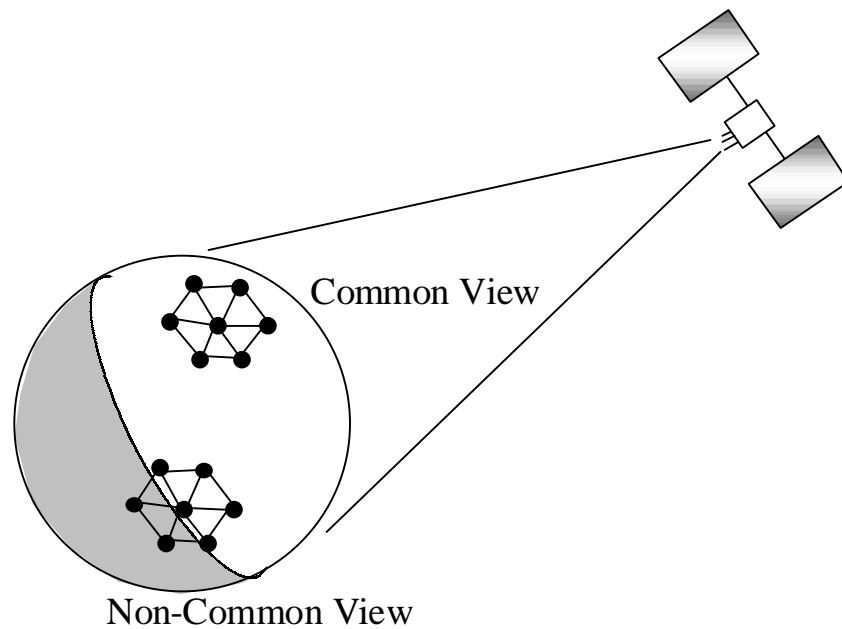


**Figure 4-3: Common View and Non-Common View Networks**

If the network designer is willing to adaptively adjust the selection of the error modelling technique based upon the number of reference stations for which the satellite is visible, the common view restriction can be eliminated. This adaptive adjustment of the modelling technique is extremely complicated, especially if the satellite is not visible at the master station. In addition, a 200-km common view network can see 97% of the sky that is visible to a non-common view network. This means that the network designer does not derive a significant benefit by using a non-common view algorithm unless the network is large (~ 400 or 500 kilometres). As a result, all of the algorithms derived in this dissertation are common view algorithms.

### **4.9.3 Centralised Vs. Decentralised Processing**

The network processing architecture is an important design constraint for CP-NDGPS. In a decentralised network, measurements from all network reference stations are sent to the user (Figure 4-4). The user processes the raw network measurements from each station to derive the measurement correction for the current location. In contrast, a centralised network collects all of the network measurements at a central processing facility. The error correction model is generated explicitly at this facility and sent to the user. Upon receiving the error model, the user computes measurement corrections for the current position. If the degrees of freedom for the selected PDA is greater than zero, then the data link of a centralised network has a lower bandwidth than that of a decentralised network. In subsequent chapters, the proposed measurement correction models fit this criterion. As a result, the networks described herein are best served by a centralised processing architecture.

### **4.9.4 Communications Architecture**

Figure 4-4 could also represent a data link communications model. Centralised data link communications imply that the DGPS corrections are sent to the user from a single transmitter. Multiple transmitters are used in a decentralised data link communications structure. The processing concept and the data link communications architecture are completely independent network design issues. There is no requirement that the location and number of data link transmitters must coincide with the location and number of network reference stations. On the other hand, the network designer may choose to co-locate the transmitters and the reference stations if such an arrangement is convenient. When deciding upon a communications architecture, the network designer must consider the availability of data link frequencies, bandwidth constraints, data link redundancy, transmitter power limitations, and line-of-sight signal blockages.

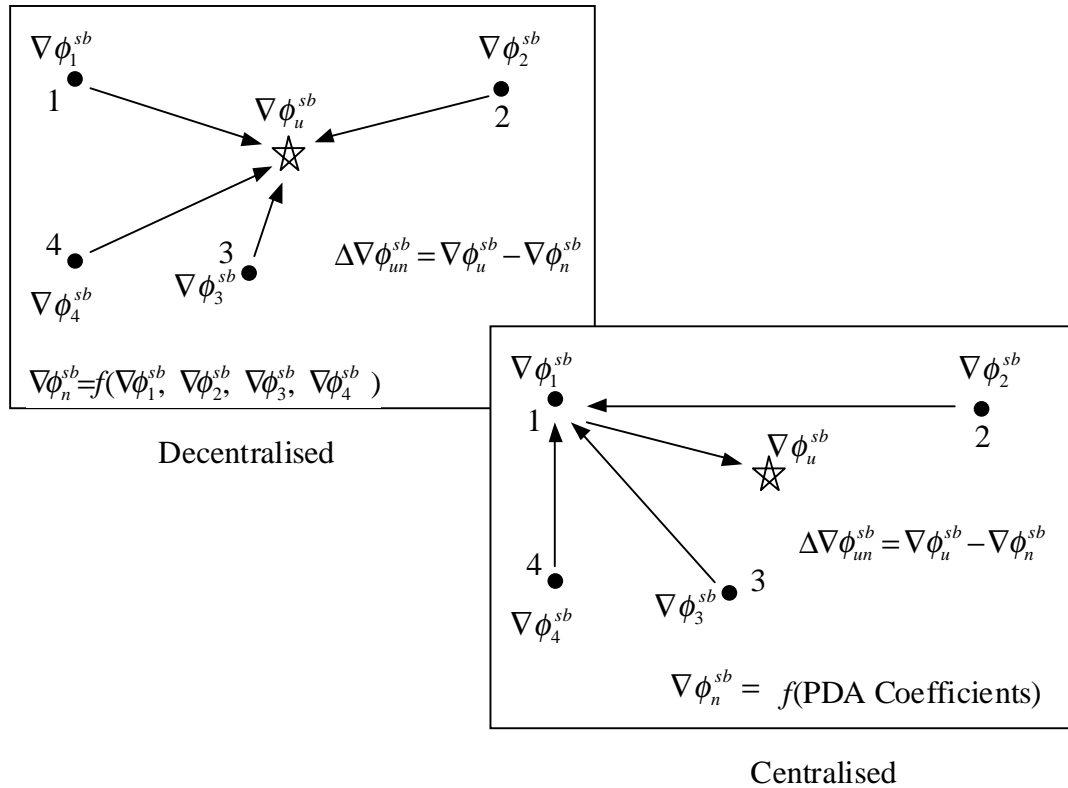


**Figure 4-4: Centralised and Decentralised Processing Models**

#### 4.10 Nearest-Station Concept

If a set of GPS reference receivers is distributed throughout an extended area, the user's DGPS position can be derived using the nearest reference station. The concept allows the user to navigate with DGPS positioning accuracy over a large area by switching from one reference station to the next as the user moves around the network area. This concept is called the "nearest-station concept". Nearest-station NDGPS is nothing more than a patchwork of local DGPS service areas, and does not attempt to combine the measurements from the various network reference stations [Loomis, et al., 1991]. If the user is deriving a position based upon a reference station that is not the closest station, network survey error will cause a differential shift and degrade the accuracy of the user's

position estimate. The USCG DGPS Service, the Canadian Coast Guard DGPS Service, and the Iceland DGPS Network are examples of DGPS networks that operate using the nearest-station concept [Alsip and Radice, 1993; Ryan et al., 1997; Thorsteinsson et al., 1996].

The nearest-station concept is simple and relatively unencumbering, but it has three problems when used with a carrier-phase network:

- 1) The accuracy level within the network has significant variability as the user moves closer to and farther from the various reference stations.
- 2) A large number of stations are required to provide coverage to an extended area.
- 3) For carrier-phase DGPS, the inter-station ambiguities must be estimated/resolved when the user switches from one reference station to the next.

The last issue in the list above only has a significant impact on real-time applications, and can be eliminated with an appropriately designed communication system. If the basic nearest-station concept is improved such that the data link communicates the inter-station ambiguities to the user, then new ambiguities do not have to be estimated when switching to a new reference station.

Anytime the user is in a position to receive differential information from more than one reference station, redundant positions can be derived. Having redundant estimates of position means that the user can perform integrity checks and verify that the position derived from the nearest reference station is correct. Though it is not the focus of this dissertation, further research regarding the subject of integrity is needed.

#### 4.11 Combined-Station Concept

A nearest-station network that is tracking its inter-station ambiguities in real-time is one of the simplest forms of a combined-station network. Other forms of combined-station networks have been promoted as methods of improving the performance of NDGPS. The three fundamental methods mentioned in Section 4.3 are the MVA [Mueller, 1994a], the CAA [Raquet, 1996], and the PDA [Varner and Cannon, 1997]. The MVA and CAA algorithms both involve decentralised processing, and are useful methods of correcting reference station errors when the network has a limited number of stations. By comparison, the PDA technique uses a reduced order error model and is easily designed to operate with a centralised processing architecture. The reduced order model discards some useful information in order to prevent data link saturation [Mueller, 1994a]. This condition can usually be met when the number of stations in the network exceeds 5 or 6.

The MVA adjusts the measurements using a spatial decorrelation function that relates the user's errors to a location within the network [Figure 4-5a]. In this sense, the error model is implicitly contained in the measurement adjustment process. The algorithm can be designed to use a predefined spatial decorrelation function selected by the network designer. Alternatively, the algorithm can be developed to estimate the parameters of the spatial decorrelation function simultaneously with the measurement adjustment [Figure 4-5b]. The method chosen by the designer depends upon the number of reference stations, the mathematical order of the spatial decorrelation function, and the amount of sophistication that the designer wishes to put into the software. Tang et al. [1989] suggested using a Kalman Filter with an implicit linear 1-dimensional decorrelation model (Equation 4.28). This model is based upon the distance between the user and the various network reference stations. A similar technique called Least Squares Collocation can provide equivalent results when the inverse distance function is used. Collocation also provides accuracy information in the form of a variance-covariance matrix, which

can be used to evaluate the performance of the inverse distance model. A technique similar to that suggested by Tang using dual frequency carrier-phase measurements has been promoted by Han and Rizos [1997], and is reportedly capable of performing instantaneous ambiguity resolution on baselines up to 100 km in length.

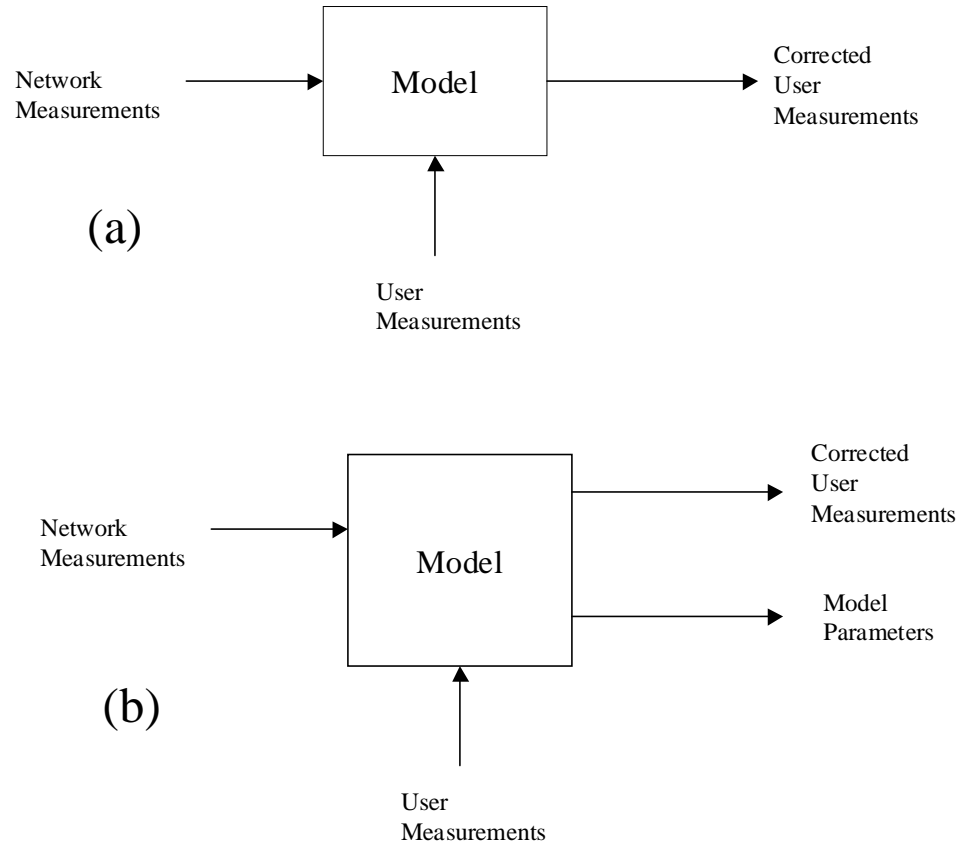


**Figure 4.5: MVA Modelling Modes**

Raquet [1996] proposed the CAA. The CAA adjusts the DGPS measurements based upon a function of spatial and non-spatial (multipath) parameters. This is an implicit algorithm that has been applied specifically to carrier-phase networks. Raquet suggested that the spatial decorrelation function could separate the DD satellite corrections into their individual satellite components. By conditioning the estimator to account for dependencies in the DD measurements, individual satellite corrections are generated.

This algorithm is based upon collocation theory, where an elevation mapping function is used to relate the errors between satellites.

$$\rho_c = \sum_i W_i \rho_i = \text{Corrected Range Measurement.} \quad (4.28)$$

Where:

$$W_i = \frac{\frac{1}{d_i}}{\sum_j \frac{1}{d_j}}$$

$d_i \equiv$  Distance to Reference Station  $i$ .

$\rho_i \equiv$  Range Measurement at Reference Station  $i$ .

As mentioned previously, MVA and CAA algorithms make use of all the information available from the network measurements. They also have the potential to overload the data link when the network consists of a large number of reference stations. Table 4-4 shows the amount of data that must be transmitted through the data link for different algorithms. As an example, a network that observes 8 satellites at 9 reference stations must send 56 separate measurements (words) to the user who is applying the MVA or CAA technique.

**Table 4-4: Data Link Throughput Requirements for Different Algorithms**

Algorithm ( $n$ = Number of Satellites)	Words of Data Transmitted
PDA ( $\tau$ = Number of PDA Parameters)	$\tau^*(n-1)$
MVA and CAA ( $l$ = Number of Reference Stations)	$(l-1)^*(n-1)$

Varner and Cannon [1997] have suggested that the PDAs reduce the bandwidth requirements for large networks because the algorithms are “reduced order” spatial functions for the DD errors that are measured at each reference station. If the PDA is a 4-parameter model, like Equation 4.23, then for parameters for each satellite pair must be

sent to the user. In the above example of 8 satellites and 9 reference stations, the PDA only needs to send 28 pieces of information (words). Raquet and Lachapelle [1997] stated that a similar technique could be applied to a grid of corrections generated by the CAA algorithm.

#### **4.12 Spatial and Non-Spatial Error Categories**

The PDA technique does not attempt to separate spatial and non-spatial errors into their physical components (e.g. orbit, ionosphere, troposphere, multipath). Rather, the individual errors are “lumped” into spatial and non-spatial categories. This “lumping of the errors can affect the accuracy of the PDA prediction. If the actual physical errors of the orbit, ionosphere, and troposphere are linear functions of the baseline length, then the “lumped” parameter is also linear. In this case, a linear PDA will give better accuracy than an algorithm that estimates each parameter separately because the solution has fewer degrees of freedom when using the “lumped” parameters. On the other hand, if the actual errors are non-linear, “lumping” the parameters into a low order spatial/non-spatial model can degrade the accuracy of the prediction. Orbital and ionospheric errors have similar effects on the DD measurements collected on short baselines. As a result, it is difficult to separate the measurement errors into their individual sources using small networks. For this reason, the errors are consolidated into spatial and non-spatial components, which can be identified by having a variety of baseline lengths within the network. This is an ideal situation in which to use a spatial/non-spatial PDA. In this dissertation, several PDA models are proposed and their accuracy analysed.

A network of reference stations can separate spatial errors from non-spatial errors because the network has a variety of baselines of differing lengths. Since the magnitude of the spatial error is directly related to the baseline length, it is possible to identify that portion of the error that is spatial.

The measurement errors that result from ionospheric advance and orbital error have strong spatial characteristics. Over small areas, these errors grow linearly with baseline length. Receiver noise is non-spatial, and its characteristics at one reference station are completely independent from its characteristics at other stations. Even though code and carrier-phase multipath have different magnitudes, they are generated by the same source or sources. The spatial nature of both forms of multipath tends to decorrelate over a few hundred metres [Parkinson and Enge, 1996]. Therefore, multipath is a non-spatial error for networks whose stations are separated by more than a 200 or 300 metres. Tropospheric error caused by the wet atmosphere decorrelates over a few kilometres [Parkinson and Enge, 1996]; but if the dry tropospheric effects are unmodelled, poorly modelled, or modelled using incorrect environmental conditions, tropospheric error can grow as a spatial function for several hundred kilometres.

#### **4.13 Network Initialisation and Recovery from Geometry Changes**

When a network first begins operations, the inter-station ambiguities for all satellites are unknown and must be estimate/resolved before network measurements can be formed, PDAs generated, and measurement corrections calculated. The period of time following start-up during which the corrections available because the inter-station ambiguities have not been fully resolved is called the initialisation period.

A problem very similar to initialisation is associated with recovering from discontinuous changes in the satellite geometry. In this case, the inter-station ambiguities of a rising satellite are unknown and must be estimated/resolved before the satellite is available for use. Ambiguity resolution can be achieved using short baseline network linking, post-process filtering, or possibly a technique called “combined ambiguity and bias estimation”. The advantages and disadvantages of these techniques will be discussed in

the following sections. Widening is also an option that makes initialisation and geometry changes easier to handle, especially when using the “ $\alpha$  only” model.

#### **4.13.1 Network Initialisation**

Network initialisation is the process of establishing the inter-station ambiguities of all visible satellites on all network baselines for the first time. When the network first starts operation – or is restarted because of some type of system wide interruption – the inter-station ambiguities are unknown for all baselines. The initialisation period is the time after start-up when the accuracy of ambiguity estimates is poor. During the period of network initialisation, the user is not provided with network reference information for any satellite, and CP-NDGPS positioning is not possible.

#### **4.13.2 Network Recovery from Geometry Changes**

Visible GPS satellites provide the carrier-phase measurements that are used to determine the user’s position. The location of these satellites in the sky defines the measurement geometry. The geometry continuously changes as the satellites move, but discontinuous changes in the geometry occur when new satellites appear (rise) or disappear (set) from view.

When a satellite rises, its ambiguities are initially unknown. These ambiguities must be estimated/resolved before the satellite PDA parameters can be supplied to the user. Other satellites can be used for positioning during the period that the rising satellite’s ambiguities are being estimated.

When a satellite sets at one of the network reference stations, there are three options:

- Continue normal operation? (Drop station; DOF must be greater than zero)
- Reduce the order of the PDA (Non-common View network)
- Stop generating PDAs (Common View network)

Normal operation can continue only if the number of secondary reference stations for which the satellite is visible is greater than the order of the PDA. In a non-common view network, the order of the PDA may be reduced if the number of secondary stations observing the affected satellite becomes insufficient to support the current PDA.

#### **4.13.3 Short Baseline Network Linking**

If the distances between the network reference stations are short (10 to 15 km for an L1 network), the inter-station ambiguities can be resolved quickly by using a “fixed baseline” ambiguity resolution technique. This technique sets the ambiguities to integers that minimise the difference between the predicted and measured carrier-phases. The predicted carrier-phase is derived from the known “fixed” length of the baseline. The assumption is that for short baselines, the differential errors are less than a half of an L1 wavelength. Therefore, selection of the integer that is nearest to the floating-point value for the ambiguity results in a correct resolution of the ambiguity. Averaging (filtering) over a short period of time can reduce the noise and improve the integrity of the resolution process. This real-time technique can be used to set the ambiguities for both the initialisation and “rising satellite” problems.

The fixed baseline resolution technique resolves ambiguities quickly. As long as the extremities of the network can be connected using a set of reference stations that form a “linked” series of short baselines, the ambiguities along the individual links can be accumulated to derive the ambiguities for any baseline in the network.

For single frequency operations, the baseline lengths are limited to a maximum of 10 to 15 km. 40 to 60 km may be tolerable baseline lengths when using the dual-frequency widelane measurements. Obviously, this technique requires a large number of reference stations if the network is of any substantial size.

The baseline separation distances quoted above depend upon the solution confidence level desired from the system. The greater the confidence desired for correct resolution of the ambiguity, the shorter must be the baseline between the reference stations.

Network linking does provide a significant benefit over a nearest station network. For L1 networks having a scale of 100-km or more, network linking requires far fewer reference stations than a fully populated nearest-station network. For example, suppose that the design requirement for an L1 network states that the DGPS correction error is to be no larger than that which would be observed by a standard DGPS user who is 15 km from a reference station. Further suppose that PDAs can reduce the DGPS correction error to this requirement across the expanse of a 105-km network. Operating in a nearest-station mode, this network requires at least 25 reference stations that are separated by no more than 30 km. By comparison, a combined network that uses network linking only needs 9 reference stations positioned along the two network diagonals.

If the network operates in a widelane mode, networks of 400 or 500 km can be serviced using a comparable number of reference stations. However, the positioning accuracy is degraded by a factor of 4 with respect to that of an L1 network (See Tables 3.1 and 3.3).

#### 4.13.4 Batch Process Filtering

Near-instantaneous ambiguity resolution using fixed baselines is unreliable for long baselines because the spatial and non-spatial errors have a high probability of exceeding a half cycle of carrier-phase wavelength. An obvious method of improving the resolution process is to filter the ambiguities as floating-point values over time using batch estimation prior to resolution. Sun et al. [1999] has shown that resolution can be achieved in a few hundred seconds for widelane observations on 100 to 300 km baselines. This estimation technique is used in Chapter 5 to analyse networks operating in Calgary and New Mexico. Batch filtering software called SEMIKIN™ [Cannon, 1990] is used to process the fixed baseline ambiguities over an estimation period of several hours in duration. This software was developed at the University of Calgary for semi-kinematic surveying and positioning applications. After the ambiguities have been resolved to integers, the original observations are used to derive network measurements for each epoch during the period of analysis.

This is a post-processing technique that significantly increases the probability of achieving correct ambiguity resolution on the network. By batch processing 3 to 5 hours of data, correct ambiguity resolution is possible on L1 networks with baselines of as much as 75 or 100 km.

This technique is not useful for real-time applications. In real-time operations the ambiguities have to be resolved as soon as possible following the time at which the satellite rises. If it takes an hour or more to resolve the ambiguities, then useful navigation is severely compromised.

#### 4.13.5 Combining Ambiguity and Parameter Estimation

If the scale of carrier-phase network is extreme (for instance, an L1 network of 300 to 500 km), an unacceptable number of reference receivers is required even when using network linking. In a case such as this, many of the reference stations serve no other purpose than to link the extremities of the network. The network measurements collected by the intermediate stations do not significantly improve the accuracy of the PDA model, but they are required because the ambiguities for the outermost stations must be resolved quickly in order to conduct real-time operations. If the ambiguities can be resolved without the need for short baseline linking, then PDAs of reasonably equivalent performance can be generated with far fewer reference stations.

Blewitt [1989] combined the process of estimating the ambiguities with that of estimating residual bias parameters. These bias parameters are the time-averaged expected value of the network measurements. Since the non-spatial errors are assumed to have a time-averaged expected value of zero, these bias parameters represent the time-averaged spatial decorrelation error at each of the secondary reference stations. The method implemented by Blewitt successfully resolved the widelane ambiguities on baselines as long as 2000 km. These results were based upon the batch estimation of four days worth of data, and do not represent a feasible real-time system. In independent tests, Dong and Bock [1989] reliably resolved the widelane ambiguities on 640-km baselines using 7.5 hours of data. Both researchers used GIPSY software [Hurst, 1995] developed at JPL in California.

Neither Blewitt nor Dong and Bock had any intention of applying this technique to real-time processes – the goal of their research was to resolve ambiguities on long baselines. Theoretically however, the common estimation of ambiguities and biases provides more information to the ambiguity resolution process than network linking. Ergo, resolution on 20 to 50-km baselines should be achievable with fewer reference stations. Unfortunately,

there has been no research to confirm this hypothesis, and to date, real-time carrier-phase networks must use some form of network linking to quickly resolve the ambiguities.

#### **4.13.6 Dual Frequency Thinning**

Large networks may be designed to use the widelane carrier-phase measurements instead of the single frequency L1 measurements [Raquet, 1998]. The ambiguities can be resolved faster, and on longer baselines, when using widelane measurements. This is a significant advantage, but it comes at a cost. Widelane networks are much more vulnerable to signal interruption because the widelane measurement is a combination of the L1 and L2 measurements. Since, both measurements are required in forming the widelane measurement, the loss of either the L1 or L2 signal causes a loss of the widelane measurement. This means that the satellite is unusable until the widelane ambiguity is once again estimated/resolved. The problem is compounded when considering that:

1. The L2 carrier-phase signal strength is designed to have a signal strength that is only a quarter of the strength of the L1 carrier-phase [Air Force, 1992], and
2. The codeless and semi-codeless technologies required for civilian GPS receivers have less signal power processing gain than the fully correlated military receiver (See Section 2.5.4.1).

Therefore, the L2 signal is more vulnerable to interference by background radio noise, especially for civilian receivers. When a satellite measurement is lost, the measurement geometry is thinned and frequent periods of poor positioning accuracy may result.

#### **4.14 Parameter Filtering**

Network parameters are normally provided for all satellites during each measurement epoch. While analysing the results obtained from widelane networks in New Mexico and Scandinavia, Raquet [1998] observed that the measurement corrections had low dynamic characteristics and suggested that epoch by epoch updates may not be required. He proposed that 1 Hz measurement corrections could be filtered and provided to the user every 5 to 20 seconds. If such is the case, the concept of parameter filtering could provide a proportional reduction in the data link bandwidth.

## Chapter 5

### PROCESSING METHODS

#### 5.1 Overview

In this chapter, the methods of processing network data are developed. These methods are described specifically in terms of the carrier-phase measurements and PDA corrections. A procedure is developed to test the performance of a network using PDA corrections at a set of static test stations. The technique relies upon batch processing data from these test stations, but potential methods of handling real-time applications are also discussed.

#### 5.2 Processing Software and Concerns

There are a variety of software products available that perform carrier-phase DGPS position solutions for the user. These products can be adapted to operate as processing engines for generating PDAs. The data analysis in Chapter 6 uses carrier-phase DGPS positioning as an underlying part of the PDA solution. The DGPS positioning solutions are computed using SEMIKIN™ [Cannon, 1990].

Carrier-phase positioning assumes that the constant ambiguity of each measurement has been accurately estimated or resolved. If the receiver stops tracking the GPS signal for even for a fraction of a second, the value of the ambiguity can change. This event is called a “cycle slip”. After a cycle slip occurs, the ambiguity estimation/resolution process must be reinitialised. For real-time systems, GPS solutions cannot use the affected measurement during the initialisation period and poor positioning performance may result. In this dissertation, the problem is avoided by post-processing the data using batch estimation.

Figure 5-1 is a generic description of the carrier-phase solution process used by SEMIKIN™. There are three fundamental events that occur during the solution process. First, cycle slips need to be detected. Second, the ambiguities are estimated/resolved; and third, the state (i.e. position, velocity, time, etc.) is estimated. Only static processing is performed during the analysis of the data in this dissertation. In a static post-processing mode, SEMIKIN™ does not require code-phase measurements to resolve the ambiguities. However, a real-time system will probably include code-phase measurements in the solution process. Since code-phase measurements may or may not be used depending upon the architecture of the solution software, their use is shown in Figure 5.1 with a dotted line.

In Figure 5-1, the GPS receiver observes the code-phase measurement ( $p^s$ ) for each satellite “s”. The combined set of all  $p^s$  is the code-phase measurement vector ( $\mathbf{p}$ ). The size of this vector is equal to the number of satellites ( $n$ ). A similar vector  $\phi$  is created for the carrier-phase measurements. The vector of estimated ambiguities ( $\hat{N}$ ) and the carrier-phase measurement vector are passed to the state estimation process, where the user’s state is derived.

During the cycle slip detection process, a cycle slip is identified by comparing the individual carrier-phase measurements with carrier-phase predictions ( $\bar{\phi}$ ). In SEMIKIN™, the state dynamics model is either a constant velocity model (Equation 5.1) or a constant position model (Equation 5.2). During static processing, it uses the constant position model, but the constant velocity model is used when the kinematic mode is selected. In both models, the carrier-phase measurements of the current epoch can be predicted from those of the previous epoch using the measurement rate of change, which is computed by differencing past measurements.

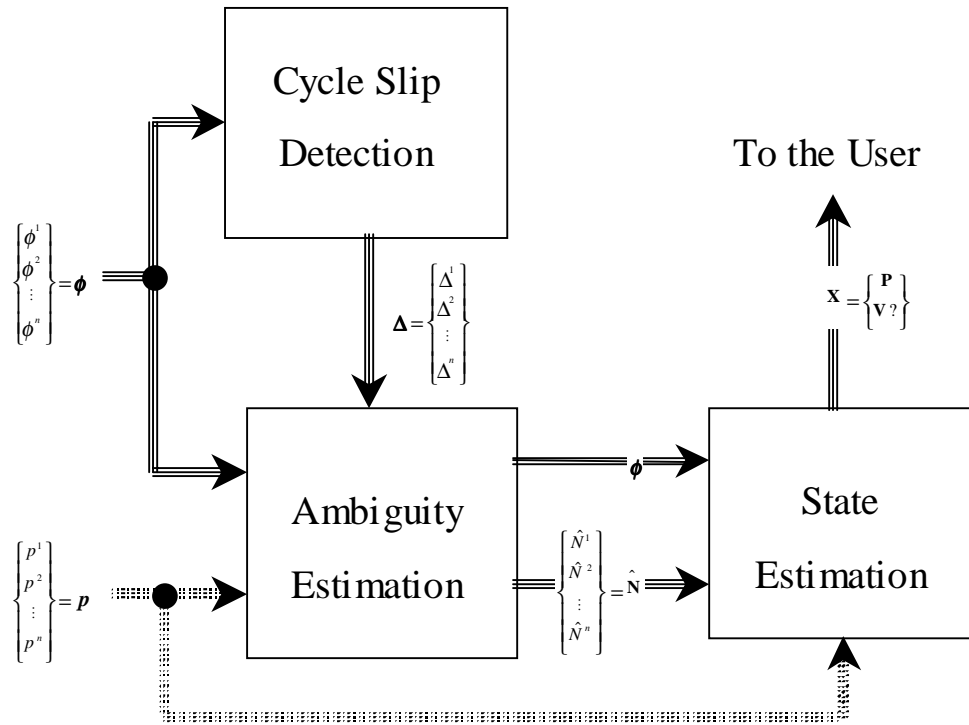


**Figure 5-1: Carrier-Phase Solution Architecture**

$$\mathbf{P} = \mathbf{P}_0 + \mathbf{V}_0 \mathbf{t} . \quad (5.1)$$

$$\mathbf{P} = \mathbf{P}_0 . \quad (5.2)$$

If the actual carrier-phase measurement at the current epoch lies outside of a tolerance envelope that is centred on the value of the predicted carrier-phase measurement, then a cycle slip is said to occur. The tolerance range is dictated by the accuracy with which the dynamics model can simulate the true state dynamics.

For example: A vehicle that is accelerating at  $6 \text{ m/s}^2$  will experience a position error of 3 metres when using a constant velocity model over a prediction period of 1 second. If the acceleration is in the direction of a particular satellite, the position error has a one-for-one mapping into the measurement (range) domain. Since, a 3-metre range error translates into a 15-cycle error in the L1 carrier-phase measurement, the cycle slip tolerance should

be set to 15 cycles when measurements are sampled every second under these dynamic conditions.

In order to support a 1 Hz sampling frequency, the default cycle slip tolerance range for SEMIKIN™ is set at 15 cycles. In Chapter 6, a carrier-phase network in California is analysed using a sampling interval of 30 seconds (frequency = 1/30 Hz). As a satellite passes over a fixed point on the Earth, the rate of change of Doppler can be more than half a cycle per second<sup>2</sup>. Over a 30-second period, a linear prediction of the carrier-phase between two static reference station can experience variations of more than 15 cycles due to the natural accelerations of the satellites themselves. The default cycle slip tolerance of 15 cycles causes too many false slips to be detected. Therefore, when analysing the California network in the next chapter, the cycle slip tolerance in SEMIKIN™ is increased to 3500 cycles and should be more than adequate for handling all, but the most stressful dynamic conditions. This is more than adequate considering that all of the test stations are static and have no appreciable acceleration.

If a cycle slip is detected for a particular satellite, a “slip detected” signal ( $\Delta^s$ ) is provided to the ambiguity filter. The vector of “slip detected” signals for all satellites ( $\Delta$ ) is also of size  $n$ .

The ambiguity estimation/resolution process estimates the ambiguity vector  $\hat{\mathbf{N}}$  and its accuracy  $\sigma_{\hat{\mathbf{N}}}$ . If possible, this process also attempts to resolve the ambiguities to their correct integer values.

In SEMIKIN™, the ambiguity estimation process is combined with the state estimation process. If ambiguity resolution is achieved, then the state estimation process is simplified by removing the ambiguity parameters from the vector of estimated parameters.

### 5.3 State and Noise Filtering

The method used to convert measurements of range into an estimate of user position is called state estimation, or state filtering [Tapley, 1990]. The user's state  $\mathbf{X}$  is defined as a vector of three parameters when estimating position {Equation 5.3(a)}. In this equation, “x”, “y”, and “z” are the three dimensional coordinates of user's position. When estimating position and velocity, the state is a vector of six parameters {Equation 5.3(b)}. In this equation, the three dimension velocity components ( $\dot{x}$ ,  $\dot{y}$ ,  $\dot{z}$ ) are also part of the state vector. 5.3(c) is the state vector if ambiguities are being estimated in conjunction with the position and velocity parameters.

Any solution which involves the estimation of the carrier-phase ambiguities is called a “float” solution because the ambiguities can change (or float) from epoch to epoch during the estimation process. Float solutions commonly have state vectors that resemble Equation 5.3(c), but the ambiguities could also be separated from the state and estimated in an independent filtering process [Cosentino, 1996]. If the ambiguities can be resolved, they are set to constant integers, and removed from the estimation process. Carrier-phase solutions in which the ambiguities are resolved are called “fixed” solutions because the ambiguities are “fixed” constants.

$$\begin{aligned} \mathbf{X}^T &= \{x \quad y \quad z\} & \text{(a)} & & \mathbf{X}^T &= \{x \quad y \quad z \quad \dot{x} \quad \dot{y} \quad \dot{z}\} & \text{(b)} \\ & & & & \mathbf{X}^T &= \{x \quad y \quad z \quad \dot{x} \quad \dot{y} \quad \dot{z} \quad N^1 \quad N^2 \quad \dots \quad N^n\} & \text{(c)} \end{aligned}$$

Equation 5.3

In order to estimate the components in  $\mathbf{X}$ , the number of range measurements – whether derived from code or carrier-phase observations – must be greater than the number of state parameters. If both position and velocity are being estimated, then measurements are normally collected at two or more time epochs. In general, multiple time epochs of

measurements must be collected when estimating the ambiguities also. When SEMIKIN™ is operated in a static mode, the velocity components are not estimated. A more detailed explanation of state estimation can be found in the work of Brown and Hwang [1997], Leva et al. [1996], Wells et al. [1986], and Axelrad and Brown [1996].

The most important aspect of state estimation is that the accuracy of the user's estimated state is directly proportional to the accuracy of the range measurements. The relationship is given by Equation 5.4, where the Dilution of Precision (*DOP*) is the constant of proportionality between the user's position accuracy ( $\sigma_x$ ) and the average range accuracy of the satellites ( $\sigma_r$ ).

$$\sigma_x = DOP \cdot \sigma_r . \quad (5.4)$$

If the DOP is relating the accuracy of the three-dimensional position to the accuracy of the range measurements, then it is called Position DOP (PDOP). An average value for PDOP is approximately 2.5 [Parkinson, 1996b], which means that when the accuracy of the average range measurement is 1.0 m, then the accuracy of the user's position is 2.5 m.

## 5.4 Ambiguity Resolution

As shown in Section 2.4.2, the ambiguity is an integer number. As the accuracy of the ambiguity estimate improves, it may become possible to select the correct integer ambiguity and remove the ambiguity parameters from the estimation process. If this does transpire, then the ambiguities are said to have been resolved.

There have been a variety of methods proposed for resolving ambiguities. Some will be discussed in the following paragraphs. Theoretically, however, ambiguity resolution can

only occur when the ambiguity confidence level  $C_N$  falls below half a cycle  $\left(\frac{1}{2}\lambda\right)$  (Equation 5.5). The ambiguity confidence level is the product of the confidence factor  $F$  and the ambiguity estimation accuracy  $\sigma_{\hat{N}}$ . The latter is a product of the state or ambiguity estimation process, and the former is obtained from the integrity requirements imposed by the application. Assuming that the errors in the ambiguity estimate are normal with zero mean, an application that requires the ambiguity estimate to be within with a confidence level of 95% must use a confidence factor of 2 [van Diggelen, 1998].

$$C_N = F \cdot \sigma_{\hat{N}} < \frac{1}{2}\lambda. \quad (5.5)$$

The theoretical technique described above is not commonly used because the time required to converge the estimates in the ambiguity filter to within  $\frac{1}{2}\lambda$  is often too great to be useful, particularly for real-time applications. Many of the fastest resolution techniques rely on empirical, or indirect, information to resolve the ambiguities. These empirical methods isolate of potential ambiguity sets, and the residual errors that result from using a specific set of ambiguities are an indirect indication of the correctness of the ambiguities in that set. The set of ambiguities that has the lowest residual errors for an epoch – or a series of epochs – is identified as the most likely solution set. Empirical constraints on the relationship between the residual errors of the different ambiguity sets are used to determine if resolution has occurred. For instance, a 2:1 ratio of the RSS residuals is often used as a resolution constraint. With this type of constraint, resolution is said to occur when the RSS of the residuals for the second most likely ambiguity set are twice as large as the RSS of the residuals for the most likely ambiguity set. While empirical techniques tend to be fast, their integrity is still the subject of much research.

The implementation of empirical resolution techniques is varied among authors. Hatch [1991], and Remondi [1991] have both discussed the use of scanning techniques in the

process of fast ambiguity resolution. Other techniques have been developed specifically for fast resolution in non-static environments. This class of ambiguity resolution methods is called On-The-Fly (OTF) ambiguity resolution. Examples of OTF methods include the Fast Ambiguity Resolution Approach, the Ambiguity Function Method, the Cholesky Decomposition Method, Lattice Transformations, and the Fast Ambiguity Search Filter [Chen and Lachapelle, 1994]. More recently, Teunissen and Tiberious [1994] have considered methods that decorrelate the ambiguities before they are resolved. SEMIKIN™ uses a fundamental Hatch scanning technique, and does not have OTF capability.

When evaluating the inter-station ambiguities of a carrier-phase network, it is important to have accurate ambiguity estimates in a short period of time. The ambiguity estimation accuracy and the time required for the resolution of ambiguities depend upon the length and number of inter-station baselines. Reducing the length of the baselines, or increasing the number of baselines can improve the ambiguity estimation accuracy and shorten the time required for resolution.

In order to achieve ambiguity resolution on all inter-station baselines, the concept of Short Baseline Network Linking is applied (see Section 4.12.3). In cases where this is not possible, the ambiguities are resolved by way of post-processing (see Section 4.12.4).

## **5.5 PDA Implementation**

The standard version of the SEMIKIN™ software has an option that allows it to record measurement residuals to a file. Measurement residuals that are computed by SEMIKIN™ are the difference between the actual carrier-phase measurements and the expected measurements. At each epoch, the position of the GPS receiver is estimated, and the expected measurements are derived from this estimated position. This

description of measurement residuals indicates that they are similar to network measurements. The difference is that the network measurements are derived from the true (surveyed) position of the receiver rather than the estimated position, which is computed by the filter at each epoch of time (See Equations 4.8 and 4.9). Because of the similarity between measurement residuals and network measurements, SEMIKIN™ was easily modified to output network measurements to a file. As described in Chapter 4, PDA parameters can be estimated for each satellite/base satellite pair by using the network measurements that are derived from this special version of SEMIKIN™. The concept is shown in Figure 5-2.

The network measurements are then used to estimate the parameters of the selected PDA for each satellite pair according to Equation 4.30. There are two pieces of software that have been developed to perform the PDA parameter estimation. One is an Excel spreadsheet that accepts network measurements and has a “macro” program to perform a worksheet estimation. The other is a C++ program called “PDAModel”. Both programs perform the same algorithmic functions. The Excel spreadsheet is useful for analysing the data and generating graphical results, while the C++ program is fast and efficient at generating alphanumeric results.

Once the PDA parameters are estimated, they are used to calculate a measurement correction ( $\Delta c^s$ ) at the user’s location according to the PDA model  $\{g(\hat{U})\}$ . Several PDA models were suggested in Chapter 4 (e.g. Equations 4.23-4.29) and are evaluated in Chapter 6. The process flow diagram is given in Figure 5-3.

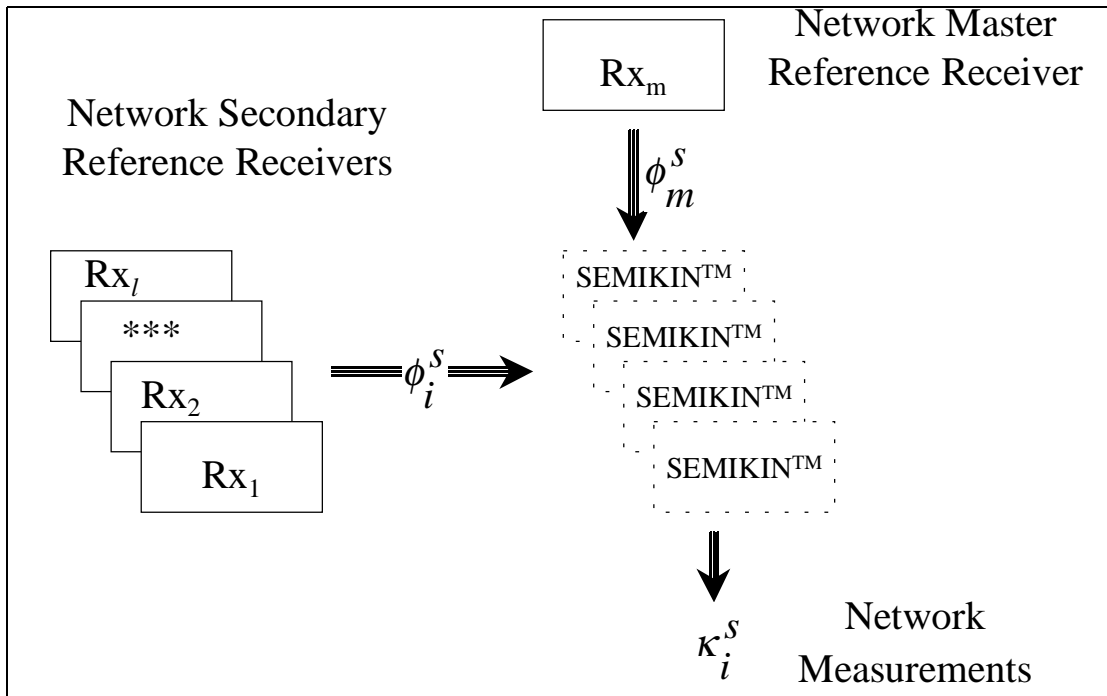


Figure 5-2: Network Processing Implementation

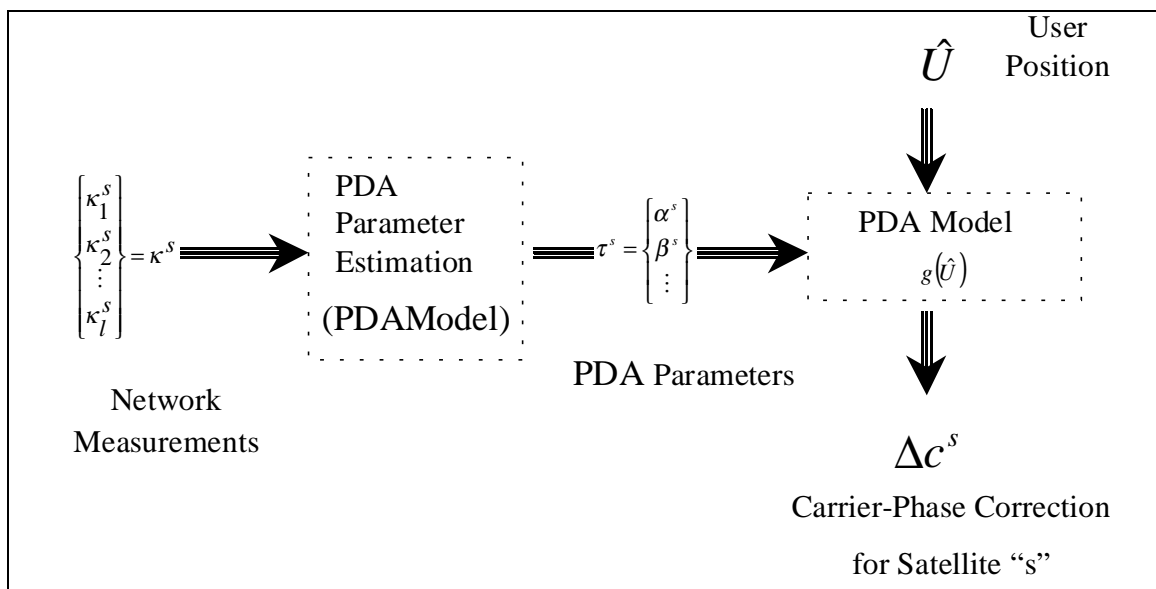


Figure 5-3: Generating Phase Corrections from Network Measurements

## 5.6 Testing Procedure

A testing procedure is created to analyse the performance of the PDA. This procedure compares the position and phase measurement errors of a standard CP-DGPS solution ( $\delta\mathbf{U}_{DGPS}$ ,  $\delta\phi_{DGPS}$ ) against the same errors that result when using PDA corrections in the solution ( $\delta\mathbf{U}_{PDA}$ ,  $\delta\phi_{PDA}$ ). In both cases, the true errors in position and phase are derived by subtracting the estimated position and phase ( $\hat{\mathbf{U}}$ ,  $\nabla\Delta\phi$ ) from the true position and phase ( $\mathbf{U}$ ,  $\nabla\Delta\phi_T$ ) at the test site. The true position and phase is computed from the surveyed location of the test site. The locations of the test sites are established from the network survey. The PDA models are generated from a subset of the reference stations within the network, but the test sites are not part of this subset. The process is described graphically in Figure 5-4.

## 5.7 Real-Time Issues

All of the results contained in this dissertation are post-processed, but the ultimate goal is to provide satellite PDA corrections to the user in real-time. It has already been indicated that real-time operations may require network linking, but issues involving the data link design, data latency, and software tuning need additional research and analysis if real-time operations are to occur.

### 5.7.1 Data Link

The data link is the interface between the reference network and the user. The measurements, corrections, or error models from the reference network are sent to the user via the data link. Since the user is often assumed to be in motion, radio data links

are the most common implementation. An excellent treatment of various types of radio data links can be found in Parkinson and Enge [1996].

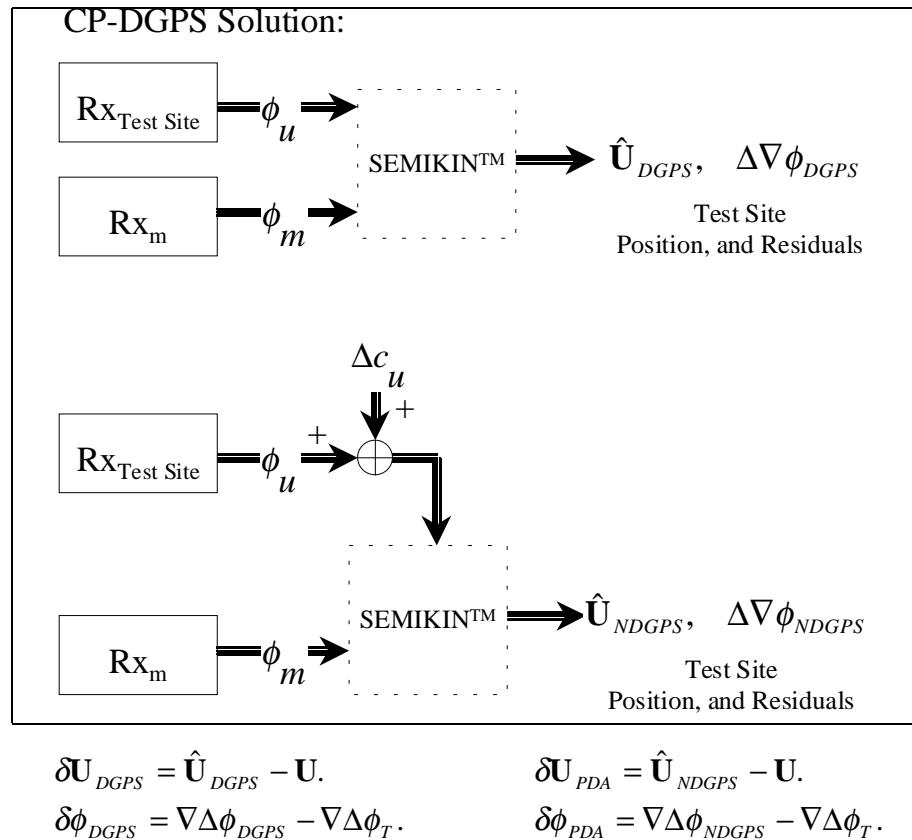


**Figure 5-4: Testing DGPS and PDA Solutions**

The data link design is the primary beneficiary of using a PDA. Many of the CP-NDGPS techniques that compete with the PDA concept are properly described as “full order” models. The PDA – as the name suggests – is a “partial order” model. The significance of this is that a “partial order” model has less data to transmit to the user, and therefore, requires a lower data link bandwidth. This is especially important when the network contains many stations. A network of 13 stations can be modelled as a 12<sup>th</sup> order function. If the network errors are instead modelled with a 4<sup>th</sup> order PDA, the data link bandwidth can be reduced by a factor of 3.

### 5.7.2 Latency

The reference station information that is being transmitted through the data link is delayed in its arrival at the user's receiver. This means that the most current measurements collected by the user do not correspond to the same time epoch as the most current reference information received from the data link. The difference in time between the collection of reference information and the currently received user measurements is called latency [RTCM 104, 1994].

Reference information collected in past epochs (latent data) is often used with the current code-phase measurements collected by the user, but the errors associated with using latent data can prevent ambiguity resolution if carrier-phase measurements are used. If ambiguity resolution is desired at the user's location, it is often necessary to "match" the time epoch of the latent data with that of past user measurements. This means that the user must store the past measurements in order to resolve the ambiguities at the match time.

After the ambiguities have been estimated and/or resolved, the user's position at "match time" can be determined. Projecting the "match time" position forward to the current epoch using the computed velocity vector is the most accepted method of deriving the user's current position. If the ambiguity estimation is performed separately from the position/velocity estimation, then the latent measurements can be modified to include the ambiguity estimates. In this case, position and velocity estimation is possible by projecting the modified latent measurements forward to the current epoch using the rate of change of the measurements. As mentioned earlier, this real-time method is not implemented in the analysis of this dissertation.

### 5.7.3 Software

The real-time user of a carrier-phase network needs to estimate ambiguities and positions at each epoch in which observations are available. This type of solution is possible with a Kalman or Bayesian filter using either “Semi-Kinematic” or OTF methods.

Semi-kinematic software resolves the ambiguities while the user is stationary. Once the ambiguities have been resolved, the software allows the user to move. SEMIKIN™ is an example of semi-kinematic software.

OTF software resolves the ambiguities regardless of whether the user is moving or not. FLYKIN™ is an example of OTF software that has been developed by The University of Calgary [Lachapelle et al., 1992].

In their post-processing versions, SEMIKIN™ and FLYKIN™ require no modifications to work with PDA corrected reference information. For real-time operations though, the PDA model must be incorporated into the software functions that preprocess the data link information. This is not trivial, and has not been attempted as part of this dissertation.

## **Chapter 6**

### **TEST CASE RESULTS AND ANALYSIS**

#### **6.0 Overview**

With the theoretical basis for using PDAs now established, empirical results that validate the theory are desired. In this chapter, three different implementations of a PDA carrier-phase network are analysed. Spatial errors are shown to exist on small carrier-phase networks using test stations as described in Chapters 4 and 5. The errors are modelled using PDAs, and the error prediction performance of the PDAs is quantified.

#### **6.1 Calgary and New Mexico Sample Networks**

Two networks were used for preliminary analysis with each one implementing dual frequency GPS receivers. Spatial errors are difficult to observe on small networks when using the widelane measurements. Therefore, both networks discussed in this section were operated as single frequency L1 networks for the PDA analysis.

The first of these networks was a small network. It was set up near Calgary where three receivers collected data over a 15-km expanse in October 1996. The other network was 70 to 100 km in size. It was installed and operated at Holloman Air Force Base in New Mexico during a three-day period in August of 1996. NovAtel MiLLennium Receivers were used in the Calgary network, while a combination of four Novatel MiLLennium receivers and one Ashtech Z-12 receiver was used at Holloman. A description of both networks is given in Figure 6-1.

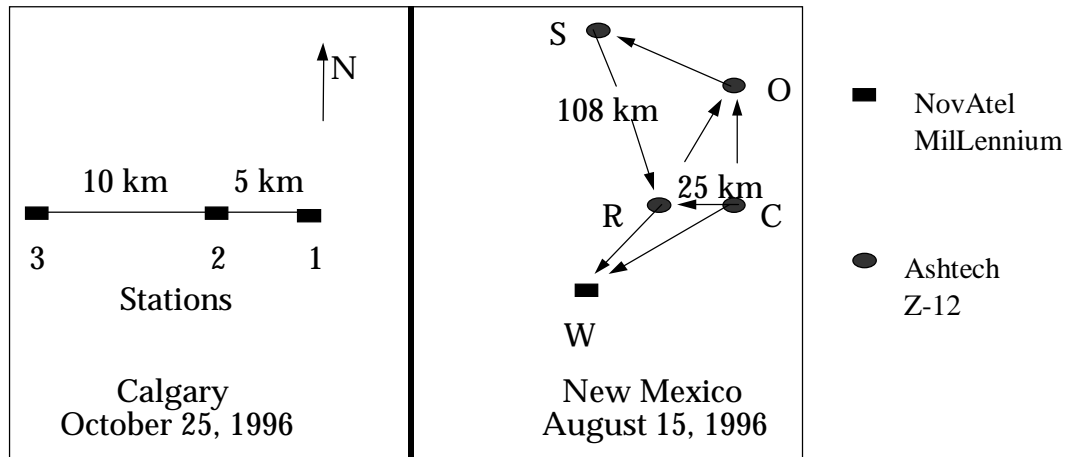


**Figure 6-1: Test Networks**

The Calgary network is a linear East/West network originally designed to detect spatial errors that are a function of baseline distance. The greatest altitude difference for the network receivers is 115 metres. It exists between Stations 2 and 3.

The New Mexico network was established under the approval and control of the U.S. 746th Air Force Test Squadron at Holloman Air Force Base [Raquet, 1998]. It is distributed in both Northing and Easting directions over an area of 18,000 km<sup>2</sup>. It spans a North/South distance of approximately 150 km, an East/West distance of 55 km, and has a vertical distribution of 300 m.

The coordinates of the stations in the Calgary network were derived from a 21-hour adjustment of the GPS observations collected on October 31, 1996. The relative network survey accuracy is estimated to be 5 mm. This estimate is obtained by dividing the 21-hour period into 64 “20-minute” sessions. Each of the 64 sessions is processed with SEMIKIN<sup>TM</sup>. For all processing sessions, the tropospheric errors were reduced using a modified Hopfield Model [Mendes and Langley, 1994]. The receiver measurements were cut-off when the satellites fell below 15° of elevation.

The errors in the receiver coordinates of each session were assumed to be normally distributed about a mean value. Of the 64 sessions, 35 resulted in fixed integer ambiguity solutions for the 15-km baseline. Two of these 35 sessions were rejected because the station coordinates did not fall within  $3\sigma$  of the mean. Therefore, the percentage of good solutions was 51%. The standard deviations of the station's coordinates for each 20-minute session were computed using the 33 good solutions and found to be 0.75 cm, 0.95 cm, and 2.75 cm in the North, East, and Vertical coordinates, respectively.

The 5-km baseline resolved correctly 62 times (96%), and had  $1\sigma$  standard deviations of 0.60 cm, 0.45 cm, and 1.15 cm, respectively. Under the assumption that the position error for each of the 20-minute sessions is statistically Gaussian, the accuracy of the 21-hour mean position was calculated from the standard deviations of each session and the number of sessions. Using the worst-case coordinate standard deviation (2.75 cm) and the least number of redundant solutions (33), the network survey accuracy over the 21-hour period was estimated according to Equation 6.1. Over a 15 km baseline, 0.48 cm accuracy is the same as 0.3 ppm and is considerably better than that which can be achieved from traditional surveys (See Table 4-1). If this positioning accuracy is mapped into the range domain using a PDOP of 2.5, the  $1\sigma$  range error that results in a 0.3 ppm survey accuracy is about 0.1 ppm.

$$\sigma_{Survey} = \frac{2.75}{\sqrt{33}} = 0.48 \text{ cm} \quad (6.1)$$

This network was established with an accuracy of 0.48 cm using 21 hours of observations. The survey accuracy is not as good when fewer hours are spent making observations. For instance, with only 10 hours of observations, the number of independent solutions would drop to 16 and the position solution would not be as accurate. As a result, the survey accuracy is inversely related to the square root of the

time spent making observations. Figure 6-2 shows how the vertical survey accuracy of Calgary's 15-km baseline is affected by the observation time under the assumption that each 20-minute solution for position is an independent measurement. This figure indicates that at least 2 hours of observations are required to obtain 1 ppm accuracy (i.e. 1.5 cm).

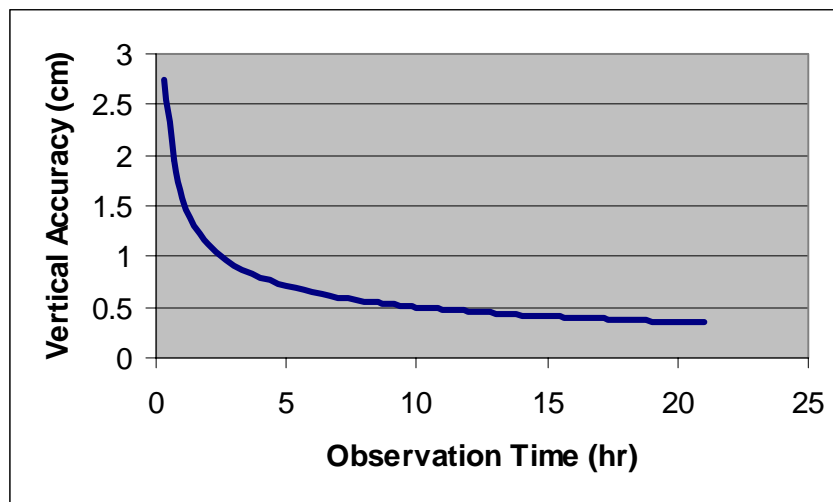


**Figure 6-2: Survey Accuracy Versus Observation Time at Calgary**

Later, it is shown that the spatial errors affecting this network are on the order of 1 cm (0.7 ppm). If the network were established using observation times of less than 2.5 hours, the spatial errors would be smaller than the survey error, and would be relatively difficult to isolate.

Station 1 in the Calgary network occupies survey pillar "N1" on the roof of the Engineering building at the University of Calgary. The coordinates of this pillar were established with respect to the ITRF through the Priddis (PRDS) reference station. The ITRF coordinates of the PRDS reference station have an accuracy of better than 3 cm [Zumberger et al., 1994]. The survey accuracy of the "N1" pillar with respect to PRDS is less than 5 cm [Varner and Henriksen, 1996]. Since the coordinates of the N1 pillar were

accurately established, the differential shift and distortion are not a factor in the performance of this network.

The adjusted survey accuracy for the Holloman Network is 1 to 3 cm horizontal and 2 to 5 cm vertical [Raquet and Lachapelle, 1997]. This is obtained by observing the fixed integer widelane position misclosures over an 18 hour period using PRIZM™ software, developed by Ashtech for surveying applications.

Reference Station “O” in the Holloman network was a test station. The PDA sub-network consisted of the remaining reference stations “R”, “S”, “C”, and “W”. Station “R” was selected as the network master station. All processing and analysis of the Holloman network was conducted using SEMIKIN™. A Hopfield tropospheric model was used on the Holloman network, and receiver measurements were cut-off below a 15° elevation mask.

### **6.1.1 PDA Development**

The primary objective of a PDA is to model the spatial and non-spatial errors as a mathematical function of partial derivatives. The assumption is that non-spatial errors exist at all network reference stations including the master station. The spatial errors decorrelate at different rates along the Northing, Easting and Vertical axis. If the network can differentiate the spatial and non-spatial errors in the Northing and Easting directions, an  $\alpha\beta\chi$  PDA (Equation 4.22) may be appropriate. However, other models may have better performance depending upon the geometry and number of stations in the network. To better understand how different PDA models perform, five models were compared, and are listed in Table 6-1.

**Table 6-1: PDAs Tested with the Holloman Network Data**

PDA	Mathematical Model
$\alpha$	$g_j = \alpha + \varepsilon_g(P_j)$
$\alpha\beta$	$g_j = \alpha + \beta * \Delta y_j + \varepsilon_g(P_j)$
$\beta\delta$	$g_j = \beta * \Delta y_j + \delta * \Delta z_j + \varepsilon_g(P_j)$
$\alpha\beta\chi$	$g_j = \alpha + \beta * \Delta y_j + \chi * \Delta x_j + \varepsilon_g(P_j)$
$\beta\chi\delta$	$g_j = \beta * \Delta y_j + \chi * \Delta x_j + \delta * \Delta z_j + \varepsilon_g(P_j)$

The testing procedure involves forming a sub-network from four of the Holloman reference stations. Reference stations “R”, “S”, “C”, and “W” form the sub-network, while station “O” is the test station. The master station for the sub-network is station “R”.

### 6.1.2 Performance Analysis

The methodology behind the performance analysis is explained using one particular PDA. Afterwards a comparison with other PDAs is provided. On the assumption that the measurement errors decorrelate linearly along the three coordinate axis at different rates, the PDA selected for the explanation is the  $\beta\chi\delta$  PDA. The network measurements  $k_j$  on the sub-network were used to estimate the parameters of the  $\beta\chi\delta$  PDA. The carrier-phase measurements at the test station were corrected by the PDA according to Equation 4.26 as described in Figure 5-3. SEMIKIN<sup>TM</sup> was then used to derive the measurement error  $\delta\phi_{PDA}$  for Test Station “O”. A second set of measurement errors  $\delta\phi_{DGPS}$  was derived using the uncorrected carrier-phase measurements for Test Station “O”. The two sets of residual errors were then compared to determine if the PDA model improved the accuracy of the measurements.

On the Holloman network, a fixed integer solution was achieved on the 108 km baseline between Stations “R” and “S” only when the elevation cut-off angle was greater than 22°. Using a cut off angle of 23°, The satellite having a pseudo-random noise number (PRN) of 17 was available to all stations in the Holloman network for the continuous period of 5 hours on August 15, 1996. During this period, five satellites had a sustained presence above 23° of elevation. Satellite 17 was selected as the base satellite, and the measurement errors were computed. The measurement errors for Station “O” are shown in Figure 6-3. The Root Mean Square (RMS) of these errors was computed for each satellite using five hours of data. An overall RMS was formed by aggregating the measurements from all satellites during the 5 hour period. Measurements that were corrected using the PDA model have an overall RMS error of 6.1 cm. When left uncorrected, the measurements had an overall RMS of 8.6 cm. Therefore, the  $\beta\chi\delta$  PDA corrections improved the measurement residuals by 30%. Because of statistical variations some satellites performed better than others when using the PDA corrections. For instance, on an individual basis, the RMS of measurement errors for Satellite 23 were improved by 66%, but other satellites showed no improvement or periods in which the corrected measurements were less accurate than uncorrected measurements.

Using corrected measurements, the time required to achieve L1 ambiguity resolution on the 70-km baseline between the master station and the test station was improved by 33% (120 minutes vs. 80 minutes). This result confirms that an improvement in the accuracy of the measurements leads to a direct improvement in the ambiguity resolution time. However, 80 minutes for initialisation is still a long time to wait for most positioning applications. Later in this Chapter, a more accurately surveyed network will be used to show that initialisation time for a 70+ km baseline can be reduced to as little as 15 minutes.

Having shown that the use of a  $\beta\chi\delta$  PDA caused a statistical reduction of the measurement errors and time required for resolution, other PDA candidate models were reviewed. To look at how the parameters of the PDA model vary with model type, the parameters for a single satellite at a single epoch of time are compared in Table 6-2. The  $\alpha\beta$  and  $\alpha\beta\chi$  models were evaluated at GPS time 416052 seconds. The results suggested that the measurement error for Satellite DD 28-17 experienced multipath errors of 2-3 centimetres. The spatial decorrelation in Northing was less than 1 mm per km (ppm). The decorrelation in Easting had a large uncertainty, and the two models in which it is predicted provided inconsistent results. Nevertheless, it appeared that the decorrelation in Easting is larger than the decorrelation in Northing. The decorrelation in the vertical

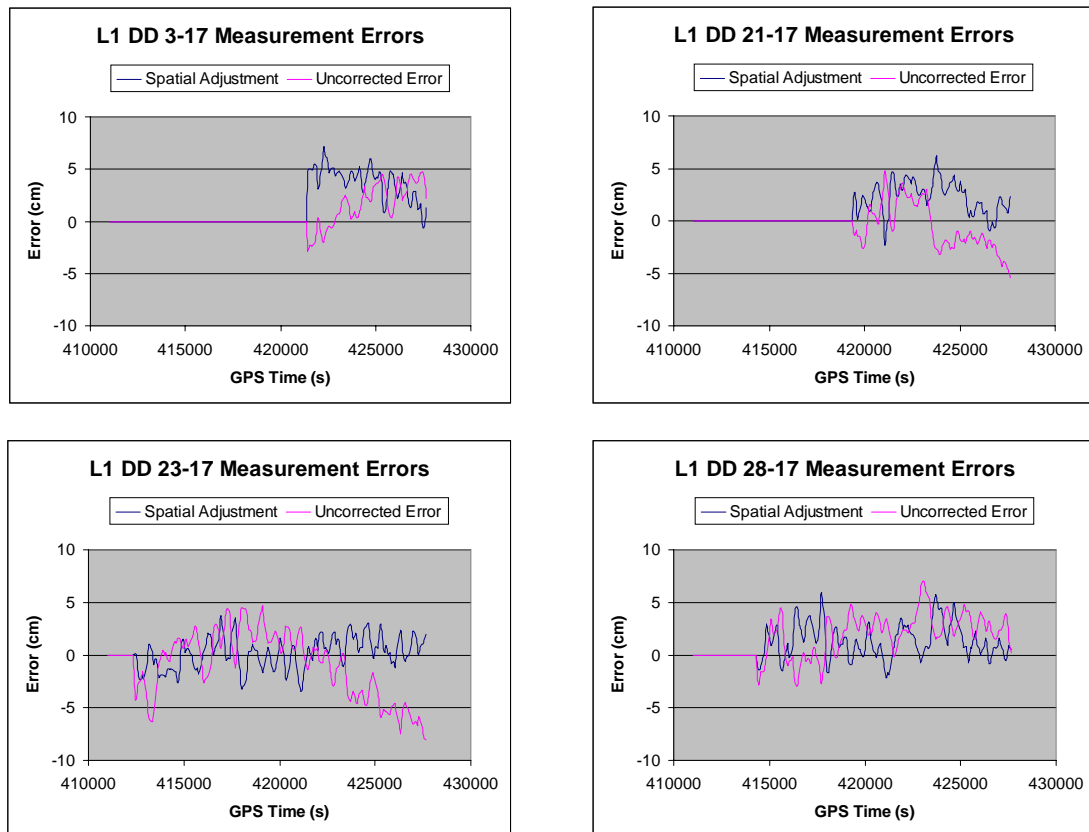


**Figure 6-3: Double Difference Carrier-Range Measurement Residuals at Holloman**

direction was between 300 and 400 ppm. This dramatic difference in the decorrelation rate results from the fact that the Holloman network did not have a large distribution in the altitude of the reference stations.

**Table 6-2: PDA Models for Satellite DD28-17 at 416052 seconds GPS Time**

Model:	$\alpha$	$\alpha\beta$	$\beta\delta$	$\alpha\beta\chi$	$\beta\chi\delta$
Parameter:					
Non Spatial ( $\alpha$ ) <cm>	-0.414	-2.855	-	-2.438	-
Northing ( $\beta$ ) <ppm>	-	0.0759	0.628	0.266	0.642
Easting ( $\chi$ ) <ppm>	-	-	-	1.292	0.475
Vertical ( $\delta$ ) <ppm>	-	-	-380	-	-350

The 5-hour root mean square error (RMS) for the uncorrected measurement errors was computed for a particular pair of satellites using the  $\beta\chi\delta$  PDA. The RMS from the  $\beta\chi\delta$  PDA was compared to the RMS of the other four PDAs of Table 6-1. For each satellite that was visible during this period, the RMS results are shown in Figure 6-4 (Satellite 17 was the base satellite).

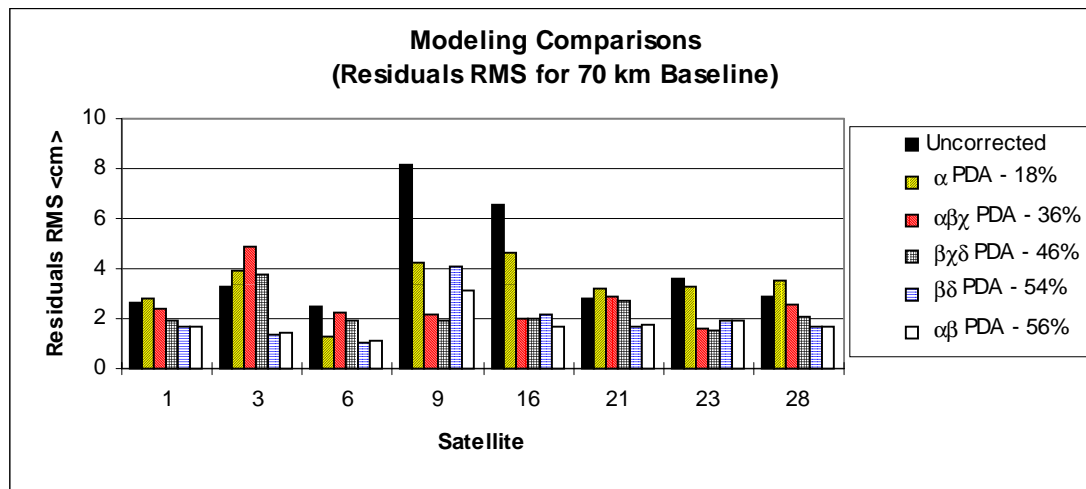


**Figure 6-4: PDA Model Comparisons**

Of the five models tested, Figure 6-4 suggests that the most appropriate PDA used with the Holloman network was a 1<sup>st</sup> order, one dimensional PDA that estimated only

non-spatial errors and the spatial decorrelation rate in the Northing direction ( $\alpha\beta$ ). This model improved the overall accuracy of the measurements by 56% when compared with the uncorrected solution. The percentage improvement for each model is given at the far right side of the legend. The non-spatial model ( $\alpha$ ) was not a good model, but the statistical performance of the other four models was similar to that of the  $\alpha\beta$  model. Models that attempted to estimate an Easting decorrelation rate tended to have weaker performance. This was expected because the North/South expanse of the Holloman network is greater than its East to West width.

A time history of the non-spatial and spatial decorrelation coefficients is shown in Figure 6-5. As expected, the non-spatial error was less than the theoretical L1 multipath limit of  $\pm 5$  cm. There were periods in which the spatial errors along the Northing direction decorrelated at rates as high as 1.3 ppm. This rate was within the limits expected for the error budget (Table 3-1). Satellite 28 was not visible at the beginning and the end of this 5-hour period, so the error and the derivative were shown as zero (see Figure 6-5).

After the corrections were made to the observed range measurements, the position was computed from those measurements using the state filter. The improvements in range are directly translated as improvements in position. Figure 6-6 depicts the DGPS and PDA positioning errors ( $\delta\mathbf{U}_{DGPS}$ ,  $\delta\mathbf{U}_{PDA}$ ) for the Test Station O. These errors were defined in Figure 5-4 as being the position errors that result from using uncorrected and corrected range measurements respectively. The corrected (PDA) results were based upon the use of an  $\alpha\beta$  PDA model. The  $\alpha\beta$  PDA model reduced the Northing error by 40% and the Vertical error by 25%. The Easting error improvement was small and not statistically significant.

The improvement in the positioning accuracy along a particular coordinate axis depended mostly on the geometry of the satellites rather than the type of PDA selected. This is because the PDA corrections are in the measurement domain, and prediction errors in the measurement domain get mapped to the position domain using the satellite geometry.

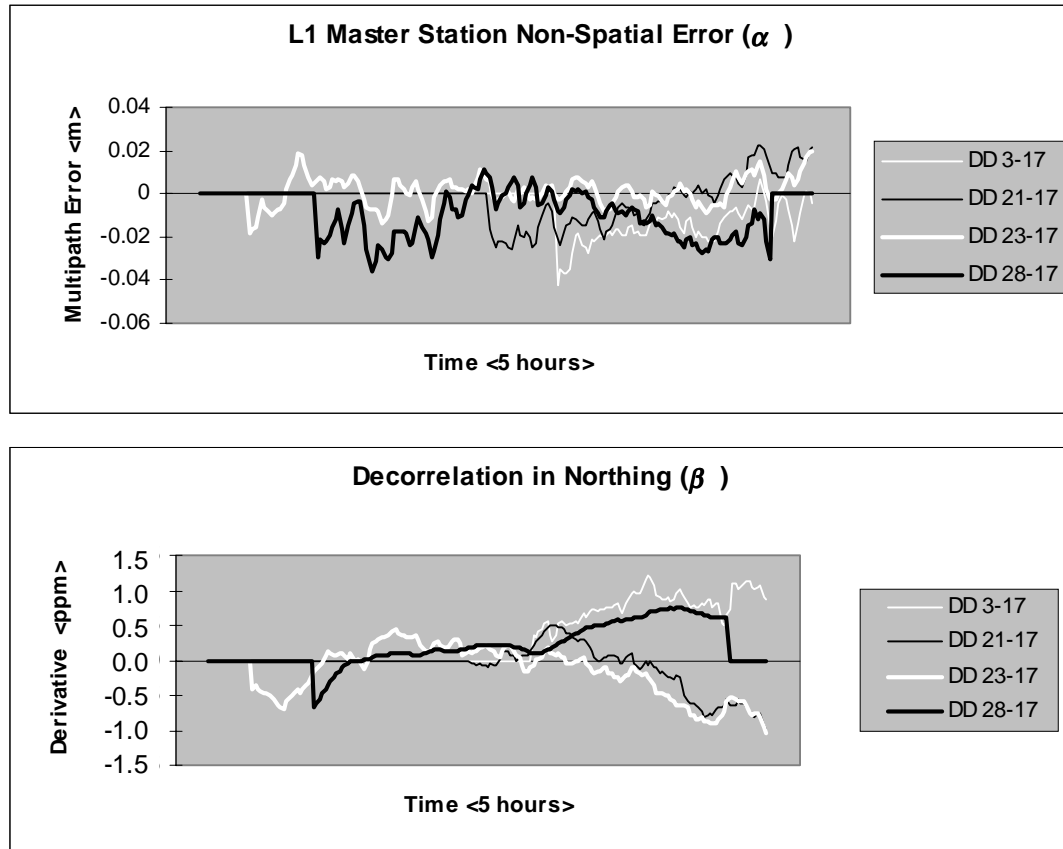


**Figure 6-5:  $\alpha\beta$  PDA Coefficient Time Histories**

During the entire period shown in Figure 6.6, five GPS satellites were visible. The geometry of these satellites was good because the PDOP remained below 2.5 throughout the analysis period.

Even though numerous models were tested, the improvement in measurement and positioning accuracy was limited to about 30%. This indicated that non-spatial errors

were dominant. Considering that the reference station positions were derived from only a few hours of GPS data, it is likely that the performance was being limited by inaccuracies in the network survey. To verify this hypothesis, another network having an accurate relative survey was tested and compared.

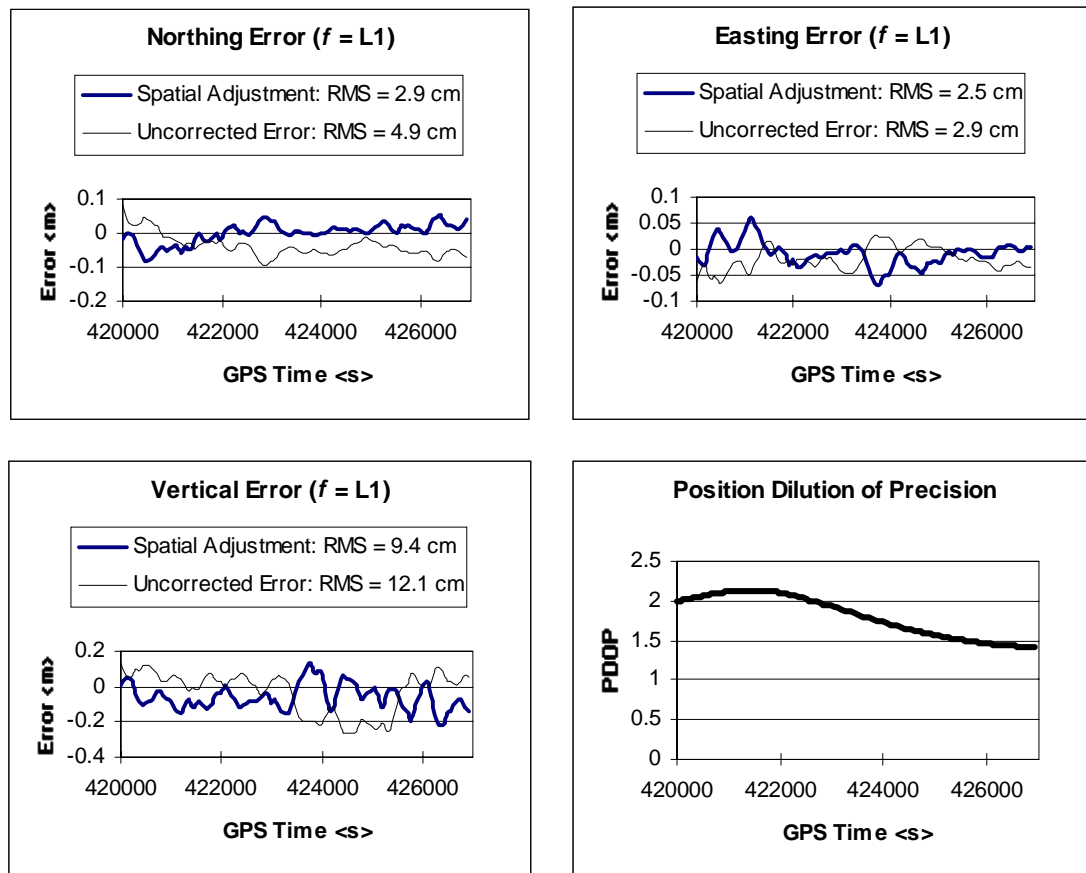


**Figure 6-6: Positioning Errors --Time Histories**

## 6.2 Southern California Integrated GPS Networks (SCIGN)

The Los Angeles region of southern California is an excellent test bed for a carrier-phase network. The IGS supports a network of more than 30 GPS reference stations within 200 km of Los Angeles. These stations are being used primarily for earthquake detection

research and have a surveyed positioning accuracy that is predicted to be between 3 mm and 3 cm [Neilan, 1997]. Figure 6-7 shows the locations of 26 stations that were available for use in June of 1997.

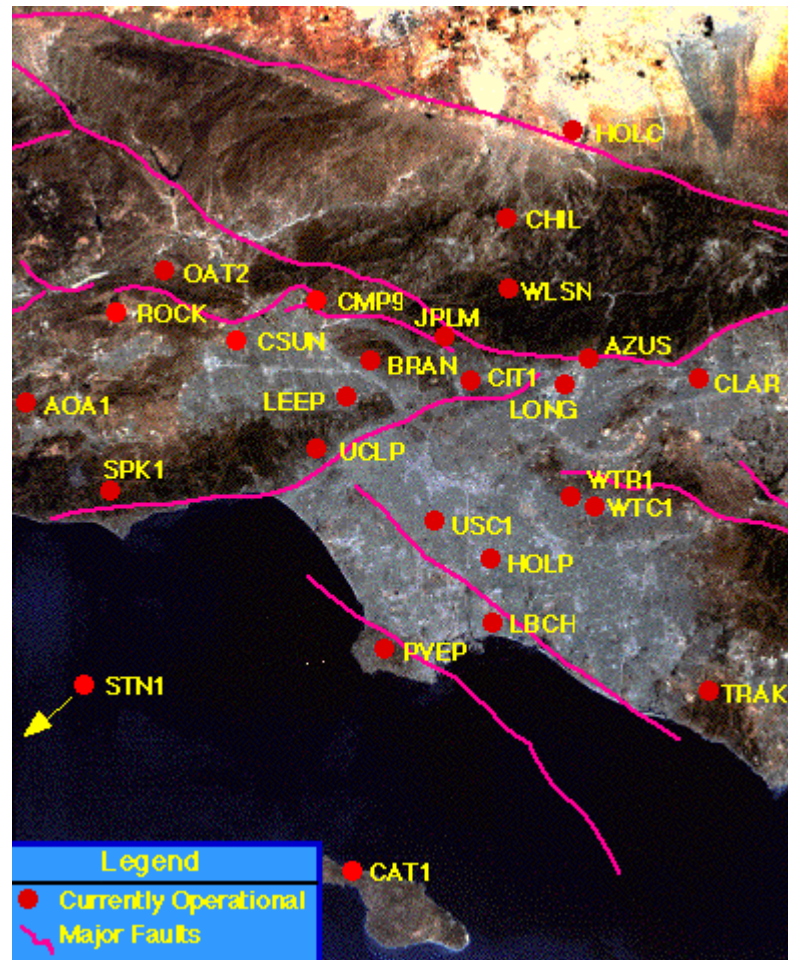


**Figure 6-7: Southern California Integrated GPS Network Site Map**  
 (Reference: SCIGN Web Page -- <http://www.scign.org/>)

A subset of the stations was selected to form a working network in which short baseline network linking was applied. The stations included in the working network are shown in Figure 6-8 as solid diamonds linked with lines that signify the short baselines of the network. The stations represented as hollow circles were test stations where the

performance of the network was evaluated. Descriptions and the ellipsoidal coordinates of the various stations are given in Appendix A. The reference station at Jet Propulsion Laboratory “jplm” was selected to be the network master station. In Figure 6-8, the coordinate system is a local horizontal planar projection of Northing and Easting having an origin, which coincides with the location of “jplm”. This coordinate system is convenient for depicting the relative positions of the network reference stations, but the positioning analysis using NDGPS was derived in WGS-84 coordinates.

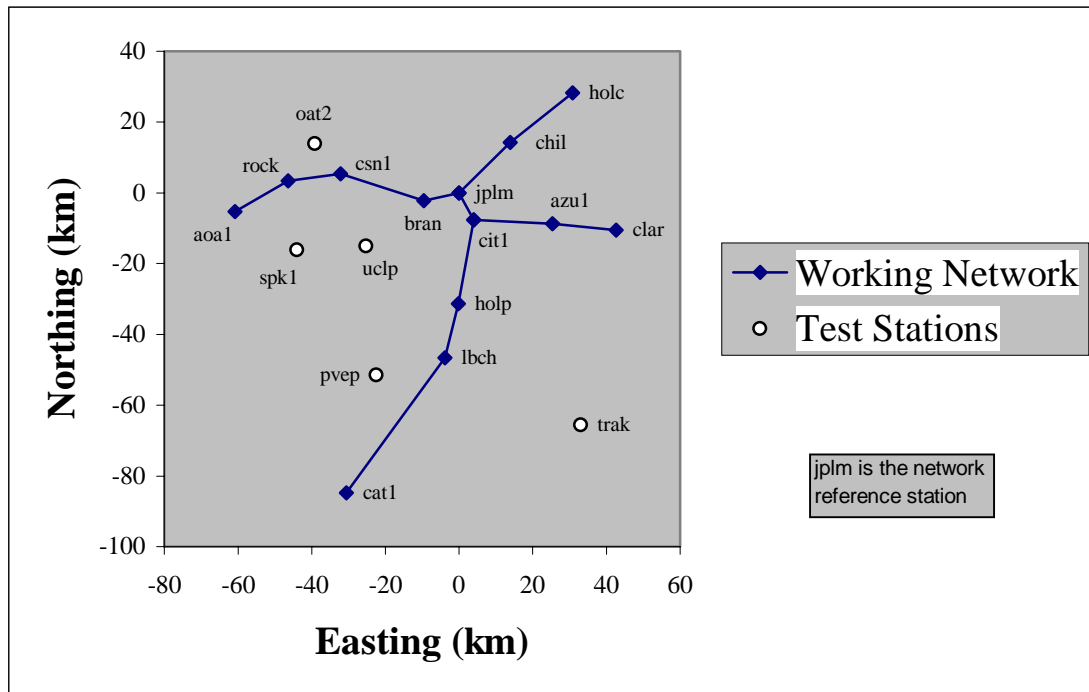


**Figure 6-8: IGS Southern California Working Network**

Distances between the various network reference stations and some important distances for the test stations are given in Table 6-3. While there were a number of other reference stations that comprise the SCIGN, only the subnet defined as the working network was used for generating PDAs. The working network’s horizontal reference axis was East and/or North, depending upon the PDA being tested. Some PDAs use both axes simultaneously.

Most baselines are less than 25 km. However, the “lbch”-“cat1” baseline is 47 km in length. Therefore, instantaneous L1 ambiguity resolution on the network was not always possible.

**Table 6-3: California Working Network Kilometrage Chart**

Network Reference Stations					Test Stations							
aoa1					oat2	pvep	spk1	trak	uclp			
azu1	86.24				Distance to "jplm"	41.57	56.21	46.97	73.35	29.37		
bran	51.25	35.62			Closest Net Station	csn1	lbch	rock	lbch	bran		
cat1	84.95	94.34	85.11		Distance to Closest	10.99	19.37	19.81	41.4	20.2		
chil	77.21	25.85	28.76	108.6								
cit1	64.92	21.33	14.73	84.56	24.04							
clar	103.6	17.4	52.98	104.3	38.11	38.72						
csn1	30.52	59.33	23.85	90.16	46.95	38.58	76.61					
holc	97.56	37.47	50.65	128.6	21.93	44.74	40.64	67.04				
holp	65.94	34.05	30.55	61.49	47.75	24.06	47.61	48.72	67.14			
jplm	61.02	26.86	9.886	90.08	19.96	8.628	43.98	32.68	41.82	31.28		
lbch	70.37	47.7	44.7	46.67	63.4	39.73	58.75	59.25	82.43	15.68	46.7	
rock	16.87	72.77	37.16	89.54	61.21	51.63	90.14	14.27	81.06	57.76	46.48	65.66
	aoa1	azu1	bran	cat1	chil	cit1	clar	csn1	holc	holp	jplm	lbch

### 6.2.1 Network Ambiguity Determination

The SCIGN collects satellite observations every 30 seconds. It is difficult to perform OTF ambiguity resolution with such a long time interval between epochs. Knowledge of the kinematic process must be well known during the 30-second period in order for ambiguity resolution to be effective. Most OTF applications tend to have strong process dynamics and a 30-second interval is unacceptably large. In static processing mode, SEMIKIN™ assumes that the kinematic process noise is zero, which is consistent with the stationary characteristics of the test stations. Therefore ambiguity resolution was accomplished using SEMIKIN™.

The ambiguities between the master station and the other secondary reference stations were resolved by network linking as described in Chapter 4 (Section 4.13.3). Because the baselines between adjacent reference stations were short and the locations of the reference stations were well established, the ambiguities were resolved in just a few epochs even with single frequency observations.

The L1 ambiguities for each short baseline were resolved. Then, the ambiguities between the network master station and each secondary station were derived by accumulating the ambiguities along the interconnecting baseline links. For example, in Figure 6-9, stations “jplm” and “aoa1” were linked using stations “bran”, “csn1”, and “rock”. The ambiguities in this figure are L1 DD ambiguities for Satellite 29. The data shown was collected on the 23 of June 1997 during a time period from 108,000 to 114,000 seconds GPS time (11 pm to 12:40 am Pacific Time). The ambiguities were resolved for the four short interconnecting baselines using two epochs of observations. Adding the ambiguities of the four baselines together resulted in a derived set of ambiguities for the full 61-km baseline between “jplm” and “aoa1”. The ambiguities shown in Figure 6-9 were calculated at 109510 seconds GPS time. Since there were no cycle slips during the period from 108,000 to 114,000 seconds GPS time, the ambiguities of Figure 6-9 were applied for this entire period.

Ambiguity resolution was checked by comparing the ambiguities derived from network linking against the ambiguities derived from batch processing as described in Section 4.13.4. The ambiguities obtained from batch processing were assumed to be correct. In the batch process, the ambiguities were resolved using the entire 6000 seconds (1 hr. 40 min.) of data.

The advantage of network linking is that the ambiguities for the 61-km baseline between “jplm” and “aoa1” were resolved in the same amount of time that it took to resolve the longest of the short baselines, i.e. 30 seconds. Without network linking, it may have

taken several hours to resolve the “jplm” ambiguities. In fact, on the Holloman network, a baseline of similar length required between 80 and 120 minutes to resolve the ambiguities.

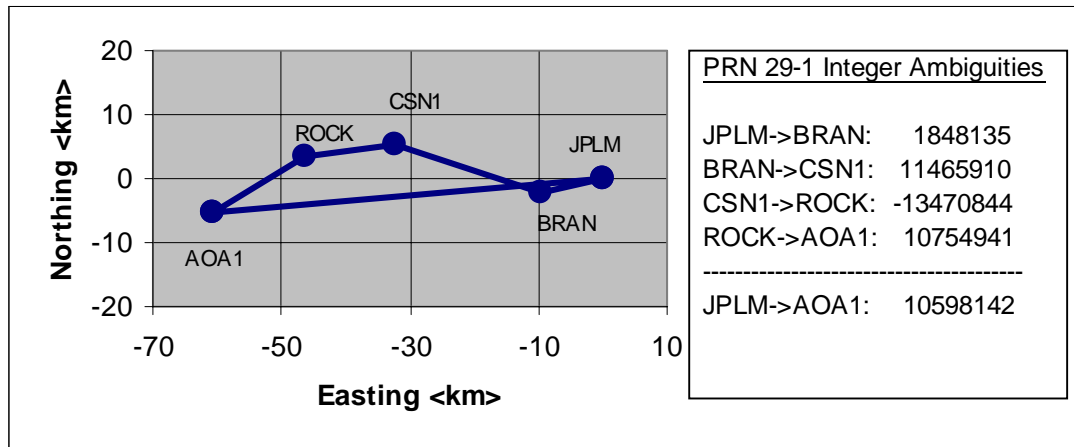


**Figure 6-9: Network Linking (Ambiguity Determination for PRN 29-1)**

## 6.2.2 Network Measurements

The network measurements were derived for all satellites at all secondary reference stations of the SCIGN working network. Figure 6-10 shows a typical set of network measurements taken on the working network at 111510 seconds GPS time. This figure depicts the network measurements at the various reference stations for the satellite combination PRN 29-14.

In Figure 6-8, the network measurements tended to become more negative for the eastern and northern stations. These trends were difficult to identify because the network measurements appeared to have fairly significant levels of network measurement noise. As indicated by Equation 4.6, this noise is the result of secondary reference station multipath, secondary reference station receiver noise, and relative survey errors between

the master and secondary reference stations. Table 4-2 predicted that this noise would have a magnitude of about 2 cm for a properly surveyed network. That prediction appears to be confirmed by the data reflected in Figure 6-10. However, the “azu1”, “clar”, and “cat1” stations seemed to be experiencing large deviations in for the network measurement noise (refer back to Figure 6-8 for station identifications).

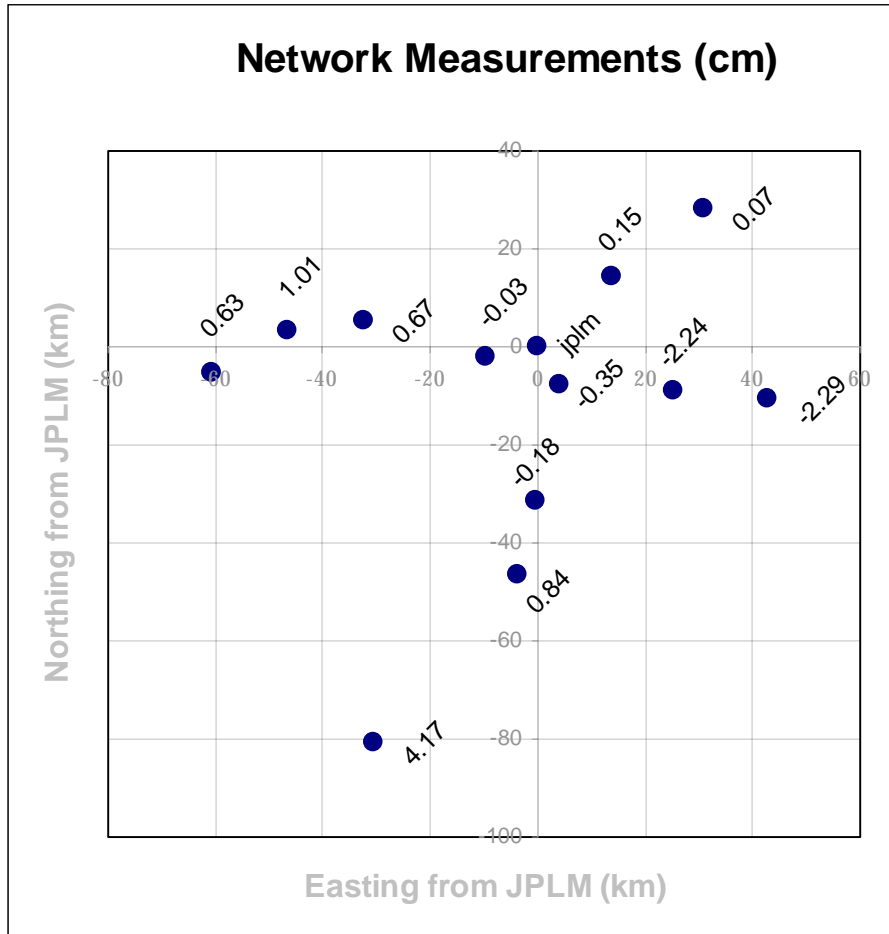


Figure 6-10: Network Measurements of PRN 29-14 at 111510 Seconds

### 6.2.3 Modelling the Errors with Partial Derivatives

It is instructive to look at the results of different PDA models using measurements from the same satellite and the same epoch of time. Using Satellite 29 at the epoch 111510 seconds, several PDA models were generated. First, the non-spatial PDA model (Equation 4.18) was solved using the Least Squares technique given by Equation 4.25. This model generates a function based upon  $\alpha$  that describes the error in the carrier-phase measurements as being a constant throughout the network. The value of this constant was 0.2 cm and represents carrier-phase non-spatial error at the master station under the assumption that the non-spatial error of the secondary stations is random with zero mean. Since part of this error includes L1 multipath, which can be as great as 5 cm, the predicted non-spatial error at the master station was very low. This result was expected because all reference stations in the SCIGN are installed with ground plane or choke ring antennas in locations that minimise the potential for multipath.

The other PDA models were also evaluated. The  $\alpha\chi$  model (Equation 4.21) was a plane surface with a West to East slope of  $-0.333$  mm/km (ppm) and an estimated master station multipath of nearly zero. The  $\alpha\beta\chi$  model (Equation 4.22) was also a plane surface with a West / East slope of  $-0.286$  ppm, a South / North slope of  $-0.246$  ppm, and a multipath estimate of  $-0.2$  cm. The  $\alpha\beta\chi\delta$  and the  $\alpha\beta\chi\delta\gamma$  models (Equations 4.23, and 4.24) form complex surfaces across the area of the network. The ground topography was modelled by fitting a smoothed surface to the published altitude of reference stations. The computed coefficients for all models are summarised in Table 6-4.

According to the theory of Chapter 4, the non-spatial error ( $\alpha$ ) is caused mostly by multipath at the master station. However, receiver noise, phase centre instabilities of the master station antenna and localised tropospheric errors also contribute. The linear spatial errors ( $\beta, \chi, \delta$ ) are caused by the combined effects of orbit error, ionospheric error,

and non-localised tropospheric errors that are not removed by the tropospheric model. The second order non-linear spatial errors ( $\gamma$ ) is assumed to be caused by inaccuracies in the tropospheric model for stations and users that are not at the same altitude as the master reference station.

On the SCIGN working network, the vertical spatial decorrelation ( $\delta$ ) rate was 5 to 10 times larger than the horizontal spatial decorrelation rates ( $\beta, \chi$ ), but was 15 to 20 times smaller than the vertical decorrelation predicted for the Holloman network. The reduction in vertical decorrelation rate with respect to the Holloman network is attributed to the improved sensitivity of the measurement system. The Holloman network has a maximum differential altitude of 303 metres between reference stations. The SCIGN spans over 1600 metres of altitude. This gives the SCIGN much better observability of altitude dependent errors. Another factor that improves the sensitivity of the SCIGN is the number of reference stations. With 13 reference stations, the SCIGN has 4 times as many measurements from which to estimate vertical decorrelation rates. Note also that even though the vertical decorrelation rate was large, it was linear because  $\gamma$  was very small in the non-linear  $\alpha\beta\chi\delta\gamma$  model.

**Table 6-4: PDA Parameter Estimates for PRN 29-1 at Epoch 96419**

Model Parameter \ Model Type	$\alpha$	$\alpha\chi$	$\alpha\beta\chi$	$\alpha\beta\chi\delta$	$\alpha\beta\chi\delta\gamma$
Non-Spatial Error [ $\alpha$ ] (cm)	0.204	0.028	-0.244	-0.521	-0.384
Easting Derivative [ $\beta$ ] (ppm)	X	-0.333	-0.286	-0.348	-0.341
Northing Derivative [ $\chi$ ] (ppm)	X	X	-0.246	-0.490	-0.537
Vertical Derivative [ $\delta$ ] (ppm)	X	X	X	22.664	29.389
Vertical Curvature [ $\gamma$ ] (ppm/km)	X	X	X	X	-0.008

Table 6-4 highlights a few other aspects of the SCIGN. The magnitude of the non-spatial error varied dramatically when the PDA model was expanded to include spatial decorrelation in the Northing and Easting directions. This indicates that errors observed across the network were heavily affected by horizontal spatial decorrelation. When spatial decorrelation parameters were not available – as is the case when using the  $\alpha$  model – spatial errors corrupt the estimation of the non-spatial errors. When the decorrelation parameters are added, the spatial error is properly related to the decorrelation parameters and its influence is removed from the non-spatial parameters. Therefore, the dominance of the spatial errors can be assumed if a large change in the non-spatial parameter occurs when spatial decorrelation parameters are added to the model.

A significant, but less dramatic, change occurs when the vertical decorrelation parameter is introduced to the model. The SCIGN working network has a vertical distribution of nearly 1600 metres (In Appendix A, the Chilao station has an altitude of 1568 metres; while the Long Beach station is 28 metres below sea level). This vertical distribution allows the network to observe errors that are associated with changes in altitude. PDA models that do not include a vertical decorrelation parameter are spreading the effects of the vertical error among the estimates of the other parameters. This induces an error in the estimated parameters. The change in the  $\alpha$ ,  $\beta$ , and  $\chi$  parameters following the introduction of the  $\delta$  parameter indicates that the vertical errors were significant on the SCIGN network. The magnitude of this error can be calculated. For instance: with a vertical decorrelation derivative of 25 mm/km, the vertical error between Chilao and Long Beach is expected to be 4 cm. On the other hand, a network that does not have a large vertical distribution between its stations should probably forgo the use of a vertical decorrelation derivative because the vertical errors between the stations are not statistically observable.

Table 6-5 gives the estimated standard deviation of the parameters for the various models tested on the SCIGN. These values are derived from the covariance matrix using an *a priori* unit variance of 2 cm. From the fourth row, there is no doubt that the standard deviation of the estimated vertical decorrelation parameter is high. This means that it is difficult for the network to estimate vertical decorrelation rates. The sensitivity of the Holloman network can be compared with that of the SCIGN by examining the covariance of the  $\delta$  model for each. For the Holloman network, the covariance of the vertical decorrelation rate when using a “ $\delta$  only” model is 61 ppm. The same covariance derived from the SCIGN is 12 ppm. Therefore, the observability of the vertical decorrelation rate is at least 5 times better when using the SCIGN than when using the Holloman network. This appears to be a minimum. The vertical decorrelation rates in Table 6-5 are 15 to 20 times smaller than those shown in Table 6-2. While observability undoubtedly is a factor, the differences in the geographical positions of the networks and differences in the environment affecting the networks could also cause the differences in these tables.

Removing the vertical decorrelation parameter from the PDA model simplifies the solution and may be justified on a “flat” network where the reference stations are all at the same altitude. The drawback is that the positioning accuracy may be degraded for the user whose altitude is not the same as that of the network. Such would be the case for aircraft that are using a ground network for navigation.

**Table 6-5: PDA Parameter Estimated Standard Deviations**

Model Parameter \ Model Type	$\alpha$	$\alpha\chi$	$\alpha\beta\chi$	$\alpha\beta\chi\delta$	$\alpha\beta\chi\delta\gamma$
Non-Spatial Error [ $\alpha$ ] (mm)	5.77	6.27	6.29	6.62	10.04
Easting Derivative [ $\beta$ ] (ppm)	X	0.201	0.206	0.273	0.378
Northing Derivative [ $\chi$ ] (ppm)	X	X	0.194	0.199	0.204
Vertical Derivative [ $\delta$ ] (ppm)	X	X	X	16.794	40.722
Vertical Curvature [ $\gamma$ ] (ppm/km)	X	X	X	X	0.042

The non-spatial error at the secondary stations ( $\alpha_j$ ) can be estimated by subtracting the network measurement at the station ( $k_j$ ) from the estimate of the network measurement at that station ( $\hat{k}_j$ ). The estimate of the network measurement is derived from the PDA model (Equation 6.4). More precisely, the estimated non-spatial error at a secondary station is equal to the innovations process of the PDA model for that station. For Satellite 29 at 111510 seconds GPS Time, the non-spatial errors for the various secondary stations are all less than 1.3 cm (Table 6-6).

$$\alpha_j = \hat{k}_j - k_j. \quad (6.4)$$

The *a posteriori* innovations process (IP) is also a measure of how well the PDA model fits the physical error environment existing within the network [Haykin, 1991]. If the model is an exact representation of the spatial decorrelation and master station non-spatial error, then the only factor contributing to non-zero IPs would be non-spatial errors at the secondary stations themselves. In general, however, the PDA model is not an exact representation of the true error environment. So, in addition to site specific errors, the IP also includes all observation errors that are not properly modelled by the PDA. This means that a poor PDA model will give an IP variance and bias that are larger than one which is obtained when using a good PDA model. The model's performance is measured using the variance and bias of the IPs. The assumption is that the performance will improve as the model order increases. Unfortunately, this assumption may not hold if the number of observations used to generate the model is not significantly greater than the number parameters within the model. In such cases, the lack of observational redundancy can cause high cross-correlation in the variance-covariance matrix for the PDA solution. This also means that the IPs can be small even when the estimates of the model parameters are poor. This situation is known as "overparameterization". The field of Information Theory provides some insight into methods that will prevent

“overparameterization”. One technique is to calculate a parameter called the Akaike Information Theoretic Criterion (AIC) [Akaike, 1974]. The criterion states that the best model to use is the one whose order minimizes Equation 6.5.

**Table 6-6: Non-Spatial Error at the Secondary Reference Stations**

Station $j$	$\alpha_j$ (cm)
bran	0.5
csn1	0.7
rock	-0.2
aoa1	-0.8
cit1	0.4
azu1	-0.6
clar	-0.7
chil	-0.7
holc	1.2
holp	-0.2
lbch	0.0
cat1	0.4

$$AIC(m) = \ln(\hat{\sigma}_m^2) + \frac{2m}{n}. \quad (6.5)$$

Where :  $m$  = Model order.

$n$  = Number of network measurements.

$\hat{\sigma}_m^2$  = Unit Power of the Innovations Process for a model of order  $m$ .

The unit power of the innovations process is the normalised variance of the observation residuals and is computed according to Equation 6.6:

$$\hat{\sigma}_m^2 = \frac{\sigma_{IP}^2(m)}{\sigma_o^2}. \quad (6.6)$$

Where :  $\sigma_{IP}^2(m) \equiv$  Variance of the innovations process for a model of order  $m$ .  
 $\sigma_o^2 \equiv$  Variance of the Network Measurements.

The Akaike analysis for Satellite 29 is summarised in Table 6-7. The power of the IP for the  $\alpha\beta\chi\delta\gamma$  model is lower than that of the  $\alpha\beta\chi\delta$  model, but the AIC value is lower for the  $\alpha\beta\chi\delta$  model. According to Akaike's theory the 4-parameter model is the best model to use. The 5 parameter model is overparameterized, and the reduction in the IP is more related to the spreading of the model error among a greater number of parameters than it is to any improvement in the model's accuracy.

The temporal variation of the PDA parameters is shown in Figures 6-11, and 6-12. These figures are time history charts of the parameters for the  $\alpha\beta\chi\delta$  model starting at epoch 108000 and ending at epoch 114000 s, i.e. 1 hour and 40 minutes later.

Table 6-7: Modelling Analysis for Satellite PRN 29-14

Model Type	$\alpha\beta\chi\delta\gamma$	$\alpha\beta\chi\delta$	$\alpha\beta\chi$	$\alpha\beta$	$\alpha$
Dimensions	3	3	2	1	1
Model Order	2	1	1	1	0
Power of the IP	0.14981	0.15414	0.39365	0.56891	0.98354
AIC Value	-1.06505	-1.20324	-0.43228	-0.23069	0.15008

Over this period of time, the estimated non-spatial error parameter ( $\alpha$ ) behaved like biased noise. The bias trend has maximum amplitude of about 1 cm. The vertical spatial decorrelation rate is more than an order of magnitude greater than the horizontal decorrelation rate.

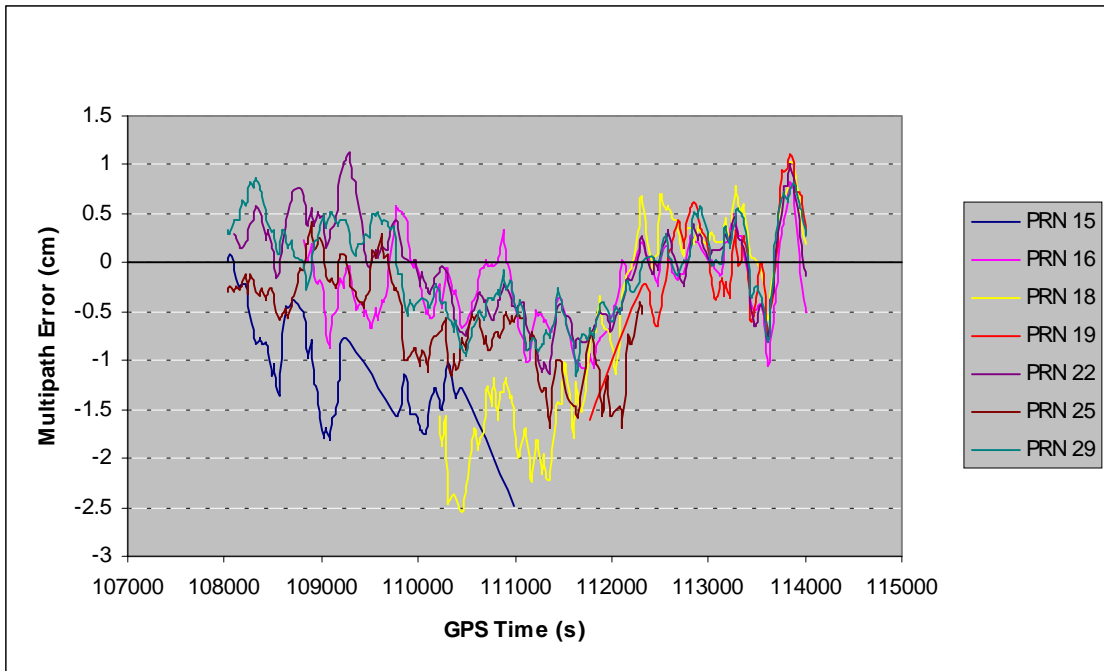


**Figure 6-11: Time History of the Master Station Non-Spatial Error Estimate ( $\alpha$ )**

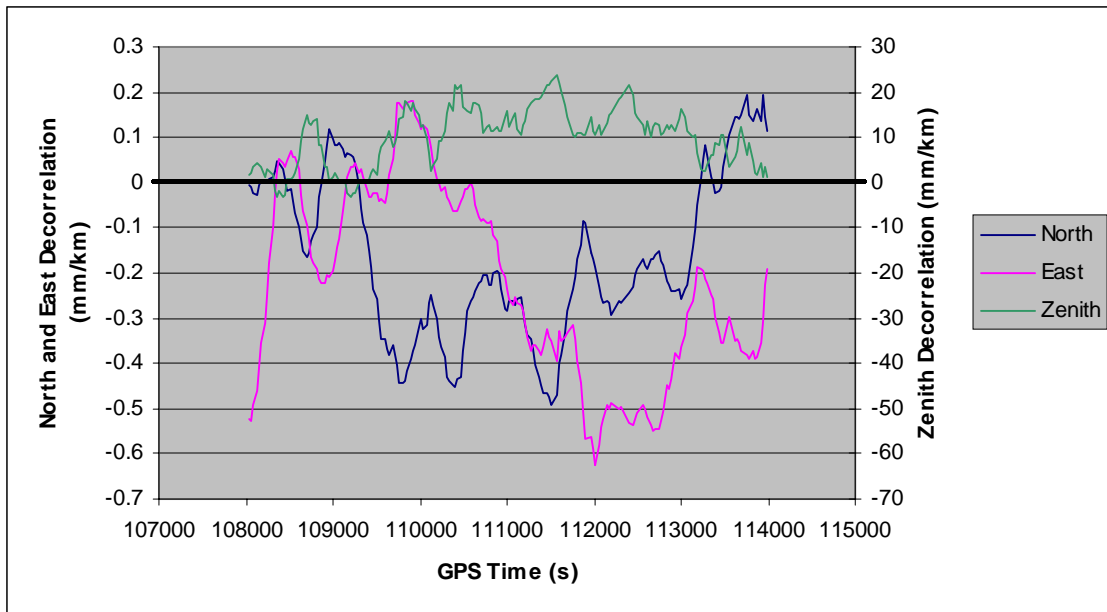


**Figure 6-12: Time History of the PRN 29-14 Spatial Decorrelation Rates**

Shown in Figure 6-13 is the AIC history for a couple of satellites using the  $\alpha\beta\chi\delta$  and the  $\alpha\beta\chi\delta\gamma$  models. The base satellite is 14. The non-base satellite is given in parentheses in the legend. Periods existed in which the five-parameter model outperformed the four-parameter model for Satellite 22. However, in general, the four-parameter model was the better one. The AIC varied substantially when using Satellite 29. Therefore, the type of model could be affected by changes in the satellite geometry. The  $\alpha\beta\chi\delta$  model was selected for further analysis because of it had good performance and was strictly linear.

#### 6.2.4 Positioning with PDA Network Phase Corrections

The positioning results from SCIGN are divided into two sections. The first section is a detail description of the analysis of a single test station, while the second section is a summary analysis of the other test sites used in the SCIGN.

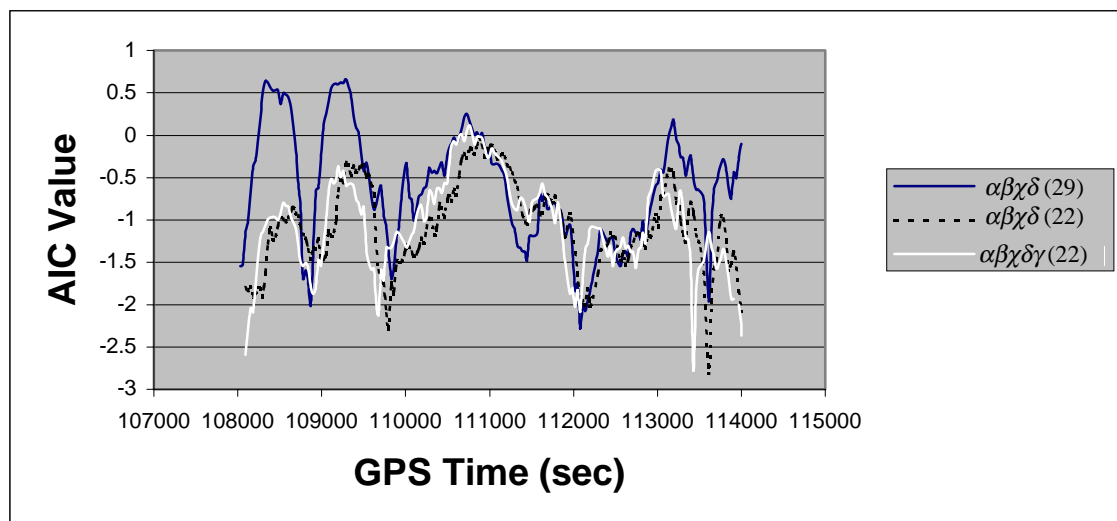


Figure 6-13: Time History of the AKAIKE Value

### 6.2.4.1 Results at the “oat2” Test Site

When the user receives the PDA parameters for visible satellites from the data link, corrections for the carrier-phase measurements are computed based upon the PDA model and the user’s current position. These corrections remove spatial and non-spatial errors from the measurements. The removal of these errors means:

1. It is easier for the user to solve for the position;
2. The floating ambiguity solution is less biased; and
3. The integer ambiguities are easier to resolve.

These points are demonstrated in two ways:

- The actual (measured) carrier-phase errors at a test station are compared with the PDA estimate of the range errors.
- The test station position errors when using standard DGPS techniques are compared with the position errors when using the network to provide DGPS range corrections as described in Figure 5-4.

The test station identified as “oat2” is taken as the first example. “oat2” is not used by the working network to generate PDA parameters (see Figure 6-8). Figures 6-14, 6-15, 6-16 and 6-17 show the actual and estimated carrier-phase measurement errors for four satellites observed at “oat2”. These figures are based on DD measurements in which Satellite 14 is the base satellite and “jplm” is the master station. The baseline distance between “jplm” and “oat2” is 42 km. The RMS of the measurement errors is given in the legend above each graph. The correlation between the actual and estimated measurement errors is also provided in the figures.

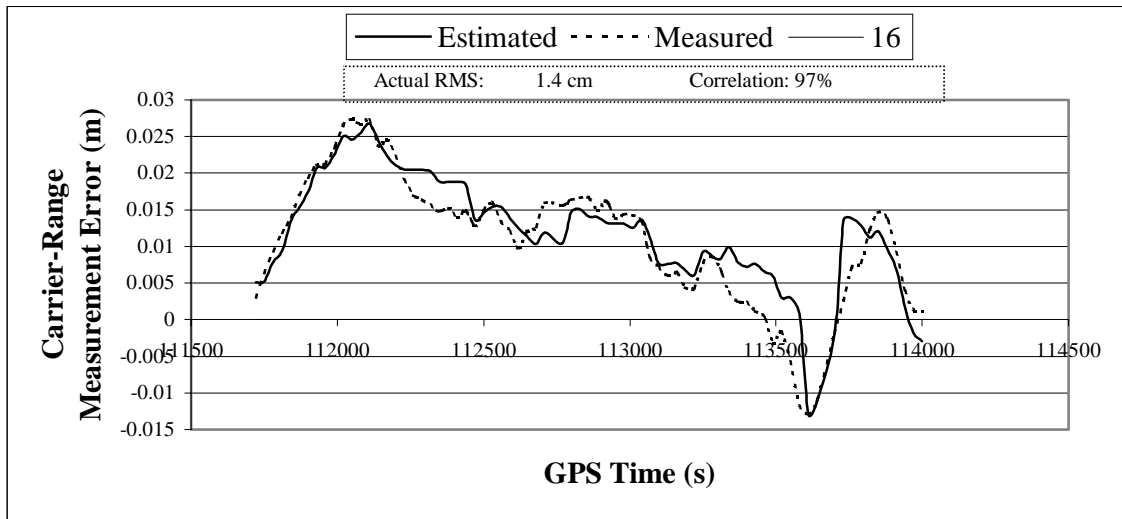


Figure 6-14: Estimated and Measured Errors for PRN 16-14 at “oat2”

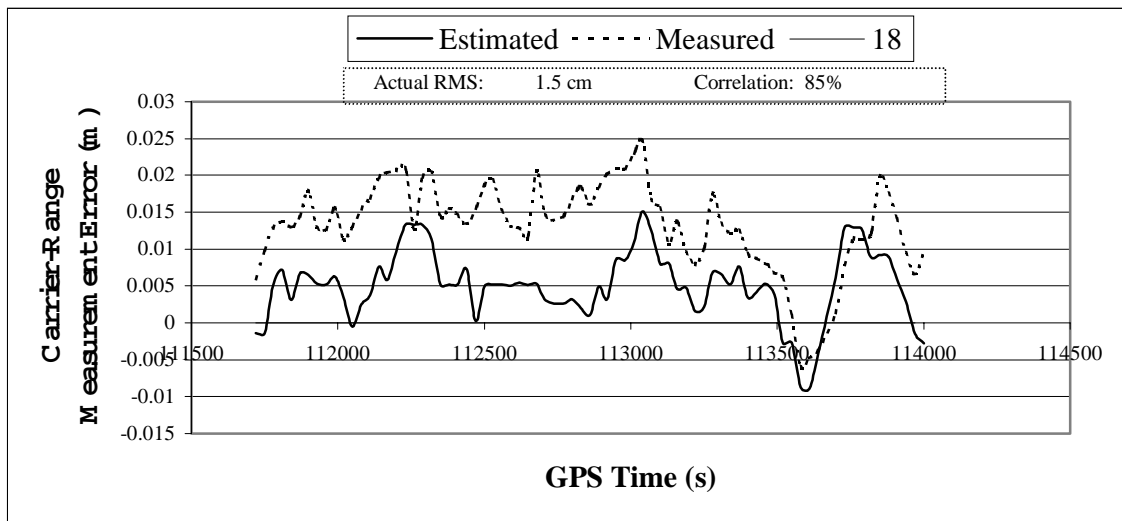
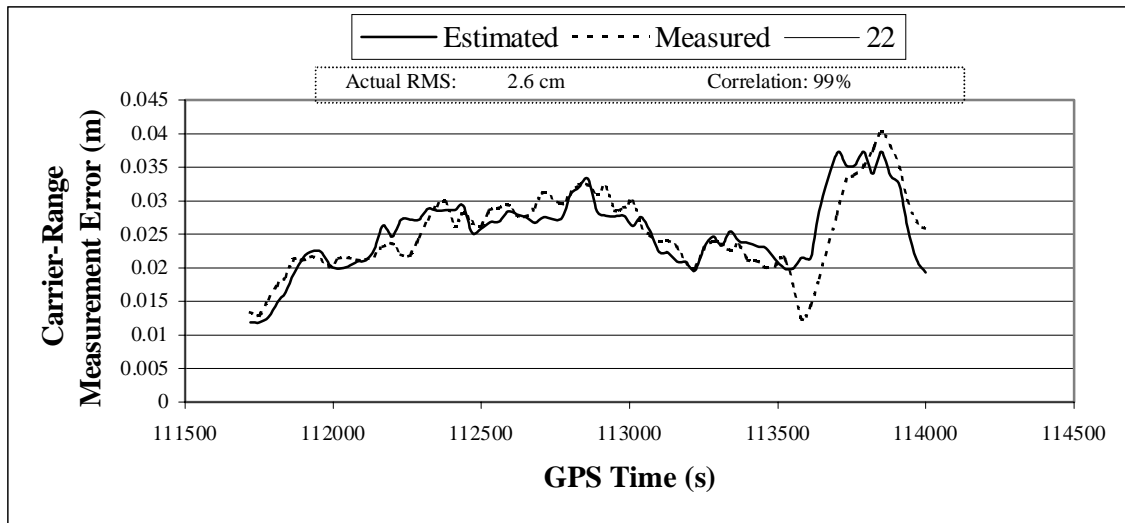
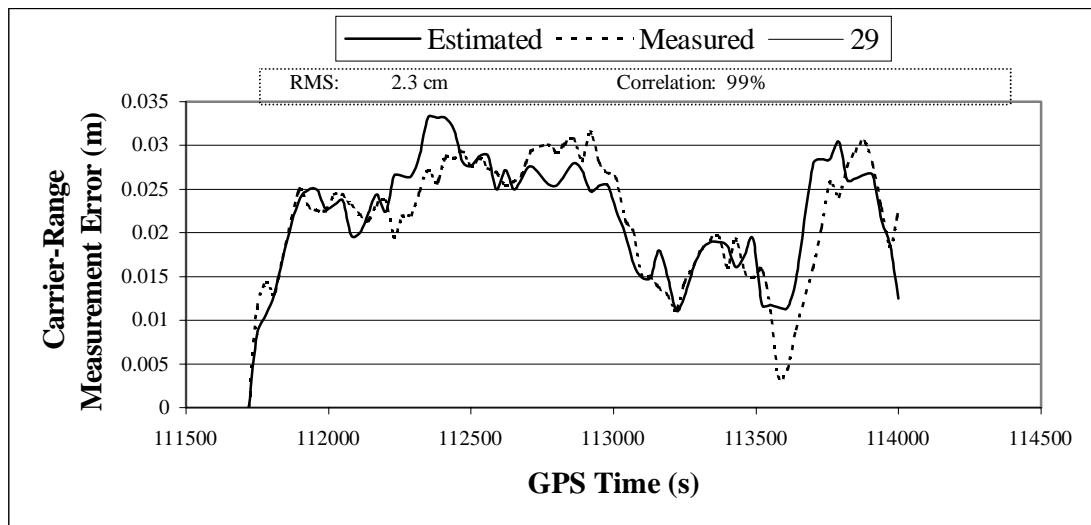


Figure 6-15: Estimated and Measured Error for PRN 18-14 at “oat2”



**Figure 6-16: Estimated and Measured Error for PRN 22-14 at “oat2”**



**Figure 6-17: Estimated and Measured Error for PRN 29-14 at “oat2”**

These charts show that there was an 85% to 99% correlation between the actual DGPS errors and the estimates of those errors using the  $\alpha\beta\chi\delta$  PDA model, and a large portion of the measurement error was removed by subtracting the PDA error estimate from the recorded measurement. In this case, more than 85% of the error could have been removed for users located near the “oat2” site.

Positioning accuracy was also improved. To demonstrate: the vertical positioning error at “oat2” is shown in Figure 6-18. The RMS of the uncorrected vertical position error was 11 cm. After the network corrections were applied, the RMS of the vertical positioning error was reduced to 1.5 cm – an 86% improvement. The dramatic variation in the uncorrected results at 112000 and 112300 seconds results from changes in the VDOP.

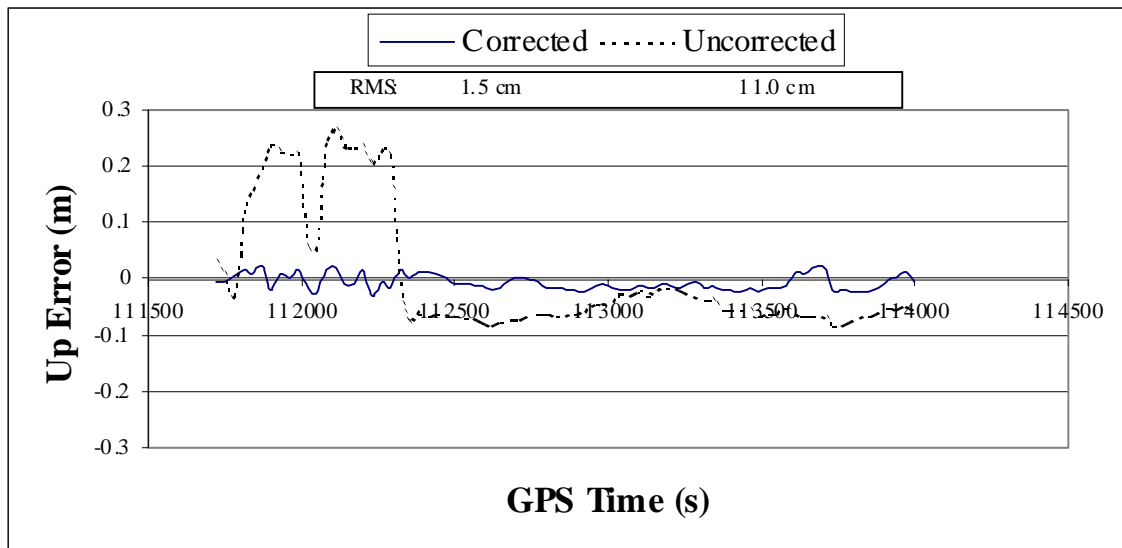


**Figure 6-18: Vertical Positioning Results for “oat2”**

Similar improvements were observed in the Easting and Northing position results, and are shown in Figures 6-19 and 6-20. When using the network corrections, the improvement in the accuracy of the Easting position was 50%. The accuracy of the Northing position was improved by 90%.

A bias remained in the corrected Easting results. This is an indication that the PDA was not a perfect model for the spatial and non-spatial errors affecting the network.

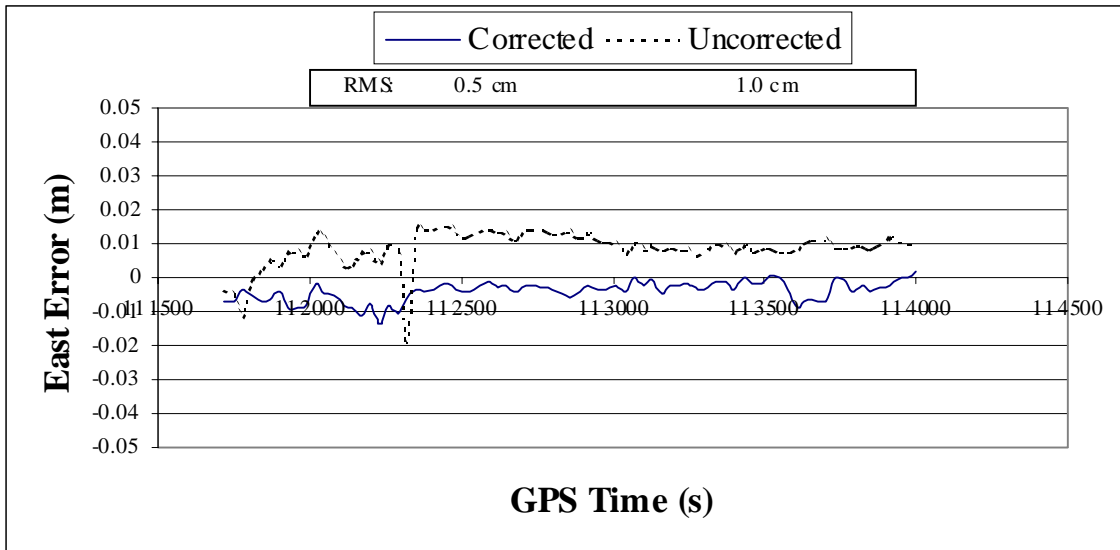


**Figure 6-19: Easting Positioning Results for “oat2”**

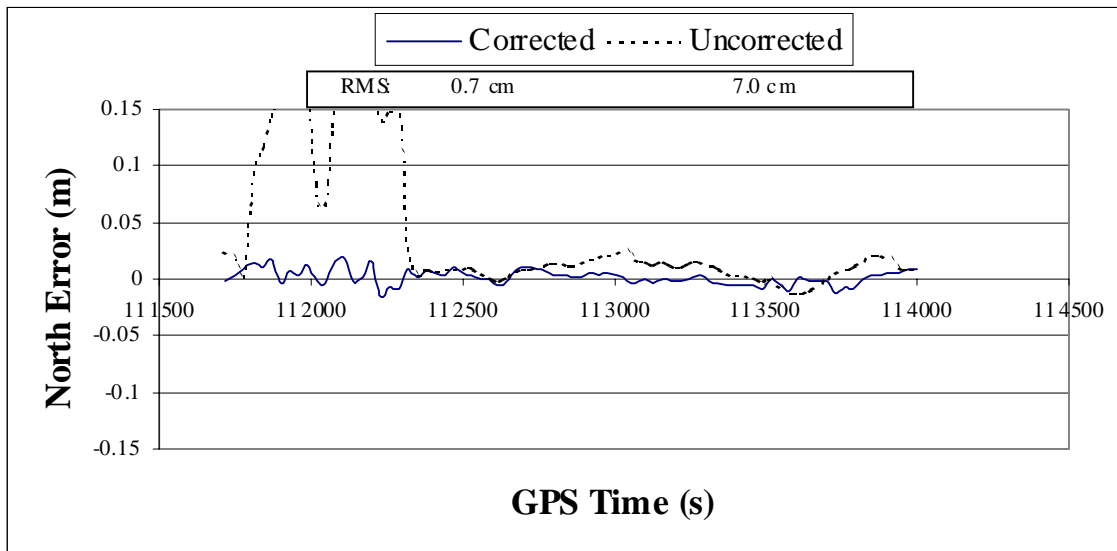


**Figure 6-20: Northing Positioning Results for “oat2”**

### 6.2.4.2 Other Test Site Results

The errors in the satellite carrier-phase measurements, as well as the errors in the user's position were calculated at all the test stations shown in Figure 6-18. In the previous section, the results of the "oat2" test station were discussed in detail. In this section, the five test stations were compared to evaluate the performance of the PDA technique at different locations within the network. The PDA model's best performance was recorded at the "oat2" station. At this location, the corrected measurements resulted in ranging and positioning errors that were 5 to 10 times smaller than those obtained using uncorrected measurements (Table 6-8). The RMS of the range measurement errors at "oat2" was 0.7 cm. "oat2" was only 10 km from the nearest network reference station ("csn1" – see Table 6-3). This could have been a factor contributing to the excellent performance at this site.

**Table 6-8: Accuracy Comparisons Between NDGPS and DGPS**

1 Sigma Statistic	oat2 (Most Improved)		trak (Least Improved)	
	Uncorrected	Corrected	Uncorrected	Corrected
	(cm)	(cm)	(cm)	(cm)
PRN 16	1.4	0.4	1.9	1.5
PRN 18	1.5	0.9	2.6	1.2
PRN 22	2.6	0.3	2.5	1.5
PRN 25	1.7	0.9	1.3	1.1
PRN 29	2.3	0.4	1.3	1.2
PRN 19	2.3	0.7	1.7	1.6
Vertical	11	1.5	7.7	4.7
Easting	1	0.5	1.6	1.1
Northing	7	0.7	3.5	2

The worst station ("trak") still showed that the PDA NDGPS technique performed better than standard DGPS techniques. At the "trak" location, the PDA NDGPS technique was 20% to 40% better than DGPS. The RMS of the measurement error at "trak" (41 km from the nearest reference station) was approximately 1.5 cm. This can be compared with the results by Raquet [1998] in which 40-km baselines had error RMS values of 0.18

cycles (3.5 cm). The performance of the single frequency SCIGN is 2 to 3 times better than Raquet's predictions using a large scale widelane network [Raquet, 1998]. The advantage of the SCIGN is attributed primarily to the density of the reference stations in the network, rather than the fidelity of the algorithm used to correct the measurements. All the other test stations had performance improvements that fell between the extremes of the "oat2" and "trak" stations.

The other performance parameter that is of interest in an NDGPS vs. DGPS comparison is the ambiguity resolution time. Carrier-phase positioning assumes that the ambiguities have either been resolved correctly or filtered until the estimation error is no longer significant. Both of these activities require numerous measurements taken over a period of time. Since integer ambiguity resolution involves reducing the ambiguity estimation error by filtering, the ambiguity resolution time is a measure of the time required to achieve accurate solutions for the user's position. Table 6-9 shows the amount of time required to achieve correct integer ambiguity resolution at two of the five test stations. In this table, 11 separate attempts to resolve the ambiguities are initiated between the time of 108000 seconds and 113000 seconds GPS time. The column titled "Uncorrected" indicates that the resolution process was completed using a regular DPGS solution. The "Corrected" column means that the resolution process was performed using an NDGPS solution with an  $\alpha\beta\chi\delta$  PDA model. If the process was applied to a regular DGPS solution, which used only those satellites that were visible to all stations in the network, it is called "Culled". Periods in which a "-" is indicated either did not resolve, or did not resolve correctly.

In Figure 6-21, the average time for resolution using each technique is shown for four of the five test stations. The uncorrected solution was only possible on the shortest baseline ("uclp" and the master station "jplm"). From Table 6-7, the uncorrected DGPS only resolved about 15% of the time on this 29-km baseline. Resolution for the uncorrected case was not possible on longer baselines. On the other hand, the culled and the corrected

cases were able to resolve the single frequency ambiguities for all test stations. It is impressive to realise that single frequency resolution was achieved more than 50% of the time on the 73-km “trak”-“jplm” baseline when using corrected measurements.

**Table 6-9: Ambiguity Resolution Results**

Start Time	uclp Time to Resolution (s)			trak Time to Resolution (min)		
	Uncorrected	Culled	Corrected	Uncorrected	Culled	Corrected
108000	-	10.0	6.7	-	-	15.8
108500	-	1.7	1.7	-	-	-
109000	-	3.3	3.3	-	-	-
109500	-	-	1.7	-	-	-
110000	-	4.2	4.2	-	-	13.3
110500	-	-	4.2	-	30.8	13.3
111000	9.2	5.0	3.3	-	-	-
111500	-	-	1.7	-	15	13.3
112000	-	-	2.5	-	15.8	8.3
112500	11.7	7.5	2.5	-	13.3	20
113000	-	-	-	-	9.2	14.2
	Average Time to Resolution (s)			Average Time To Resolution (min)		
	10.4	5.3	3.2	-	16.8	14.0

Another important conclusion can be derived from Figure 6-21. The “culled” case, in which the network simply indicates which satellites are observable to all stations, performs respectably well. This means that knowing which satellites should not be used is nearly as important as knowing the errors affecting the satellite measurements. Those satellites that are being obstructed at one or more reference stations are often low elevation satellites that provide the poorest performance at the stations for which they are visible.

Finally, there is one other issue that deserves some discussion. The SCIGN working network has shown that the station with the best performance (“oat2”) was very close to network’s Eastern axis, while the test station with the worst performance (“trak”) was the farthest test station from any network axis. This fact indicates the spatial decorrelation errors may not follow a linear East/North relationship for off-axis locations. Since the

linear PDA appears to be an adequate selection for network locations near the axes, it would not be advantageous to sacrifice this fit in order to improve the performance at of axis locations. Perhaps a PDA model that has a non-linear cross-correlation parameter between the two horizontal axes could improve the off-axis accuracy without sacrificing on-axis performance.

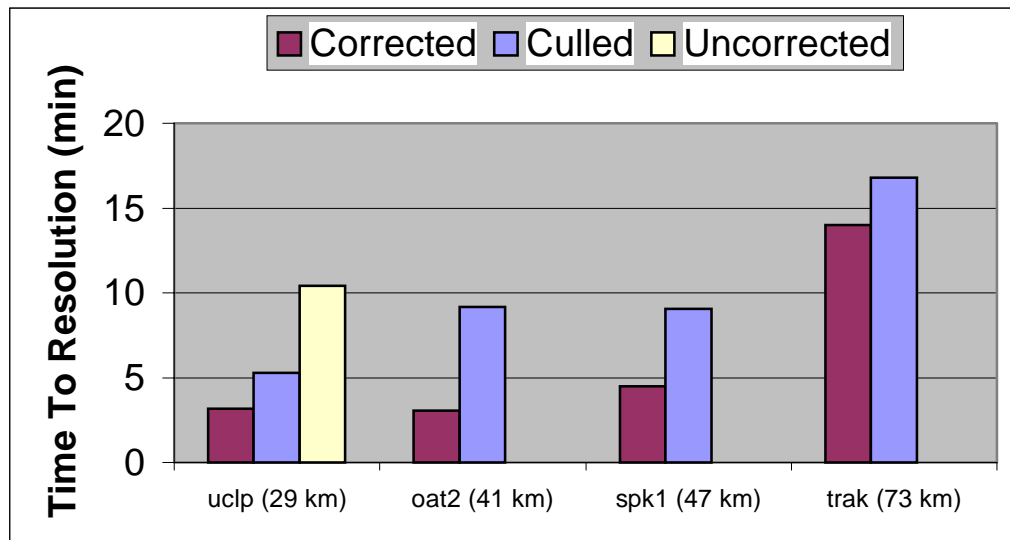


**Figure 6-21: Resolution Time Vs. Distance**

## Chapter 7

### CONCLUSIONS AND RECOMMENDATIONS

#### 7.1 Summary

A new approach has been proposed for substantially reducing the spatial and non-spatial errors in differential GPS navigation using accumulated carrier-phase measurements. Experimental results have shown that this approach can provide corrections for spatial error without deriving explicit estimates for the uncertainties of the ionosphere, troposphere, or satellite orbit. The previous chapters have demonstrated that a carrier-phase network can reduce the spatial errors that have traditionally limited the operational domain of carrier-phase DGPS applications. This research is the first time that PDAs have been used to explicitly estimate DGPS measurement errors on a carrier-phase network.

Several network implementations have been analysed in the preceding chapters. The “nearest-station” network is a simple concept, but suffers from several problems: First, the positioning accuracy degrades rapidly as the user moves away from the network reference stations. The simulated user at the “oat2” reference station in Southern California was shown to have a single-station positioning accuracy that was 90% poorer than that which was achieved when using a combined station network of 13 stations employing an  $\alpha\beta\chi\delta$  PDA. Second, discontinuities in the user’s position occur at the transition boundaries between adjacent reference stations. Finally, the ambiguities must be estimated/resolved each time the user transitions from one reference station to the next.

A “combined station” network is more difficult to implement, but has many advantages. Even the simplest combined station network eliminates the ambiguity transition issue by passing the inter-station ambiguities to the user via the data link. The non-spatial errors that affect each reference station are reduced as part of the solution’s filtering process, while spatial errors are estimated and removed.

In the preceding chapters, spatial and non-spatial errors have been shown to exist on networks in the United States and Canada. For standard DGPS applications, these errors can exceed 10 cm on 50 to 70 km baselines. The PDA estimates of these errors for each satellite. The estimated errors are then provided to the user as corrections for the user’s measurements. The analysis from the Holloman and SCIGN networks has indicated that the removal of estimated errors improves the measurement accuracy by 30% to 90%.

Three networks were used to verify the PDA theory presented in Chapter 4. The results from these networks are summarised as follows:

- 1) The Calgary network showed that the accuracy of the carrier-phase measurements and the ability to resolve the single-frequency ambiguities is degraded by spatial errors on baselines as short as 15 km.
- 2) The New Mexico network used an  $\alpha\beta$  PDA to improve measurement accuracy and ambiguity resolution by 30%. At the same time, it was suggested that relative survey errors and the lack of measurement redundancy are the limiting factors for the network’s performance.
- 3) The California network showed that, with sufficient redundancy and a precise network survey, the measurement accuracy was improved 50% to 90%. Network linking can be used to establish the inter-station ambiguities in real-time. However, many reference stations will be required for large networks. This

means that real-time networks will be expensive unless and alternative to network linking is developed.

## 7.2 Specific Results

Station “O” of the Holloman network was used as a test station to compare CP-NDGPS performance against that of standard DGPS performance. The baseline between Station “O” and the master reference station was 70 km in length, and the CP-NDGPS position of Station “O” using an  $\alpha\beta$  PDA had an accuracy between 2.5 and 9.5 cm. This was 30% better than the 3 to 12-cm accuracy obtained from standard DGPS positioning on the same baseline. The ambiguity resolution time using the PDA corrected measurements was 30% faster than for uncorrected DGPS measurements.

The SCIGN was also used to demonstrate how CP-NDGPS outperforms standard DGPS positioning. The close proximity of more than 25 reference stations provided the opportunity to test:

- ✓ Different PDA models
- ✓ The effects caused by having stations located at different altitudes
- ✓ The ability to instantly determine ambiguities at all stations within the network
- ✓ The accuracy and the ambiguity resolution performance at a variety of test stations

Five different PDA models were examined; the simplest involved only estimating the non-spatial error at the network master station ( $\alpha$  model). The most complicated model estimated the non-spatial error, the spatial decorrelation in the East, North, and Vertical axes, as well as non-linear effects along the vertical axis ( $\alpha\beta\chi\delta\gamma$  model). A full 12<sup>th</sup> order algorithm would saturate most data links in use today. However, it was shown that the best performance was derived from a 4<sup>th</sup> order PDA ( $\alpha\beta\chi\delta$  model).

The performance of each of the five models was compared using AIC. The AIC analysis attempts to minimise the residual errors or the power of the innovations process (IP) while considering the effects of over-parameterisation. The problem of over-parameterisation was clearly demonstrated when the power of innovations process for the complicated  $\alpha\beta\chi\delta\gamma$  model (0.150 m) was observed to be lower than that for the less complicated  $\alpha\beta\chi\delta$  model (0.154 m). Without the AIC analysis, the lower IP value would have been attributed to better modelling rather than over-parameterisation. This would have resulted in the incorrect selection of the  $\alpha\beta\chi\delta\gamma$  model as the best PDA for the SCIGN. It was also suggested that over-parameterization could be detected by looking for high cross-correlation in the covariance between PDA parameters.

The Southern California network had a variety of test stations at which the performance of the CP-NDGPS concept was tested. It was possible to measure the actual carrier-phase error at each test site because the locations of the test sites were known from a large-scale network survey. Each PDA model was used to predict the error at the test site, and a high correlation was established between the predicted errors and those actually measured.

Like the New Mexico network, the performance of the various PDA models was compared against the performance of a standard carrier-phase DGPS solution. The “oat2” test station was more than 40 km from the “jplm” master station, and standard DGPS positioning accuracy was estimated at between 7 and 11 cm. The CP-NDGPS positioning accuracy was below 1.5 cm. The other four test stations also showed improved positioning accuracy and confirmed that the performance improvements observed at “oat2” were the result of using a PDA. The improvement in positioning accuracy ranged from 20% to 90% at the various reference stations

The use of PDAs with CP-NDGPS also improved the ambiguity resolution times for the various test sites on the SCIGN. Standard CP-DGPS methods failed to resolve the single frequency ambiguities on the 73-km baseline connecting the “trak” and “jplm” reference stations. Using CP-NDGPS however, the single frequency ambiguities were resolved in less than 20 minutes when using the  $\alpha\beta\chi\delta$  PDA.

### 7.3 Network Design Issues

The network frequency is also an important design issue. A carrier-phase network can provide PDA models for several carrier-phase frequencies. These include L1, L2, both L1 and L2, or widelane. Sub-decimetre level positioning accuracy was achieved with the single frequency networks discussed in this dissertation. However, for large operational areas having few reference stations, it may be more convenient to use a widelane network and accept lower performance. If the data link has sufficient bandwidth, the network designer provides the user with the greatest utility by supplying PDAs for both the L1 and L2 frequencies separately. Such a design allows the user to switch from single frequency to widelane depending upon the conditions.

Rapid ambiguity resolution is desired on the inter-station baselines during the PDA modelling process. The PDA algorithm relies on the assumption that the errors in measurements are solely due to spatial and non-spatial factors. If the ambiguities are not resolved, the estimation error increases the network measurement noise and confuses the PDA solution process. Accurate estimates of the ambiguity must be nearly instantaneous for real-time operations. This is the greatest challenge facing the development of carrier-phase networks. In Chapter 6, the selected method of solving this problem was to form a set of short baseline links to the outermost reference stations (network linking). Ambiguity resolution on the short links was achieved in 30 seconds using two epochs of data from the SCIGN. The link ambiguities were accumulated to derive the ambiguities

for the outermost stations. This technique is simple and straightforward, but it requires the network reference stations to be within 10 to 30 km of one another when using a single frequency network. The New Mexico test network was unable to achieve instantaneous ambiguity resolution because the stations were not close enough together. The result was that PDAs could only be derived in post-processing using batch estimation of the ambiguities. Except for the data collection rate, the SCIGN working network had the potential for being used as a real-time network. However, the requirements of network linking forced the continuous operation of 13 reference stations.

#### **7.4 Future Perspectives**

The future of PDA development is broad and offers a variety of research opportunities. The PDA parameters have been shown to be relatively constant with time, and there is reason to believe that the non-spatial errors at satellite cross-over points are the highly correlated. The possibility of filtering the parameters may improve the parameter estimation accuracy. This may make it possible to use more complex PDA functions, or reduce the requirements for data link bandwidth.

If ambiguity resolution can be assured, increasing in the complexity of the PDA may reduce in the number of reference stations required to achieve a specific level of performance. Network linking is the primary factor limiting the use of CP-NDGPS in real-time applications. Combined ambiguity and bias estimation is one alternative to network linking that could provide equivalent accuracy with fewer reference stations. Another intriguing aspect of combined ambiguity and bias estimation is that the PDA parameters may be estimated along with the inter-station ambiguities. Future development in this area will be a key factor in reducing the costs associated with real-time carrier-phase networks.

The PDA models tested in this dissertation are not the only models that can be used. One non-linear model was tested, but other non-linear models may be justified with certain network configurations. A model having a non-linear horizontal correlation parameter was suggested as a possible method of improving the off-axis performance of the SCIGN working network.

Testing involving kinematic vehicles is needed. Neither the SCIGN nor the New Mexico networks were adequate test beds for kinematic analysis. The New Mexico network did not have enough stations to provide reliable ambiguity resolution, while the SCIGN working network did not have an appropriate data observation rate. Future kinematic testing in ground and airborne vehicles is going to require a dense network having a data rate of 1 Hz or better. A dense network where stations are separated by 15 to 50 km is necessary for real-time network linking and research into real-time ambiguity resolution for long baselines is needed. The 1 Hz data rate is important for establishing the performance capabilities of dynamic applications.

Further research is also needed to improve the accuracy of PDA corrections along the vertical axis. Networks having reference stations at a diverse set of altitudes will be important tools for defining methods that provide the best vertical positioning accuracy.

In addition to the generation and transmission of PDAs, real-time software needs to be developed to collect PDA information and produce measurement corrections. Standards that currently exist for the transmission of DGPS corrections need to be revised to accommodate PDA data link requirements.

## REFERENCES

- Air Force (1992), *Interface Control Document GPS-ICD-200 with IRN-200B-PR001*, Department of the Air Force, July 1.
- Akaike, H., (1974), "A New Look at the Statistical Model Identification", *IEEE Transactions on Automatic Control*, vol. AC-19.
- Alsip, D.H., and Radice, J. (1993), "The U.S. Coast Guard's Differential GPS Program", *Navigation, Journal of The Institute of Navigation, Alexandria, VA, Vol. 39, No. 4, Winter 1992-1993.*
- Axelrad, P., and Brown, R., (1996), "GPS Navigation Algorithms", *Global Positioning System: Theory and Applications*, Vol. 1, Edited by Parkinson, B., and Spilker Jr., J., The American Institute of Aeronautics and Astronautics, Progress in Astronautics and Aeronautics Series Volume 163, Washington D.C.
- Basker, S. (1995), "The Connection of Multiple Regional Wide Area Networks", *Proc. of DSNS 95*, Vol. 1, Bergen, Norway, April 28.
- Beser J, and B. Parkinson, (1984), "The Application of NAVSTAR Differential GPS in the Civilian Community", *Global Positioning System: Papers published in NAVIGATION*, Vol. II, The Institute of Navigation, Alexandria, VA.
- Blewitt, G. (1989), "Carrier-phase Ambiguity Resolution for the Global Positioning System Applied to Geodetic Baselines up to 2000 km", *Journal of Geophysical Research*, Vol 94, No. B8, August, 10.
- Boucher, C., and Altamimi, Z. (1996), "Innovation: International Terrestrial Reference Frame", *GPS World News and Applications of the Global Positioning System*, Vol. 7, Number 9, Advanstar Communications, Eugene OR, September.
- Braff, R., Powel, J.D., and Dorfler, J., (1996), "Applications of GPS to Air Traffic Control", *Global Positioning System: Theory and Applications*, Vol. 1, Edited by Parkinson, B., and Spilker Jr., J., The American Institute of Aeronautics and Astronautics, Progress in Astronautics and Aeronautics Series Volume 163, Washington D.C.
- Braff, R. (1997), Description of the FAA's Local Area Augmentation System (LAAS), MITRE Technical Report MTR 97W0000076, Center for Advanced Aviation Systems Development, The MITRE Corporation, McLean, VA, December.

- Braasch, M., (1996), "Multipath Effects", *Global Positioning System: Theory and Applications*, Vol. 1, Edited by Parkinson, B., and Spilker Jr., J., The American Institute of Aeronautics and Astronautics, Progress in Astronautics and Aeronautics Series Volume 163, Washington D.C.
- Brown, G., and Hwang, P., (1997), *Introduction to Random Signals and Applied Kalman Filtering*, Third Ed., John Wiley & Sons, Inc., New York, NY.
- Cannon M E, Berry E, and King M (1993), "Testing a Light weight GPS/GIS Terminal for Sub-Meter DGPS Positioning", *Proc. of ION GPS-93*, The Institute of Navigation, Alexandria, VA.
- Cannon M E, and Varner C (1995), *Final Report on the AvCan Network RTK Project*, University of Calgary Department of Geomatics Engineering Report, Calgary Canada, October.
- Cannon, M.E., (1990), "High Accuracy GPS Semikinematic Positioning: Modeling and Results", *Navigation*, Vol. 37, No.1, The Institute of Navigation, Alexandria, VA
- Chen D, Lachapelle G, (1994) "A Comparison of FASF and Least-Squares Search Algorithms for Ambiguity Resolution On The Fly", *Proc. of KIS 94*, The University of Calgary Department of Geomatics Engineering, Calgary, Canada, August 30.
- Collier Encyclopedia* © 1997, Collier Newfield, Bellevue, WA.
- Cosentino, R.J., and Diggle, D. (1996), "Differential GPS", *Understanding GPS: Principles and Applications*, Edited by Kaplan, E., Artech House Publishers, Mobil Communications Series, Norwood, MA.
- Dong, D., and Bock, Y., (1989), "Global Positioning System Network Analysis With Phase Ambiguity Resolution Applied to Crustal Deformation Studies in California", *Journal of Geophysical Research*, Vol. 94, No. B4, April 10
- DOD/DOT (1997), *1996 Federal Radionavigation Plan*, U.S. Department of Transportation and U.S. Department of Defense, Washington, DC, Rep. DOT-VNTSC-RSPA-97-2/DOD-4650.5, July 1997.
- (1997) *Encarta 97 Encyclopedia*, Microsoft Corporation, Seattle WA.
- El-Arini, M. B., Conker, R., Albertson, T., Reagan, J., Klobuchar, J., and Doherty, P., (1995), "Comparison for Real-Time Ionospheric Algorithms for a GPS Wide-

Area Augmentation System (WAAS)”, *Navigation*, Journal of the Institute of Navigation, Vol. 41, No. 4, The Institute of Navigation, Alexandria, VA, Winter 1994-1995, pp. 393-413.

Ford, T.J. and Neumann, J. (1994). “NovAtel’s RT20 - A Real Time Floating Ambiguity Positioning System”, *Proc. of ION GPS-94*, The Institute of Navigation, Alexandria, VA, September 20-23.

Galijan R, J. Gilkey, and R. Turner, (1994), “Results of a Study Into the Utility of Carrier-phase GPS for Automated Highway Systems”, *Proc. of ION GPS-94*, The Institute of Navigation, Alexandria, VA, September 20-23.

Garin, L., van Diggelen, F., and Rousseau, J. (1996). “Strobe & Edge Correlator Multipath Mitigation for Code”, *Proc. of ION GPS-96 (Kansas City)*, The Institute of Navigation, Alexandria, VA, September 17-20.

GPS JPO (1991), *NAVSTAR GPS User Equipment*, ANP2, NAVSTAR GPS Joint Program Office, Las Angeles, CA.

GPS World (1995), “AFSC Says GPS Constellation Fully Operational”, *GPS World News and Applications of the Global Positioning System*, Vol. 6, Number 6, Advanstar Communications, Eugene OR, June.

Han, S., and Rizos, C. (1997), “An Instantaneous Ambiguity Resolution Technique for Medium-Range GPS Kinematic Positioning”, *Proc. of ION GPS-97 (Kansas City)*, The Institute of Navigation, Alexandria, VA, September 16-19.

Hatch, R., (1991), “Instantaneous Ambiguity Resolution”, *Proc. of KIS 1990*, Banff, Canada, pp. 299-308.

Haykin, S., (1991), *Adaptive Filter Theory*, 2<sup>nd</sup> Edition, Prentice Hall, Englewood Cliffs, NJ, pp.107-108.

Hurst, K., (1995), “Precise Orbital Products Available from JPL”, *GIPSY-OASIS II Newsletter*, Fall 1995, Jet Propulsion Laboratory, Pasadena, CA.

Hoffmann-Wellenhof, B., Liechtenegger, H. and Collins, J., (1994), *GPS Theory and Practice*, Third Revised Ed., Springer-Verlag, Wien, New York.

Kee, C. (1996), “Wide Area Differential GPS”, *Global Positioning System: Theory and Applications*, Vol. 1, Edited by Parkinson, B., and Spilker Jr., J., The American

Institute of Aeronautics and Astronautics, Progress in Astronautics and Aeronautics Series Volume 163, Washington D.C.

- Kee, C., Parkinson, B., and Axelrad, P., (1991), "Wide Area Differential GPS", *Navigation*, Journal of the Institute of Navigation, Vol. 38, No. 2, The Institute of Navigation, Alexandria, VA, Summer.
- Kee C. and Parkinson, B.W., (1992), "Algorithms and Implementation of Wide Area Differential GPS", *Proc. of ION GPS-92 (Salt Lake)*, The Institute of Navigation, Alexandria Virginia, September.
- Krakiwsky, E. (1990), *The Method of Least Squares: A Synthesis of Advances*, UCGE Report # 10003, The University of Calgary, Department of Geomatics Engineering, Calgary, Alberta, Canada.
- Klobuchar, J., (1996), "Ionospheric Effects on GPS", *Global Positioning System: Theory and Applications*, Vol. 1, Edited by Parkinson, B., and Spilker Jr., J., The American Institute of Aeronautics and Astronautics, Progress in Astronautics and Aeronautics Series Volume 163, Washington D.C., pp. 485-515.
- Klobuchar, J., Doherty, P., and El-Arini, B., (1995), "Potential Ionospheric Limitations to the GPS Wide-Area Augmentation System", *Navigation*, Vol. 42, No.2, The Institute of Navigation, Alexandria, VA, pp. 353-370.
- Lachapelle, G., and Cannon, M.E. and Lu, G., (1992), "High Precision GPS Navigation with Emphasis on Carrier-Phase Ambiguity Resolution, Marine Geodesy, Vol 15, 4, pp. 253-269.
- Langley R. (1997), "GPS Receiver System Noise", *GPS World News and Applications of the Global Positioning System*, Advanstar Communications, Eugene OR, June, pp. 40-45.
- Lapucha, D. and Huff, M, (1994), "Two Methods of Multiple Reference Station DGPS – Performance Comparison", *Proc. of KIS-94*, Department of Geomatics Engineering, The University of Calgary, Calgary, Canada, August 30 - September 2.
- Lapucha, D. and Barker, R, (1994), "Multi-Site Real-Time DGPS Systems Using Starfix Link; Operational Results", *Proc. of ION GPS-94 (Salt Lake)*, The Institute of Navigation, Alexandria, Virginia, September 24.

- Leick, A. (1995), *GPS Satellite Surveying*, 2nd ed., John Wiley & Sons Inc., New York, NY.
- Leva, J., Uijt de Haag, M., Van Dyke, K. (1996), "Performance of Standalone GPS", *Understanding GPS: Principles and Applications*, Edited by Kaplan, E., Artech House Publishers, Mobil Communications Series, Norwood, MA.
- Loomis, P., Sheynblatt, L., and Mueller, T. (1991), "Differential GPS Network Design", *Proc. of ION GPS-91 (Albuquerque)*, The Institute of Navigation, Alexandria, VA, September 11-13.
- Malys, S. Slater, J., Smith, R., Kunz, L. and Kenyon, S. (1997), "Status of the World Geodetic System 1984", *Proc. of KIS-97*, Department of Geomatics Engineering, The University of Calgary, Calgary, Canada, June 3-6.
- Martin, E. H., (1980), "GPS User Equipment Error Models", *Global Positioning System: Papers published in NAVIGATION*, Vol. 1, Edited by Janiczek, P. M., The Institute of Navigation, Washington D.C.
- Mendes, V.B. and Langley, R.B. (1994), "A Comprehensive Analysis of Mapping Functions Used in Modelling Tropospheric Propagation Delay in Space Geodetic Data", *Proc. of KIS-94*, Department of Geomatics Engineering, The University of Calgary, Calgary, Canada, September 2.
- MITRE (1998), *Potential Economic Benefits of Adding a Third Civil GPS Frequency*, MTR98W0000145, The MITRE Corporation, McLean, VA, 30 October 1998.
- Mueller, T. (1994a), "Minimum Variance Network DGPS Algorithm", *Proc. of IEEE PLANS 94 (Las Vegas)*, Institute of Electrical and Electronic Engineers, Publishing Services, New York, NY, April 11-15.
- Mueller, T. (1994b), "Wide Area Differential GPS", *GPS World*, Advanstar Communications, Eugene, OR, June.
- Neilan, R., (1997), *IGS, International GPS Service for Geodynamics, Resource Information*, Jet Propulsion Laboratory, Pasadena, CA, January.
- Parkinson, B. (1996a), "Introduction and Heritage of NAVSTAR", *Global Positioning System: Theory and Applications*, Vol. 1, Edited by Parkinson, B., and Spilker Jr., J., The American Institute of Aeronautics and Astronautics, Progress in Astronautics and Aeronautics Series Volume 163, Washington D.C.

- Parkinson, B., (1996b), "GPS Error Analysis", *Global Positioning System: Theory and Applications*, Vol. I, Edited by Parkinson, B., and Spilker Jr., J., The American Institute of Aeronautics and Astronautics, Progress in Astronautics and Aeronautics Series Volume 163, Washington D.C.
- Parkinson, B. and Enge, P., (1996), "Differential GPS", *Global Positioning System: Theory and Applications*, Vol. II, Edited by Parkinson, B., and Spilker Jr., J., The American Institute of Aeronautics and Astronautics, Progress in Astronautics and Aeronautics Series Volume 163, Washington D.C.
- PDD, (1996), *Fact Sheet: U.S. Global Positioning System Policy*, Office of Science and Technology Policy, National Security Council, Presidential Decision Directive NSTC-6, March 29.
- Raquet, J. (1996), "Multiple Reference GPS Receiver Multipath Mitigation Technique", *Proc. of the ION 52<sup>nd</sup> Annual Meeting*, The Institute of Navigation, Alexandria VA.
- Raquet, J. and Lachapelle, G. (1997), "Long Distance Kinematic Carrier-Phase Ambiguity Resolution Using a Simulated Reference Receiver Network", *Proc. of ION GPS 97 (Kansas City)*, The Institute of Navigation, Alexandria, Virginia, September 16-19.
- Raquet, J. (1998), *Development of a Method for Kinematic GPS Carrier-Phase Ambiguity Resolution using Multiple Reference Receivers*, PhD Dissertation, The University of Calgary, Department of Geomatics Engineering, Calgary, Alberta, Canada.
- Ray, J., Cannon, M. E., and Fenton P., (1998), Mitigation of Static Carrier Phase Multipath Effects Using Multiple Closely-Spaced Antennas", ", *Proc. of ION GPS 98 (Nashville)*, The Institute of Navigation, Alexandria, Virginia, September 15-18, pp. 1025-1034.
- Remondi, B., (1991), "Kinematic GPS Results without Static Initialization", *Proc. of 47<sup>th</sup> Annual Meeting*, The Institute of Navigation, Washington D.C., pp.87-111.
- RTCM 104 (1994), *RTCM Recommended Standards for Differential NAVSTAR GPS Service, Version 2.1*, Radio Technical Commission for Maritime Services, Washington D.C., January 1994, Appendix IV.
- Ryan, S., Forbes, F., and Wee, S. (1997), "Avoiding the Rocks – Then Canadian coast Guard Differential GPS System", *Proc. of KIS-97 (Banff)*, The University of

Calgary, Department of Geomatics Engineering, Calgary, Alberta, Canada, June 3-6.

- Sams M. (1995), "CAT II/III Accuracy and Availability for Local Area Differential GPS Including Geostationary Satellite and Pseudolite Augmentations", *Proc. of ION 51<sup>st</sup> Annual Meeting*, The Institute of Navigation, Alexandria, Virginia, June 5.
- Sauer D, Beutler G, Euler H, (1994), "Phase Measurements in Kinematic GPS Applications Theory and Summary of Processing Strategies", *Proc. of KIS-94*, The University of Calgary Department of Geomatics Engineering, Calgary, Canada, August 30.
- Sinnott, J., Ahn, I., and Pietraszewski, D., (1996), "Marine Applications", *Global Positioning System: Theory and Applications*, Vol. 1, Edited by Parkinson, B., and Spilker Jr., J., The American Institute of Aeronautics and Astronautics, Progress in Astronautics and Aeronautics Series Volume 163, Washington D.C.
- Skone, S., M.E. Cannon, K. Lochhed, P. Heroux, F. Lahaye, (1996), "Performance Evaluation of NRCAN Wide Area System", *Proc. of ION GPS-96 (Kansas City)*, The Institute of Navigation, Alexandria, VA, September 20-23, pp 1793-1802.
- Skone, S., and M.E. Cannon, (1998), "Detailed Analysis for Auroral Zone WADGPS Ionospheric Grid Accuracies during Magnetospheric Substorm Event", *Proc. of ION GPS-98 (Nashville)*, The Institute of Navigation, Alexandria, VA, September 15-18, pp 701-710.
- Sluiter P., J. Zomerdijsk, and G. Husti, (1994), "A Comparison of Geodetic Receivers Under A-S Conditions: Survey of Baselines", *Proc. of ION GPS-94*, The Institute of Navigation, Alexandria, VA, September 20-23.
- Spilker Jr., J., (1980), "GPS Signal Structure and Performance Characteristics", *Global Positioning System: Papers published in NAVIGATION*, Vol. 1, Edited by Janiczek, P. M., The Institute of Navigation, Washington D.C.
- Spilker Jr., J., (1996), "GPS Navigation Data", *Global Positioning System: Theory and Applications*, Vol. 1, Edited by Parkinson, B., and Spilker Jr., J., The American Institute of Aeronautics and Astronautics, Progress in Astronautics and Aeronautics Series Volume 163, Washington D.C.
- Sun H., Cannon M.E., Miligard T., (1999), "Real-Time GPS Reference Network Carrier-Phase Ambiguity Resolution", *Proc. of ION NTM-99 (San Diego)*, The Institute of Navigation, Alexandria, VA, January 25-27.

- Swokowski E., (1979), *Calculus with Analytic Geometry*, Second Ed., Prindle, Weber, and Schmidt, Boston, MA.
- Tang, C. (1996), *Accuracy and Reliability of Various DGPS Approaches*, Master's Thesis, The University of Calgary, Department of Geomatics Engineering, Calgary, Alberta, Canada, May.
- Tang, W., Johnson, N., and Graff, J., (1989), "Differential GPS Operation with Multiple Ground Reference Stations", *Proc. of ION GPS-89 (Colorado Springs)*, The Institute of Navigation, Alexandria, VA, September 27-29.
- Tapley, B. (1990), *Statistical Estimation Theory*, The University of Texas, Department of Aerospace Engineering, ASE 381P Course Notes Spring Session, Austin, Texas.
- Taveira-Blomenhofer, T, and G. Hein (1993), "Investigations on Carrier-phase Corrections for High-Precision DGPS Navigation", *Proc. of ION GPS-93 (Salt Lake City)*, The Institute of Navigation, Alexandria, VA, pp. 1461-1467.
- Teunissen, P., and Tiberious, C., (1994), "Integer Least-Squares Estimation of the GPS Phase Ambiguities", *Proc. of KIS-94 (Banff)*, The University of Calgary, Department of Geomatics Engineering, Calgary, Alberta, Canada, August 30-September 2.
- Thomson, D., E. Krakiwsky, and B. Nickerson, (1987), *A Manual for the Establishment and Assessment of Horizontal Survey Networks*, UCGE Report # 10005, The University of Calgary, Department of Geomatics Engineering, Calgary, Alberta, Canada.
- Thorsteinsson, S., T. Gunnarsson, G. Gudmundsson, G. Tryggvason, P. Enge, D. Young, L. Sheynblat, B. Westfall, C. Daniell, J. Helgason (1996), "Iceland's Network of Differential GPS Radiobeacons", *Navigation*, Journal of The Institute of Navigation, Vol.42, No. 4, Winter 1995-1996, Alexandria, VA.
- Townsend B, Fenton P, Van Dierendonck K, Richard Van Nee D J, (1995), "Performance Evaluation of the Multipath Estimating Delay Lock Loop", *Navigation*, Journal of the Institute of Navigation, Vol. 42, No. 3. Fall.
- Van Dierendonck A.J. (1995), "Innovation: Understanding GPS Receiver Terminology: A Tutorial", *GPS World News and Applications of the Global Positioning System*, Vol. 6, Number 1, Advanstar Communications, Eugene OR, January.

- Van Dierendonck, A.J., (1996), "GPS Receivers", *Global Positioning System: Theory and Applications*, Vol. 1, Edited by Parkinson, B., and Spilker Jr., J., The American Institute of Aeronautics and Astronautics, Progress in Astronautics and Aeronautics Series Volume 163, Washington D.C.
- Van Dierendonck A. J., Fenton P., and Ford T., (1992), "Theory and Performance of Narrow Correlator Spacing in a GPS Receiver", *Navigation*, Journal of the Institute of Navigation, Vol. 39, No. 3., Fall, The Institute of Navigation, Alexandria VA.
- Van Dierendonck, A.J., Klobuchar, J., and Hua, Q. (1994), "Ionospheric Scintillation Monitoring Using Commercial Single Frequency C/A Code Receivers", *Proc. of ION GPS-94*, The Institute of Navigation, Alexandria, VA, September 20-23.
- van Diggelen, F. (1998), "Innovation: GPS Accuracy: Lies, Damn Lies, and Statistics", *GPS World News and Applications of the Global Positioning System*, Vol. 9, Number 1, Advanstar Communications, Eugene OR, January.
- van Graas, F., and Braasch, M., (1996), "Selective Availability", *Global Positioning System: Theory and Applications*, Vol. 1, Edited by Parkinson, B., and Spilker Jr., J., The American Institute of Aeronautics and Astronautics, Progress in Astronautics and Aeronautics Series Volume 163, Washington D.C.
- Varner, C., and Henriksen, J. (1996), *Roof Co-ordinates for the Pillars above the Geomatics Engineering Satellite Laboratory*, University of Calgary Department of Geomatics Engineering Internal Memorandum, Calgary, Alberta, Canada, August 14.
- Varner, C., and Cannon, M.E. (1997), "The Application of Multiple Reference Stations to the Determination of Multipath and Spatially Decorrelating Errors", *Proc. of ION NTM-97 (Santa Monica)*, The Institute of Navigation, Alexandria, VA, January 14-16.
- Wells D E, Beck N, Delikaraoglou D, Kleusberg A, Krakiwsky E J, Lachapelle G, Langley R B, Nakiboglu M, Schwarz K P, Tranquilla J M, Vanicek P (1987), *Guide to GPS Positioning*, Canadian GPS Associates, Fredericton, N.B., Canada.
- Weisenberger, S. (1997), *Effect of Constraints and Multiple Receivers for On-The-Fly Ambiguity Resolution*, Master's Thesis, The University of Calgary, Department of Geomatics Engineering, Calgary, Alberta, Canada, April.

- White House Press Release* (1998), Office of the Vice President of the United States, March 30.
- Wübbena, G., Bagge, A., Seeber, G., Boder, V., and Hankemeier, P., (1996), “Reducing Distance Dependent Errors for Real-Time Precise DGPS Applications by Establishing Reference Station Networks”, *Proc. of ION GPS-96 (Kansas City)*, The Institute of Navigation, Alexandria, VA, September 17-20.
- Wübbena, G., (1989), “The GPS Adjustment Software Package GEONAP – Concepts and Models”, *Proc. Of the Fifth International Geodetic Symposium on Satellite Positioning, Las Cruces, New Mexico, March 13-17, Vol. 2: pp. 452-461.*
- Yunck, T., Bar-Sevar, Y., Bertiger, W., Iijima, B., Lichten S., Lindqwister, U., Mannucci A., Muellerschoen R., Munson, T., Romans, L., and Wu, S., (1996), “A Prototype WADGPS System for Real Time Sub-Meter Positioning Worldwide”, *Proc. of ION GPS 96 (Kansas City)*, The Institute of Navigation, Alexandria, Virginia, September 17-20.
- Zumberge, J., and Bertiger, W., (1996), “Ephemeris and Clock Navigation Message Accuracy”, *Global Positioning System: Theory and Applications*, Vol. 1, Edited by Parkinson, B., and Spilker Jr., J., The American Institute of Aeronautics and Astronautics, Progress in Astronautics and Aeronautics Series Volume 163, Washington D.C.
- Zumberge, J., Neilan, R., Beutler, G., and Gurtner, W., (1994), “The International GPS Service for Geodynamics – Benefits to Users”, *Proc. of ION GPS-94 (Salt Lake)*, The Institute of Navigation, Alexandria, Virginia, September 24.

## Appendix A: Site Coordinates for SCIGN Working Network

The following tables provide co-ordinate information about the SCIGN Working network and the test stations used to evaluate the performance of various network models studied in the previous chapters.

### Working Network

<b>ID</b>	<b>Location</b>	<b>Latitude (°N)</b>	<b>Longitude (°E)</b>	<b>Hgt (m)</b>
Aoa1	Westlake Village	34.157441609	-118.830312157	246.5564
Azu1	Azusa High School	34.126017062	-117.896482446	144.9654
Bran	Burbank	34.184892868	-118.277045172	246.2571
Cat1	Catalina Island	33.445769785	-118.483002578	3.9102
Chil	Chilao	34.333421463	-118.025994527	1568.1050
Cit1	Caltech	34.136707191	-118.127280456	215.3439
Clar	Clarmont	34.109926804	-117.708805114	373.7772
Csn1	CSU at Northridge	34.253548259	-118.523806750	261.5295
Holc	Pearblossom	34.458185352	-117.845157504	1238.1722
Holp	Hollydale	33.924538071	-118.168165982	-6.5385
Jplm	Jet Propulsion Lab	34.204818782	-118.173222161	423.9820
Lbch	Long Beach	33.787767976	-118.203337924	-27.5406
Rock	Simi Valley	34.235672474	-118.676425725	553.5277

### Test Station Site Coordinates

<b>ID</b>	<b>Location</b>	<b>Latitude (°N)</b>	<b>Longitude (°E)</b>	<b>Hgt (m)</b>
Oat2	Oat Mountain	34.329890245	-118.601374481	1112.5745
Pvep	Palos Verdes	33.743288116	-118.404242706	69.4243
Bran	Burbank	34.184892868	-118.277045172	246.2571
Cat1	Catalina Island	33.445769785	-118.483002578	3.9102
Chil	Chilao	34.333421463	-118.025994527	1568.1050